Fluctuating Selection and its Effects on Neutral Genetic Variation

Olivia Lenore Johnson

Principal Supervisor: Asst. Prof. Christian D. Huber

Co-Supervisors: Assoc. Prof. Raymond Tobler and Dr. Joshua M. Schmidt

Department of Ecology and Evolutionary Biology

School of Biological Sciences

The University of Adelaide

THE UNIVERSITY of ADELAIDE

This thesis is submitted in fulfilment of the requirements for the degree of Doctor of Philosophy

January 2024

I acknowledge the Kaurna people, the original custodians of the Adelaide Plains and the land on which I live and work. I extend my respects to Elders past, present, and emerging. I acknowledge that sovereignty was never ceded.

Table of Contents

Thesis Abstract

Natural selection has become a pervasive theory of evolution since its first proposal over 160 years ago. Some forms of selection have been intensively studied such that we now have a robust understanding of their dynamics, can predict their effects, and have wide-ranging evidence in empirical data from natural populations. Fluctuating selection, when selection shifts in strength or direction over time, is a form of natural selection that has been studied sporadically over the last century. As a consequence, we have a number of models of fluctuating selection but a comprehensive understanding of its effect on genomic variation has remained elusive. Fluctuating selection was originally studied in the form of phenotype observations, for example, Fisher and Ford studied wing patterns in a population of scarlet tiger moth and noticed patterns varied in proportion over time. More recently, fluctuating selection has been identified at the molecular level using allele frequencies. With recent advances in sequencing and decreases in associated costs, the last decade has seen a multitude of evidence of fluctuating selection in natural and experimental populations. A large quantity of this has stemmed from investigations of cosmopolitan *Drosophila melanogaster* populations over seasonal time scales but is also observed in other species such as *Arabidopsis thaliana*, non-biting midge, and stickleback. This thesis contains a methodical investigation of fluctuating selection, with an emphasis on its effects on neutral genetic variation.

In Chapter 1, I perform an updated review of the field of fluctuating selection, compiling the abundance of recent evidence of fluctuating selection in natural and experimental populations as well as analytical studies of the dynamics of loci under this form of selection. Additionally, I highlight the gaps that remain in our current knowledge of fluctuating selection, with the hope of filling some with the subsequent work in this thesis.

In Chapter 2, I benchmark population genetic simulation frameworks to identify an efficient and robust way to simulate non-standard forms of natural selection using fluctuating selection as an example. I compare four simulation frameworks using classical and updated data-recording methods to identify the workflow that confers the most efficient computational resource usage for use in the following chapters.

Chapter 3 comprises a population genetic analysis of the effects of seasonally fluctuating selection on linked neutral genetic variation. A single-locus model of fluctuating selection is used to characterise its effect on linked neutral genetic variation using a range of population genetic statistics. I then compare the signatures of fluctuating selection to common selection types (i.e. positive and balancing selection) to determine if fluctuating selection can be differentiated from these forms.

In Chapter 4, I simulate multilocus fluctuating selection to examine its impact on genome-wide effective population size. A recent theoretical study found that seasonally fluctuating selection can decrease diversity genome-wide. I find that under realistic model parameters estimated from *Drosophila* data, fluctuating selection indeed leads to a strong reduction in effective population size, and thus reduces genome-wide genetic diversity. I discuss the results in the context of Lewontin's Paradox, the observation that the range of genetic diversity across species is much smaller than the extent of variation in population size.

Together, this thesis synthesises and expands our knowledge of fluctuating selection and its implications on population genetic measures and approaches.

Thesis Declaration

I certify that this work contains no material which has been accepted for the award of any other degree or diploma in my name, in any university or other tertiary institution and, to the best of my knowledge and belief, contains no material previously published or written by another person, except where due reference has been made in the text. In addition, I certify that no part of this work will, in the future, be used in a submission in my name, for any other degree or diploma in any university or other tertiary institution without the prior approval of the University of Adelaide and where applicable, any partner institution responsible for the joint-award of this degree.

I acknowledge that copyright of published works contained within this thesis resides with the copyright holder(s) of those works.

I also give permission for the digital version of my thesis to be made available on the web, via the University's digital research repository, the Library Search and also through web search engines, unless permission has been granted by the University to restrict access for a period of time.

I acknowledge the support I have received for my research through the provision of an Australian Government Research Training Program Scholarship.

Olivia Lenore Johnson

Acknowledgements

I would first like to extend my utmost thanks and gratitude to my supervisors Christian Huber, Raymond Tobler, and Joshua Schmidt. We did it, we successfully completed a zoom PhD! While my PhD experience was not at all what I imagined it to be when we first discussed it back in 2019, your dedication to this work and my project has made for a thesis and a PhD journey I am really proud of.

To Christian, thank you for all your guidance and support over this project, all the nights you've stayed up late and worked overtime to ensure I was never impacted by the fact that you were on the other side of the world. I have learnt so much from you, and hope, if I ever supervise someone, I can be half the supervisor you have been to me. Thank you also for welcoming me into your lab at Penn State, and I thank Matt and Vanessa, Abby, Dina, Troy, and the Huber family for making my time in the US such an enjoyable experience.

To Ray, perhaps unbeknownst to you, you have made such an impact on the trajectory of my academic career. From our first interaction when I was first introduced to ACAD and all it entailed almost 7 years ago, your passion for your work and your willingness to share your knowledge and skills has encouraged me to follow my interest in this field. Your constant enthusiasm, curiosity, and unique perspective has been so valuable throughout my PhD journey, and I am so grateful that you have been a part of this project.

Finally, to Josh, thank you for your dedication to seeing out this project in the face of unexpected upheaval and uncertainty. You have brought invaluable insight and contributions that have not only improved this thesis but also expanded my knowledge and understanding.

To the members of ACAD, thank you to Jeremy, Bastien, Vilma, and Yassine for your support and advice on the ground. Particularly to Yassine who has not only supported but

encouraged me from the start of my journey at ACAD. To all the students past and present who have shared their experiences and who I have learnt from, especially Caitlin M, Robbi, Xavi, Gludi, Shyam, Matt, Evelyn, Adrien, and Gina who have helped and supported me on this journey.

To the Westpac Scholars Trust, thank you for choosing me as a Future Leader for 2020, the experiences, opportunities, and people that have been brought into my life by this scholarship have helped me be the well-rounded leader you saw I could be. Special thanks go to Georgina, Scott, Alicia, Kealan, and Shanna. Our monthly catch ups have kept me sane and taught me so much that is not related to my research, I'm so glad the scholarship program brought you all into my life.

To my friends, thank you for all your support and encouragement over this journey. Most of all, to Tamara, thank you for letting me have a life vicariously through you over the last 4 years, and for continuing to study so I'm not the only one complaining about 'uni work'.

And finally, to my family. Thank you for sharing the highs and lows of this journey with me, I hope you know I appreciate every time you pretended to care about fluctuating selection, and shared my excitement when I made breakthroughs you didn't understand. Thanks especially go to Mae and Henry for keeping me company while I work, Dad for keeping me supplied with ice creams and lollies, and Mum for wiping my tears when times have been tough and taking me for some retail therapy when that didn't work. I couldn't have made it through without you.

Publications

Published Articles

Johnson OL, Tobler R, Schmidt JM, Huber CD. 2023. Fluctuating selection and the determinants of genetic variation. Trends Genet. 39:491–504. doi: 10.1016/j.tig.2023.02.004.

Accepted Manuscripts

Johnson OL, Tobler R, Schmidt JM, Huber CD. 2024. Population genetic simulation: Benchmarking frameworks for non-standard models of selection. Mol Ecol Resour. *In press.*

Unsubmitted Manuscripts

Johnson OL, Tobler R, Schmidt JM, Huber CD. Discerning the genetic footprints of seasonal fluctuating selection: A comparison with established selection forms. *In preparation.*

Johnson OL, Tobler R, Schmidt JM, Huber CD. The effect of fluctuating selection on effective population size. *In preparation.*

Thesis Introduction

Natural selection, the theory that species promote their survival by adapting to changes in their environment, was first proposed by Charles Darwin over 160 years ago (Darwin 1859). Since then, selection has been observed in a wide variety of species and in a number of different forms.

Early studies of natural selection used observations of phenotype to identify traits under selection (Darwin 1859; Tutt 1891; Fisher 1930; Ford 1937; Fisher & Ford 1947). However, the advent of affordable sequencing technologies has led to an abundance of genetic data, enabling us to study selection at the molecular level in the context of genetic variation. Natural selection can have significant impacts on neutral diversity at sites linked to a selected locus (Smith & Haigh 1974; Charlesworth et al. 1993), and these patterns can be identified when assessing genetic variation in a population, allowing for the identification of selection. In addition, increased computational capability and new algorithmic methods have resulted in powerful population genetic simulators being developed which can model complex selective processes and examine their effects on genetic diversity (Baumdicker et al. 2022; Haller & Messer 2023).

Several features of genetic variation can be leveraged using population genetic statistics to identify natural selection, this includes the distribution of allele frequencies, i.e. site frequency spectrum (Tajima 1989; Bitarello et al. 2023); levels of variation across a region (Smith & Haigh 1974; Watterson 1975; Tajima 1983); and haplotype frequencies (Garud & Rosenberg 2015). These can then be compared to expectations of these statistics under neutral evolution to determine if distortions have occurred that can be attributed to natural selection.

Simple forms of selection that assume constant selection pressures in homogeneous populations are now well understood, owing to a substantial body of research not only

examining the dynamics and implications of loci under these forms of selection but identifying them in empirical data. Positive selection is one such form, where a beneficial variant increases in frequency in a population until reaching fixation, thereby decreasing diversity in surrounding regions (Smith & Haigh 1974; Fay & Wu 2000; Pritchard et al. 2010; Coop & Ralph 2012; Hermisson & Pennings 2017). Positive selection has been found in a wide range of species, spanning all forms of life, in natural populations and experimentally (Petersen et al. 2007; Garud et al. 2015; Souilmi et al. 2022; Zhong et al. 2022; Harris & Garud 2023). Other well-studied forms of selection include balancing selection, in the form of heterozygote advantage where alleles are held at intermediate frequencies, thereby maintaining genetic variants in a population (Tian et al. 2002; Hedrick 2007; Andrés et al. 2009; Sellis et al. 2011; Key et al. 2014; Bitarello et al. 2018; Chapman et al. 2019; Bitarello et al. 2023), and background selection, the purging of neutral variation linked to deleterious alleles in a population (Charlesworth et al. 1993; Hudson & Kaplan 1995; Charlesworth 2012; Comeron 2014; Matheson & Masel 2023). Theoretical, experimental, and empirical methods have been developed and refined for the study of these selection types. However, selection cannot always be expected to be simple or constant (Bell 2010), and consequently, attention has now moved to the investigation of more complex forms of selection.

Fluctuating selection is a form of selection that was first proposed almost a century ago and has been periodically examined over the following decades (Fisher & Ford 1947; Haldane & Jayakar 1963; Hedrick et al. 1976; Gillespie 1991, 1997; Barton 2000; Huerta-Sanchez et al. 2008; Bell 2010; Taylor 2013; Wittmann et al. 2017). Fluctuating selection occurs when selection pressures shift in magnitude or direction over time and is often considered a form of balancing selection as it is able to maintain segregating alleles longer than expected under neutral evolution (Wittmann et al. 2017). By maintaining multiple variants segregating across time, fluctuating selection allows populations to withstand changing environments by

carrying adaptations suited to different conditions across generations. In recent years, whole-genome resequencing studies of populations across time have led to the identification of seasonally fluctuating selection, i.e. hundreds to thousands of alleles that oscillate on a seasonal time scale, in plants and insects with short generation times (reviewed in depth in Chapter 1; Bergland et al. 2014; Busoms et al. 2018; Garcia-Elfring et al. 2021; Machado et al. 2021; Behrman & Schmidt 2022; Kelly 2022; Pfenninger et al. 2022; Pfenninger & Foucault 2022; Rudman et al. 2022; Bitter et al. 2023; Lynch et al. 2023; Nunez et al. 2023). However, there have also been studies using ancient DNA to identify changing selection pressures at individual loci in larger mammals with longer generation times, including studies in humans (Ludwig et al. 2015; Jagoda et al. 2018; Mathieson & Mathieson 2018; Yair et al. 2021; Mathieson & Terhorst 2022). In addition to this evidence from empirical data, there has been a number of studies modelling the dynamics of fluctuating loci (Haldane & Jayakar 1963; Wittmann et al. 2017; Bertram & Masel 2019; Park & Kim 2019; Kim 2023). Theoretical studies of the impact of fluctuating selection on linked neutral diversity have been examined (Gillespie 1997; Huerta-Sanchez et al. 2008; Taylor 2013; Wittmann et al. 2023). However, the only study of regular fluctuations used a coalescent approach (Wittmann et al. 2023), leaving the effects of regularly fluctuating selection on other patterns of population genetic variation and genome-wide effective population size to be investigated. Most of these studies have been published since the last review of the field of fluctuation selection (Bell 2010). In this time, there have also been a number of simulation methods developed that may allow for the effective simulation of fluctuating selection, however, these have yet to be consistently benchmarked. This thesis concentrates on the population genetic signatures and implications of fluctuating selection using simulation approaches. It is structured as follows.

Chapter 1 - Fluctuating selection and the determinants of genetic variation.

In this chapter, I review the field of fluctuating selection as it currently stands, summarising recent evidence from natural populations and experimental studies, examining new theoretical models, and discussing these findings and their implications in the context of wider population genetic theory. This published review also highlights the gaps remaining in our current knowledge, some of which are filled by the following studies in this thesis.

Chapter 2 - Population genetic simulation: Benchmarking frameworks for non-standard models of natural selection.

The work in this thesis is conducted using population genetic simulation to explore seasonally fluctuating selection, a non-standard model of natural selection. This chapter explores simulation workflows that allow for the simulation of complex models of selection while also comparing the computational resource usage of each approach.

Chapter 3 - Discerning the genetic footprints of seasonal fluctuating selection: A comparison with established selection forms.

In my third thesis chapter, I simulate single-locus seasonally fluctuating selection to elucidate the signatures of this form of selection using population genetic statistics including diversity, site frequency spectrum, and haplotype-based statistics. I then compare this with common forms of balancing and positive selection to determine if fluctuating selection can be discriminated for these types of selection using population genetic statistics. This study provides a detailed understanding of the effect of fluctuating selection on linked neutral variation and how this differs from more common and well-understood forms of selection (i.e. positive and balancing selection).

Chapter 4 - The effect of fluctuating selection on effective population size.

This chapter investigates the effect of seasonally fluctuating selection on effective population size (N_e), a key parameter in population genetics and conservation. It has previously been proposed, based on theoretical modelling, that fluctuating selection can lead to a wide-ranging decrease in diversity even at regions that are unlinked from any selected sites. Diversity is a commonly used indicator of effective population size, but the direct influence of fluctuating selection on effective population size has yet to be quantified. In this chapter, I explore multilocus seasonally fluctuating selection and examine the impacts on variance effective population size using realistic model parameters derived from empirical *Drosophila* data. I discuss the findings in relation to the resolution of Lewontin's Paradox, the observation that the variance in diversity (and effective population size) across species is orders of magnitude smaller than the variance in census population size.

References

Andrés AM et al. 2009. Targets of balancing selection in the human genome. Mol. Biol. Evol. 26:2755–2764. doi: 10.1093/molbev/msp190.

Barton NH. 2000. Genetic hitchhiking. Phil. Trans. R. Soc. Lond. B. 355:1553–1562. doi: 10.1098/rstb.2000.0716.

Baumdicker F et al. 2022. Efficient ancestry and mutation simulation with msprime 1.0. Genetics. 220. doi: 10.1093/genetics/iyab229.

Behrman EL, Schmidt P. 2022. How predictable is rapid evolution? bioRxiv. 2022.10.27.514123. doi: 10.1101/2022.10.27.514123.

Bell G. 2010. Fluctuating selection: The perpetual renewal of adaptation in variable environments. Philos. Trans. R. Soc. Lond. B Biol. Sci. 365:87–97. doi: 10.1098/rstb.2009.0150.

Bergland AO, Behrman EL, O'Brien KR, Schmidt PS, Petrov DA. 2014. Genomic evidence of rapid and stable adaptive oscillations over seasonal time scales in Drosophila. PLoS Genet. 10:e1004775. doi: 10.1371/journal.pgen.1004775.

Bertram J, Masel J. 2019. Different mechanisms drive the maintenance of polymorphism at loci subject to strong versus weak fluctuating selection. Evolution. 73:883–896. doi:

10.1111/evo.13719.

Bitarello BD et al. 2018. Signatures of long-term balancing selection in human genomes. Genome Biol. Evol. 10:939–955. doi: 10.1093/gbe/evy054.

Bitarello BD, Brandt DYC, Meyer D, Andrés AM. 2023. Inferring balancing selection from genome-scale data. Genome Biol. Evol. 15. doi: 10.1093/gbe/evad032.

Bitter MC et al. 2023. Continuously fluctuating selection reveals extreme granularity and parallelism of adaptive tracking. bioRxiv. 2023.10.16.562586. doi: 10.1101/2023.10.16.562586.

Busoms S et al. 2018. Fluctuating selection on migrant adaptive sodium transporter alleles in coastal Arabidopsis thaliana. Proc. Natl. Acad. Sci. U.S.A. 115:E12443–E12452. doi: 10.1073/pnas.1816964115.

Chapman JR, Hill T, Unckless RL. 2019. Balancing selection drives the maintenance of genetic variation in Drosophila antimicrobial peptides. Genome Biol. Evol. 11:2691–2701. doi: 10.1093/gbe/evz191.

Charlesworth B. 2012. The role of background selection in shaping patterns of molecular evolution and variation: evidence from variability on the Drosophila X chromosome. Genetics. 191:233–246. doi: 10.1534/genetics.111.138073.

Charlesworth B, Morgan MT, Charlesworth D. 1993. The effect of deleterious mutations on neutral molecular variation. Genetics. 134:1289–1303. doi: 10.1093/genetics/134.4.1289.

Comeron JM. 2014. Background selection as baseline for nucleotide variation across the Drosophila genome. PLoS Genet. 10:e1004434. doi: 10.1371/journal.pgen.1004434.

Coop G, Ralph P. 2012. Patterns of neutral diversity under general models of selective sweeps. Genetics. 192:205–224. doi: 10.1534/genetics.112.141861.

Darwin C. 1859. *On the Origin of Species by Means of Natural Selection Or the Preservation of Favoured Races in the Struggle for Life*. H. Milford; Oxford University.

Fay JC, Wu CI. 2000. Hitchhiking under positive Darwinian selection. Genetics. 155:1405–1413. doi: 10.1093/genetics/155.3.1405.

Fisher RA. 1930. *The genetical theory of natural selection*. The Clarendon Press: Oxford.

Fisher RA, Ford EB. 1947. The spread of a gene in natural conditions in a colony of the moth Panaxia dominula L. Heredity. 1:143–174. doi: 10.1038/hdy.1947.11.

Ford EB. 1937. Problems of heredity in the Lepidoptera. Biol. Rev. Camb. Philos. Soc. 12:461–501. doi: 10.1111/j.1469-185X.1937.tb00642.x.

Garcia-Elfring A et al. 2021. Using seasonal genomic changes to understand historical adaptation to new environments: Parallel selection on stickleback in highly-variable estuaries. Mol. Ecol. 30:2054–2064. doi: 10.1111/mec.15879.

Garud NR, Messer PW, Buzbas EO, Petrov DA. 2015. Recent selective sweeps in North

American Drosophila melanogaster show signatures of soft sweeps. PLoS Genet. 11:e1005004. doi: 10.1371/journal.pgen.1005004.

Garud NR, Rosenberg NA. 2015. Enhancing the mathematical properties of new haplotype homozygosity statistics for the detection of selective sweeps. Theor. Popul. Biol. 102:94–101. doi: 10.1016/j.tpb.2015.04.001.

Gillespie JH. 1997. Junk ain't what junk does: Neutral alleles in a selected context. Gene. 205:291–299. doi: 10.1016/s0378-1119(97)00470-8.

Gillespie JH. 1991. *The causes of molecular evolution*. Oxford University Press.

Haldane JBS, Jayakar SD. 1963. Polymorphism due to selection of varying direction. J. Genet. 58:237–242. doi: 10.1007/BF02986143.

Haller BC, Messer PW. 2023. SLiM 4: Multispecies eco-evolutionary modeling. Am. Nat. 201:E127–E139. doi: 10.1086/723601.

Harris M, Garud NR. 2023. Enrichment of hard sweeps on the X chromosome in Drosophila melanogaster. Mol. Biol. Evol. 40. doi: 10.1093/molbev/msac268.

Hedrick PW. 2007. Balancing selection. Curr. Biol. 17:R230–R231. doi: 10.1016/j.cub.2007.01.012.

Hedrick PW, Ginevan ME, Ewing EP. 1976. Genetic polymorphism in heterogeneous environments. Annu. Rev. Ecol. Syst. 7:1–32. doi: 10.1146/annurev.es.07.110176.000245.

Hermisson J, Pennings PS. 2017. Soft sweeps and beyond: Understanding the patterns and probabilities of selection footprints under rapid adaptation. Methods Ecol. Evol. 8:700–716. doi: 10.1111/2041-210X.12808.

Hudson RR, Kaplan NL. 1995. Deleterious background selection with recombination. Genetics. 141:1605–1617. doi: 10.1093/genetics/141.4.1605.

Huerta-Sanchez E, Durrett R, Bustamante CD. 2008. Population genetics of polymorphism and divergence under fluctuating selection. Genetics. 178:325–337. doi: 10.1534/genetics.107.073361.

Jagoda E et al. 2018. Disentangling immediate adaptive introgression from selection on standing introgressed variation in humans. Mol. Biol. Evol. 35:623–630. doi: 10.1093/molbev/msx314.

Kelly JK. 2022. The genomic scale of fluctuating selection in a natural plant population. Evol Lett. 6:506–521. doi: 10.1002/evl3.308.

Key FM, Teixeira JC, de Filippo C, Andrés AM. 2014. Advantageous diversity maintained by balancing selection in humans. Curr. Opin. Genet. Dev. 29:45–51. doi: 10.1016/j.gde.2014.08.001.

Kim Y. 2023. Partial protection from fluctuating selection leads to evolution towards wider population size fluctuation and a novel mechanism of balancing selection. Proc. Biol. Sci. 290:20230822. doi: 10.1098/rspb.2023.0822.

Ludwig A et al. 2015. Twenty-five thousand years of fluctuating selection on leopard complex spotting and congenital night blindness in horses. Philos. Trans. R. Soc. Lond. B Biol. Sci. 370:20130386. doi: 10.1098/rstb.2013.0386.

Lynch M, Wei W, Ye Z, Pfrender ME. 2023. The genome-wide signature of short-term temporal selection. bioRxiv. 2023.04.28.538790. doi: 10.1101/2023.04.28.538790.

Machado HE et al. 2021. Broad geographic sampling reveals the shared basis and environmental correlates of seasonal adaptation in Drosophila. eLife. 10:e67577. doi: 10.7554/eLife.67577.

Matheson J, Masel J. 2023. Background selection from unlinked sites causes non-independent evolution of deleterious mutations. bioRxiv. 2022.01.11.475913. doi: 10.1101/2022.01.11.475913.

Mathieson I, Terhorst J. 2022. Direct detection of natural selection in Bronze Age Britain. Genome Res. 2022.03.14.484330. doi: 10.1101/2022.03.14.484330.

Mathieson S, Mathieson I. 2018. FADS1 and the timing of human adaptation to agriculture Heyer, E, editor. Mol. Biol. Evol. 35:2957–2970. doi: 10.1093/molbev/msy180.

Nunez JCB et al. 2023. A cosmopolitan inversion facilitates seasonal adaptation in overwintering Drosophila. Genetics. doi: 10.1093/genetics/iyad207.

Park Y, Kim Y. 2019. Partial protection from cyclical selection generates a high level of polymorphism at multiple non-neutral sites. Evolution. 73:1564–1577. doi: 10.1111/evo.13792.

Petersen L, Bollback JP, Dimmic M, Hubisz M, Nielsen R. 2007. Genes under positive selection in Escherichia coli. Genome Res. 17:1336–1343. doi: 10.1101/gr.6254707.

Pfenninger M, Foucault Q. 2022. Population genomic time series data of a natural population suggests adaptive tracking of fluctuating environmental changes. Integr. Comp. Biol. doi: 10.1093/icb/icac098.

Pfenninger M, Foucault Q, Waldvogel A-M, Feldmeyer B. 2022. Selective effects of a short transient environmental fluctuation on a natural population. Mol. Ecol. doi: 10.1101/2022.02.10.479864.

Pritchard JK, Pickrell JK, Coop G. 2010. The genetics of human adaptation: hard sweeps, soft sweeps, and polygenic adaptation. Curr. Biol. 20:R208–R215. doi: 10.1016/j.cub.2009.11.055.

Rudman SM et al. 2022. Direct observation of adaptive tracking on ecological time scales in *Drosophila*. Science. 375:eabj7484. doi: 10.1126/science.abj7484.

Sellis D, Callahan BJ, Petrov DA, Messer PW. 2011. Heterozygote advantage as a natural consequence of adaptation in diploids. Proc. Natl. Acad. Sci. U.S.A. 108:20666–20671. doi: 10.1073/pnas.1114573108.

Smith JM, Haigh J. 1974. The hitch-hiking effect of a favourable gene. Genet. Res. 23:23–35. doi: 10.1017/S0016672300014634.

Souilmi Y et al. 2022. Admixture has obscured signals of historical hard sweeps in humans. Nat. Ecol. Evol. 1–13. doi: 10.1038/s41559-022-01914-9.

Tajima F. 1983. Evolutionary relationship of DNA sequences in finite populations. Genetics. 105:437–460. doi: 10.1093/genetics/105.2.437.

Tajima F. 1989. Statistical method for testing the neutral mutation hypothesis by DNA polymorphism. Genetics. 123:585–595. doi: 10.1093/genetics/123.3.585.

Taylor JE. 2013. The effect of fluctuating selection on the genealogy at a linked site. Theor. Popul. Biol. 87:34–50. doi: 10.1016/j.tpb.2013.03.004.

Tian D, Araki H, Stahl E, Bergelson J, Kreitman M. 2002. Signature of balancing selection in Arabidopsis. Proc. Natl. Acad. Sci. U.S.A. 99:11525–11530. doi: 10.1073/pnas.172203599.

Tutt JW. 1891. *Melanism and melanochroism in British Lepidoptera*. S. Sonnenschein and Company.

Watterson GA. 1975. On the number of segregating sites in genetical models without recombination. Theor. Popul. Biol. 7:256–276. doi: 10.1016/0040-5809(75)90020-9.

Wittmann MJ, Bergland AO, Feldman MW, Schmidt PS, Petrov DA. 2017. Seasonally fluctuating selection can maintain polymorphism at many loci via segregation lift. Proc. Natl. Acad. Sci. U.S.A. 114:E9932–E9941. doi: 10.1073/pnas.1702994114.

Wittmann MJ, Mousset S, Hermisson J. 2023. Modeling the genetic footprint of fluctuating balancing selection: From the local to the genomic scale. Genetics. 223. doi: 10.1093/genetics/iyad022.

Yair S, Lee KM, Coop G. 2021. The timing of human adaptation from Neanderthal introgression. Genetics. 218:iyab052. doi: 10.1093/genetics/iyab052.

Zhong L, Zhu Y, Olsen KM. 2022. Hard versus soft selective sweeps during domestication and improvement in soybean. Mol. Ecol. 31:3137–3153. doi: 10.1111/mec.16454.

Chapter 1

Fluctuating selection and the determinants of genetic variation

Statement of Authorship

Title of Paper	Fluctuating selection and the determinants of genetic variation
Publication Status	[X] Published [ ] Accepted for Publication [ ] Submitted for Publication [ ] Unpublished and Unsubmitted work written in manuscript style
Publication Details	Johnson, Olivia L., Raymond Tobler, Joshua M. Schmidt, and Christian D. Huber. 2023. "Fluctuating Selection and the Determinants of Genetic Variation." Trends in Genetics 39 (6): 491–504. https://doi.org/10.1016/j.tig.2023.02.004.

Principal Author

Name of Principal Author (Candidate)	Olivia L. Johnson
Contribution to the Paper	Conceptualisation, reviewed literature, interpretation, and wrote the manuscript.
Overall percentage (%)	70%
Certification:	This paper reports on original research I conducted during the period of my Higher Degree by Research candidature and is not subject to any obligations or contractual agreements with a third party that would constrain its inclusion in this thesis. I am the primary author of this paper.
Signature	Date: 08/01/2024

Co-Author Contributions

By signing the Statement of Authorship, each author certifies that:

i. the candidate's stated contribution to the publication is accurate (as detailed above);

ii. permission is granted for the candidate in include the publication in the thesis; and

iii. the sum of all co-author contributions is equal to 100% less the candidate's stated contribution.

Name of Co-Author	Christian D. Huber
Contribution to the Paper	Conceptualisation, reviewed literature, interpretation, wrote the manuscript, and acted as corresponding author.
Signature	Date: 08/01/2024

Name of Co-Author	Raymond Tobler
Contribution to the Paper	Conceptualisation, reviewed literature, interpretation, wrote the manuscript.
Signature	Date: 08/01/24

Name of Co-Author	Joshua M. Schmidt
Contribution to the Paper	Conceptualisation, reviewed literature, interpretation, wrote the manuscript.
Signature	Date: 09/01/24

Trends in Genetics

CellPress OPEN ACCESS

Review

Fluctuating selection and the determinants of genetic variation

Olivia L. Johnson,[1] Raymond Tobler,[1,2] Joshua M. Schmidt,[3] and Christian D. Huber[1,4,*]

Recent studies of cosmopolitan *Drosophila* populations have found hundreds to thousands of genetic loci with seasonally fluctuating allele frequencies, bringing temporally fluctuating selection to the forefront of the historical debate surrounding the maintenance of genetic variation in natural populations. Numerous mechanisms have been explored in this longstanding area of research, but these exciting empirical findings have prompted several recent theoretical and experimental studies that seek to better understand the drivers, dynamics, and genome-wide influence of fluctuating selection. In this review, we evaluate the latest evidence for multilocus fluctuating selection in *Drosophila* and other taxa, highlighting the role of potential genetic and ecological mechanisms in maintaining these loci and their impacts on neutral genetic variation.

Highlights

Recent observations of seasonally fluctuating allele frequencies at hundreds to thousands of loci across the genome in cosmopolitan *Drosophila* populations have highlighted fluctuating selection as a potentially important factor in the maintenance of genetic variation in natural populations.

Empirical evidence also suggests that fluctuating selection may influence genetic diversity across large portions of the genome through linkage.

Several single and multilocus theoretical treatments have been presented for fluctuating selection over the past decades, but these models have not been evaluated in light of these recent empirical findings.

We highlight evidence of fluctuating selection in species beyond *Drosophila* and explore potential causal genetic and ecological mechanisms.

The combined evidence suggests that fluctuating selection will need to be incorporated in future population genetic models that seek to understand variation in genetic diversity across species.

The maintenance of genetic variation

Determining the mechanisms responsible for maintaining genetic variation in natural populations has been a central goal of evolutionary biologists for more than a century [1]. In the past decade, the availability of population genomic datasets for numerous species has allowed this question to be directly evaluated in natural populations, reigniting historical debates regarding the role of **genetic drift** (see Glossary) and natural selection as the predominant evolutionary mechanisms shaping population genetic diversity (Box 1). Among the more intriguing findings has been the discovery that hundreds to thousands of polymorphic loci in cosmopolitan *Drosophila melanogaster* populations appear to be maintained by selection pressures that oscillate across seasons [2,3]. This has revived interest in the contribution of **fluctuating selection** to the maintenance of genetic variation within populations and the genetic and ecological factors that underlie it [4–7]. Here we examine recent empirical evidence for multilocus temporally fluctuating selection in natural and experimental populations and evaluate a range of theoretical treatments to provide an overview of recent developments in this area while highlighting the importance of these findings for the age-old question, what maintains genetic variation in natural populations?

Evidence of seasonally fluctuating selection in natural populations

Early field studies of fluctuating selection utilized phenotype observations as proxies for changes in underlying gene frequencies [8]. For instance, Fisher and Ford's classic 1947 study showed that different morphs in a natural population of the scarlet tiger moth, *Panaxia dominula*, were 'affected by selective action varying from time to time in direction and intensity, and of sufficient magnitude to cause fluctuating variation in all gene-ratios' to an extent that could not be attributed to genetic drift [9]. The development of genomic sequencing technologies in the past few decades has facilitated the direct discovery of fluctuating selection at the molecular level, with studies having used allele frequency time-series data to identify fluctuating selection acting at a single locus [10] and multiple loci [2,3,11–13] in natural populations.

[1]Australian Centre for Ancient DNA, School of Biological Sciences, University of Adelaide, Adelaide, Australia
[2]Evolution of Cultural Diversity Initiative, The Australian National University, Canberra, Australia
[3]Flinders Health and Medical Research Institute (FHMRI) Eye and Vision, Flinders University, Bedford Park, Adelaide, Australia
[4]Department of Biology, Pennsylvania State University, University Park, PA, USA

*Correspondence:
cdh5313@psu.edu (C.D. Huber).

Box 1. Evolutionary causes of population genetic diversity

The first empirical evaluations of population genetic variation in 1966 used **allozyme** assays in fruit flies [49] and humans [78] to reveal surprisingly high levels of segregating genetic variation in both species, eventually prompting the development of the Neutral Theory of Molecular Evolution [79,80]. The Neutral Theory asserts that newly arising beneficial mutations are exceedingly rare relative to neutral variants, such that levels of standing genetic variation are predominantly shaped by genetic drift rather than positive selection. Later revisions of the Neutral Theory argued that the key determinant of neutrality is the strength of selection acting on a variant relative to the effective population size [81], thereby broadening the role of genetic drift to include weakly selected mutations.

An alternative to the Neutral Theory states that levels of genetic diversity can be largely explained by the action of selection on functional variants and its effects on neutral variation linked to the selected sites [64,82–84]. Such models typically consider positive and background selection [57,84] but also balancing selection [85]. Balancing selection is a form of natural selection that maintains allelic diversity at selected loci across generations [60]. Distinct mechanisms for balancing selection include **heterozygote advantage**, **sexually antagonistic selection**, fluctuating selection, and **frequency-dependent selection** [86]. Notably, while many forms of balancing selection result in polymorphisms being maintained at stable equilibrium frequencies [87], both fluctuating and frequency-dependent selection can result in oscillating allele frequencies. To distinguish between these two modes of selection, we note that fluctuating selection is mediated by an alternating environmental variable, such as temperature, resource availability, predator abundance, or population size [88], whereas frequency-dependent selection is conditional on the allele frequency (i.e., the selective value of an allele is causally dependent on its relative abundance rather than the environment).

Population genomic studies have inferred balancing selection in several species, including humans. Estimates of loci under selection have generally been small in number (tens of loci; [89–91]) and largely circumscribed to immune-related genes [92]. However, recent studies using more powerful methods and larger sample sizes suggest that balancing selection, including fluctuating selection, directly maintains hundreds of independent causal loci [2,3,93–95], suggesting a more prominent role for balancing selection in maintaining functional genetic variation than has been previously appreciated.

To date, the strongest empirical evidence for multilocus fluctuating selection at the molecular level comes from studies of *D. melanogaster* populations from temperate North American and European environments. A study of North American *D. melanogaster* conducted by Bergland and colleagues identified approximately 1750 sites fluctuating seasonally from a total of ~500 000 surveyed SNPs (false discovery rate <0.3) in a Pennsylvanian population sampled in the spring and fall seasons across 3 years in succession [2] (Figure 1, Key figure). The frequency of selected loci changed by an average of 20% between spring and fall across the 3 years, equating to selection coefficients of 5–50% per locus per generation. When accounting for the limited statistical power of their study, the authors estimate that the total number of sites that cycle either as a direct result of seasonally fluctuating selection or through linkage to such a site could be ten times the number identified. Bergland and colleagues also found evidence that many seasonal SNPs were shared polymorphisms with *Drosophila simulans*, a sister species to *D. melanogaster* that diverged several million years ago [14], implying that these loci had either been segregating prior to their divergence or are recurrent mutations that are maintained by oscillating seasonal selection pressures over millions of years. Nonetheless, seasonal changes in life history traits measured for *D. simulans* and *D. melanogaster* populations sampled from the same Pennsylvanian orchard showed substantial interspecies differences, suggesting that these putative shared seasonal SNPs may not be maintained by selection pressures that are common to both species [15].

A subsequent study examined allele frequency fluctuations within 20 *D. melanogaster* populations distributed across North America and Europe [3], with Machado and colleagues reporting average shifts of 4–8% and associated selection coefficients of 10–30% per season, among the top 1% (i.e., most significant) of all common ~775 000 SNPs surveyed. Interestingly, the fluctuating SNPs identified by Bergland and colleagues in the Pennsylvanian population were only slightly enriched among the top 1% of SNPs identified in this study, and this enrichment was not statistically significant using a permutation approach (p_{perm} = 0.0512). This discrepancy may be due to the addition of many more populations in the more recent study, leading to increased statistical sensitivity for alleles exhibiting small but consistent seasonal fluctuations across

Glossary

Adaptive tracking: continuous adaptation in response to a rapid environmental change.
Allozyme: enzymes that have the same function but are structurally different.
Antagonistic pleiotropy: when loci contribute to multiple traits with contrasting effects.
Background selection: loss of neutral genetic variations due to negative selection of linked deleterious alleles.
Balancing selection: classically defined as the maintenance of genetic variants at intermediate frequencies over long periods of time. More broadly defined, it is an evolutionary force that leads fitness-affecting variants to segregate within a population longer than expected.
Boom–bust: exponential population growth (boom; summer season) followed by collapse (bust; winter season) where selection on the beneficial summer allele weakens at higher population densities.
Chromosomal inversion: a type of mutation where a segment of DNA has been flipped in place in the genome.
Diminishing-returns epistasis: a form of epistasis where, as more loci with beneficial alleles are present in a genome, there is less fitness advantage gained from each additional beneficial allele.
Dominance: describes the relationship between the phenotype and the genotype at a diploid locus in heterozygotes; quantified by the dominance coefficient d. In this context, $d > 0.5$ indicates that the allele is dominant and masks the alternative allele, whereas $d < 0.5$ indicates that the allele is recessive.
Dominance modifier: an allele, or epigenetic process, that changes the dominance of another locus.
Effective population size (N_e): the hypothetical number of individuals in an idealized Wright–Fisher population that has the same rate of genetic drift as the population of interest.
Fitness: a measure of reproductive success, or the likelihood that an individual or genotype can survive long enough to reproduce or be passed on to the next generation.
Fluctuating selection: when the strength and/or direction of selection shifts over time.
Frequency-dependent selection: where fitness depends on the frequency

Key figure

Detecting loci with seasonally fluctuating allele frequencies

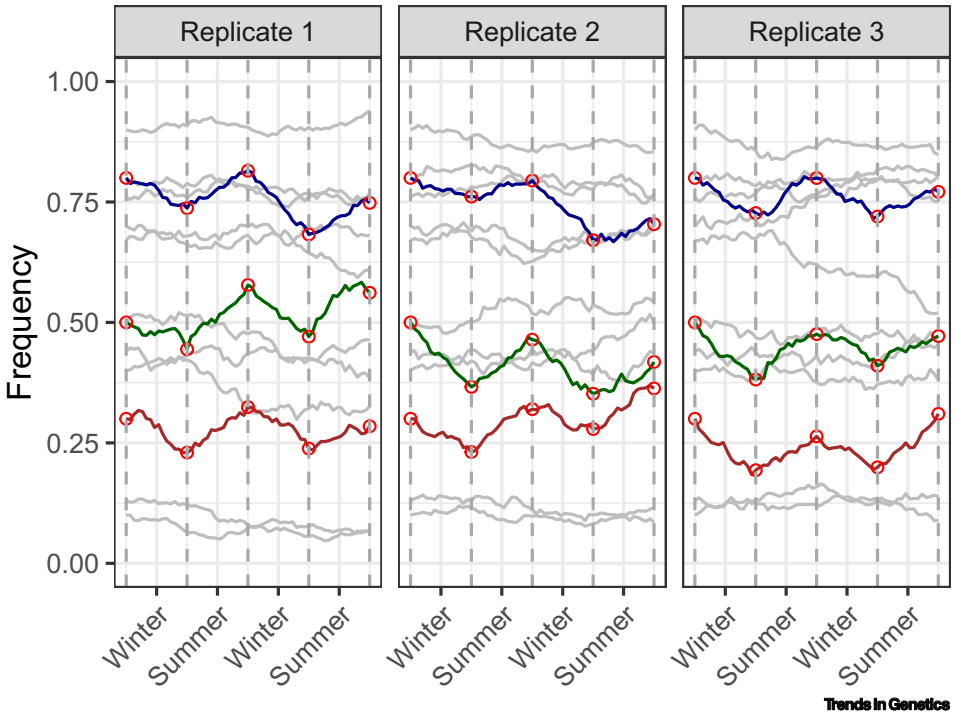

Figure 1. Allele frequency trajectories were simulated under seasonally oscillating selection pressures. Three loci displaying parallel seasonal allele frequency oscillations within replicates (i.e., across years) and between replicates are highlighted (red, green, and blue lines). This repeated seasonal change in frequency across replicates is the underlying pattern used to statistically identify seasonally fluctuating loci. The null hypothesis is that neutral loci unlinked to selected sites (grey trajectories) will not experience such regular seasonal oscillations. Statistical analyses have employed a binomial logit-linked generalized linear model (GLM) that regresses the frequency of each locus on season (i.e., spring and fall) encoded as a dummy variable [2,3,13]. More complex statistical models that account for repeated measures produce similar results [2,3]. The Bergland *et al.* study [2] compared parallel shifts measured across successive seasonal time points, whereas both the Machado *et al.* [3] and the Rudman *et al.* [13] studies had replication at the temporal and population levels. While genetic drift (e.g., grey lines) and migration from neighboring demes violate model assumptions, these were rejected as likely explanations for the observed seasonal frequency fluctuations based on simulations [2]. Statistical models that explicitly account for genetic drift and time-varying selection pressures are under active development and could be applied in the future to more robustly infer selected polymorphisms and quantify the contribution of fluctuating selection to allele frequency changes across the genome [28,108].

the majority of sampled populations (Figure 1), while being less likely to detect seasonal fluctuations that are population-specific[3]. Nonetheless, the study demonstrated that seasonal adaptation is a general phenomenon that impacts numerous loci in temperate fruit fly populations.

D. melanogaster harbors several large **chromosomal inversions** that have been shown to influence adaptive clinal variation across multiple continents [16], suggesting that these structural variants might also contribute to the quantity and dynamics of fluctuating loci reported for this species. However, while an excess of seasonally fluctuating SNPs was found in several different inversions by Machado and colleagues [3], the identity of enriched inversions tends to be

of the phenotype or genotype in the population.

Genetic drift: shifts in allele frequency in a population over time due to random sampling of alleles for the next generation from the gene pool of the current generation.

Geometric mean fitness: the geometric mean of the fitnesses of a genotype across generations. It is the relevant criterion for the maintenance of polymorphism in models with discrete generations.

Harmonic mean fitness: the reciprocal of the mean of the reciprocals of the fitnesses of a genotype across space; a key quantity in models of spatially maintained genetic variation.

Heterozygote advantage: also termed overdominance; when the heterozygote genotype has higher fitness than either homozygous genotype.

Hitchhiking: where the linked flanking regions of loci under selection are carried along with the selected allele to a high frequency.

Positive epistasis: a form of epistasis where fitness benefit per allele increases with each additional beneficial allele across loci.

Positive selection: selection on a genetic variant that confers a beneficial trait in a given environment, causing it to increase in frequency.

Protection from selection: also known as the storage effect; each season, a proportion of the population is replaced by juveniles. The remaining adult individuals are not subject to selection.

Sexually antagonistic selection: when a trait that is favorable in one sex is unfavorable in the other.

Tajima's D: a neutrality test statistic that measures the difference in mean number of pairwise nucleotide differences and the number of segregating sites across a region. Negative values signify an abundance of low-frequency variants, associated with positive selection or population expansion. An excess of intermediate-frequency alleles, associated with balancing selection, population bottlenecks, or structure, results in a positive value.

inconsistent across different studies [3,17,18], and no such enrichment was observed among segregating inversions in the North American *D. melanogaster* population studied by Bergland and colleagues [2]. This suggests that the role of inversions may be strongly dependent on the local population genetic profile.

Attempts to identify the potential environmental pressures underlying the seasonally fluctuating *Drosophila* loci also suggest that local factors may predominate over any shared ecological drivers [2,3,18,19]. For instance, allele frequency changes were well predicted by maximum temperature prior to sampling in a North American *D. melanogaster* population but not in European populations, where average temperature and humidity were better predictors [18]. Accordingly, adaptive seasonal allele fluctuations in *D. melanogaster* appear to be strongly influenced by local genetic and environmental factors that invoke highly population-specific dynamics, and this might partly explain the lack of common candidate seasonal SNPs observed across the different studies.

Experimental validation of rapid seasonal adaptation

Recently, a novel **adaptive tracking** field experiment involving outbred *D. melanogaster* populations was deployed to explicitly evaluate the role of selection in maintaining seasonally oscillating loci and its associated **hitchhiking** effects [13]. The experimental design involved rearing fruit flies in outdoor cages that contained features of a natural orchard – for example, fruit trees, natural ground cover, and insect and microbial community – along with regularly replenished food and egg-laying substrate. This aimed to allow the experiment to capture natural shifts as a result of local ecological features rather than experimental artefacts. Because the experiment was designed to preclude opportunities for gene flow events, all allele frequency changes could be attributed to either genetic drift or selection acting on pre-existing variants. Around 9000 SNPs exhibited significant parallel allele frequency shifts across ten replicated populations measured at multiple points between midsummer and late fall in a single year, with changes ranging from 2% to 8% between consecutive sampling periods and up to 5% when comparing the first and final samples taken during the experiment.

Applying a statistical approach that accounts for linkage among the putatively selected sites resulted in a total of 165 unlinked independent genomic clusters that exhibited parallel directional changes indicative of rapid adaptation to seasonal changes in selection pressures over the year, a pattern consistent with strong fluctuating selection. Remarkably, selection at these loci was inferred to have impacted the frequencies at >60% of the 1.9 million genome-wide SNPs screened during the study. Only three clusters were found to be strongly linked with known inversions, indicating that the seasonal signal seen in this study is not strongly driven by common segregating inversions. Consistent with theoretical results [20,21], simulations under a truncation selection model showed that the observed frequency shifts are feasible despite the large number of independently selected loci (i.e., 4.5 loci per chromosome per month, changing at least 2% in frequency) that are competing against each other [13]. Combined with the two studies of wild *Drosophila* populations, these results provide strong evidence for fluctuating selection targeting at least hundreds of independent loci in *Drosophila* populations in temperate environments. They indicate that fluctuating selection is likely to affect allele frequency changes at linked neutral alleles across a large portion of the genome, and suggest that it also has a major role in shaping genome-wide diversity in these populations. Interestingly, while this study provides further support for multilocus fluctuating selection being a common feature in *Drosophila* populations living in temperate climates, we found no significant overlap between the candidate SNPs reported in Bergland *et al.* [2] and Machado *et al.* [3] and the genomic clusters of Rudman *et al.* [13] (Bergland–Rudman overlap p_{perm} = 0.813, Machado–Rudman overlap p_{perm} = 0.445). While

this lack of overlap suggests that a substantial fraction of the seasonally adapting loci might be population specific and/or temporally constrained (see Outstanding questions), it remains unknown to what extent this lack of replicability was caused by the imperfect mirroring of selection pressures between the experimental regime and natural environments.

Evidence for fluctuating selection beyond *Drosophila*

While most evidence for multilocus fluctuating selection comes from observations of *Drosophila* populations, fluctuating selection has been identified in several other species, suggesting it may be found throughout all life.

A study of non-biting midge (*Chironomus riparius*) over a cold-snap period found evidence of fluctuating selection at 19 SNPs, of which ten were unlinked [12]. Frequency changes of at least 50% were observed for all ten independent SNPs, with all but one returning to their pre-cold-snap frequency after 6 months. **Balancing selection** was inferred at four of the SNPs using **Tajima's D**, with one other SNP showing signs of a recent selective sweep. A separate study of the same species sampled seasonally over 3 years also found that nearly 360 000 SNPs were impacted by selection (among ~22.7 million SNPs), with alleles changing frequency by at least 15% between two consecutive sampling periods or the first and last sampling points. Notably, while some loci were found to switch direction in concert with environmental changes, the majority did not covary with seasonal change [11] (Box 2). Rapid adaptation was also observed in a study of six populations of threespine stickleback (*Gasterosteus aculeatus*) inhabiting bar-built estuaries that undergo seasonal environmental changes due to intermittent connectivity to the ocean. Analyses of pooled sequencing data sampled in spring and fall of 2016 revealed significant parallel allele frequency shifts at thousands of loci across the six populations [22]. Functional enrichment analysis of the candidate genes suggests rapid osmoregulatory adaptation to temporal changes in salinity. Similar patterns were reported for coastal *Arabidopsis thaliana* populations, where alleles conferring differential levels of salinity tolerance were found to be maintained by annual fluctuations in soil salinity levels [23].

Because of a lack of long-term genetic time-series data for most species, direct molecular evidence for fluctuating selection pressures operating over super-seasonal ecological timescales is largely limited to species for which ancient DNA is available. For instance, alleles associated with leopard complex spotting (LP), a speckled coat pattern, were found to fluctuate in frequency in ancient horse genomes between the Late Pleistocene (approximately 17 000 years ago) and the Iron Age [24]. This is suspected to result from waves of artificial selection for the speckled coat pattern favoring the LP allele, which eventually becomes detrimental as LP homozygotes exhibit congenital night blindness. In humans, studies of ancient genomes have revealed that selection pressures often vary over millennial timescales, with some introgressed Neanderthal alleles persisting at low frequencies for tens of thousands of years before being targeted by selection

Box 2. Non-oscillating or aperiodic fluctuating selection

Natural environmental fluctuations can follow periodic cycles (diurnal, seasonal, or pluriannual) but also exhibit random variation or noise that is aperiodic. While such non-oscillatory fluctuations do not exhibit regular temporal changes by nature, they can result in serial changes in the direction of selection (i.e., where the beneficial allele alternates through time) that are sufficiently frequent to preserve genetic variation at the selected locus [8,11]. Accordingly, non-oscillating environmental fluctuations are unlikely to result in the distinct frequency fluctuations observed in *Drosophila* but might still affect genetic diversity and be detected in genetic time-series data. For example, time-series data for the non-biting midge (*Chironomus riparius*) shows non-neutral changes in allele frequency at hundreds of loci across the genome, which cluster in distinct temporal patterns. In this case, seasonal patterns were of relatively minor importance, and only a few temporal patterns could be related to measured environmental variables [11]. Although our review largely focuses on cyclical environmental change, theoretical work on randomly changing adaptive environments has demonstrated that non-oscillatory fluctuations in selection pressures can also maintain genetic polymorphism and phenotypic/genetic variance of quantitative traits under certain conditions [38,85,96].

[25,26]. Similarly, alleles associated with adaptation to agricultural diets were initially introduced into early European farming populations at the start of the Neolithic, but only became strongly selected some 5000 years later in the Bronze Age [27,28]. Furthermore, recent research has demonstrated that causative variants for many human traits and diseases have population-specific effects [29,30], implying the intensity of the underlying selection pressures has changed over time in at least some of the studied populations [31].

Beyond genomic data, evidence for temporally varying selection pressures operating at the phenotypic level has been reported in studies of vertebrate species that measured trait and **fitness** components over time [8]. For example, the strength of selection on breeding dates was estimated for 31 populations of 21 species of birds and mammals, showing that variation in the strength of selection and/or fluctuations of an optimum phenotype had strong statistical support across all taxa [32].

These examples suggest that fluctuations in the strength and direction of selection may be a reasonably common feature for a wide variety of species and that these fluctuations can be tracked through time and are influencing the allele frequency dynamics of many genomic loci. However, in many of these cases, the lack of long-term temporal coverage means that it remains unclear whether the fluctuating selection pressures also alter the direction of selection frequently enough to avoid the fixation of adaptive alleles – a necessary condition to maintain polymorphisms in models of fluctuating selection [33]. In the future, the analysis of ancient DNA datasets covering successive ecological and/or climate cycles and long-term field studies will help improve our understanding of the environmental drivers of fluctuating selection pressures and their temporal characteristics.

Theoretical models of fluctuating selection

Theoretical studies have aimed to evaluate the conditions under which genetic variants are maintained in fluctuating environments. Haldane and Jayakar first proposed a general condition for a temporally fluctuating polymorphism in a biallelic single-locus model [33] where the favored allele alternates across two opposing environments (e.g., hot and cold). Stable polymorphism at a single locus requires the heterozygote to have a greater **geometric mean fitness** than the homozygous alternatives [33]. This contrasts with spatial selection models, where the difference in **harmonic mean fitness** between genotypes is key [34–36]. Since this seminal study by Haldane and Jayakar, fluctuating selection has been explored through models of temporally fluctuating selection coefficients [37] as well as Gillespie's SAS-CFF (stochastic additive scale–concave fitness function) model, which was designed to provide a mechanistic explanation for genetic variation in enzymes [38–48]. The SAS-CFF model uses a SAS to imitate enzyme activity under a random continuous environment, with the enzyme activity being mapped to a CFF. These properties result in random fluctuations in selection pressures (Box 2), which produce stable polymorphic loci when the average effect of each allele is the same and only weakly correlated across different environments [38].

Although a single stable polymorphism can be well explained by these models, extending them to the multilocus case (i.e., potentially explaining the hundreds of fluctuating loci seen in *Drosophila*) is nontrivial [4]. For instance, the evolutionary applicability of genetic models that permit non-additive loci and multiplicative epistasis was questioned for requiring seemingly unrealistic levels of genetic load (i.e., whereby some individuals would have to produce an astronomically large number of offspring to avoid population extinction) [49–51]. By contrast, models of fluctuating selection where loci contribute additively to a trait can maintain polymorphism at only one or two loci [4,52]. Accordingly, multilocus fluctuating selection has long been considered unrealistic as a mechanism for the maintenance of a large number of polymorphic sites [4].

In light of the compelling empirical evidence emerging from population genomic studies of *Drosophila* [2], recent theoretical work has re-evaluated the plausibility of multilocus fluctuating selection by drawing on a wider class of selection models that include various forms of **dominance** and epistasis [4]. In particular, the 'segregation lift' (SL) model proposed by Wittmann and colleagues can maintain polymorphism at hundreds of loci under seasonally oscillating selection pressures without generating unrealistic levels of genetic load (Figure 2) [4]. The SL model decomposes fitness into two parts: (i) the seasonal score (z) contributed by each locus, scaled by a seasonal dominance coefficient; and (ii) a fitness function [$w(z)$] that allows for epistasis across selected loci and is constant across seasons (Figure 2). Both **positive** and **diminishing-returns epistasis** were examined; however, maintenance of long-term fluctuating loci under positive epistasis required that seasonally favored alleles are almost completely dominant (i.e., extreme dominance reversal, Box 3; dominance approaches 1 as the number of loci increases), resulting in large changes in dominance between seasons. By contrast, with diminishing-returns epistasis, more moderate changes in dominance were permissible – as the number of loci increases, permissible dominance values approach 0.5 – making diminishing-returns epistasis more plausible overall [4]. Moreover, beneficial mutations often exhibit diminishing-returns epistasis in empirical studies [53–55].

Wittmann and colleagues also investigated a more complex version of their SL model that allowed dominance and effect sizes of selected loci to take random values that are potentially asymmetric

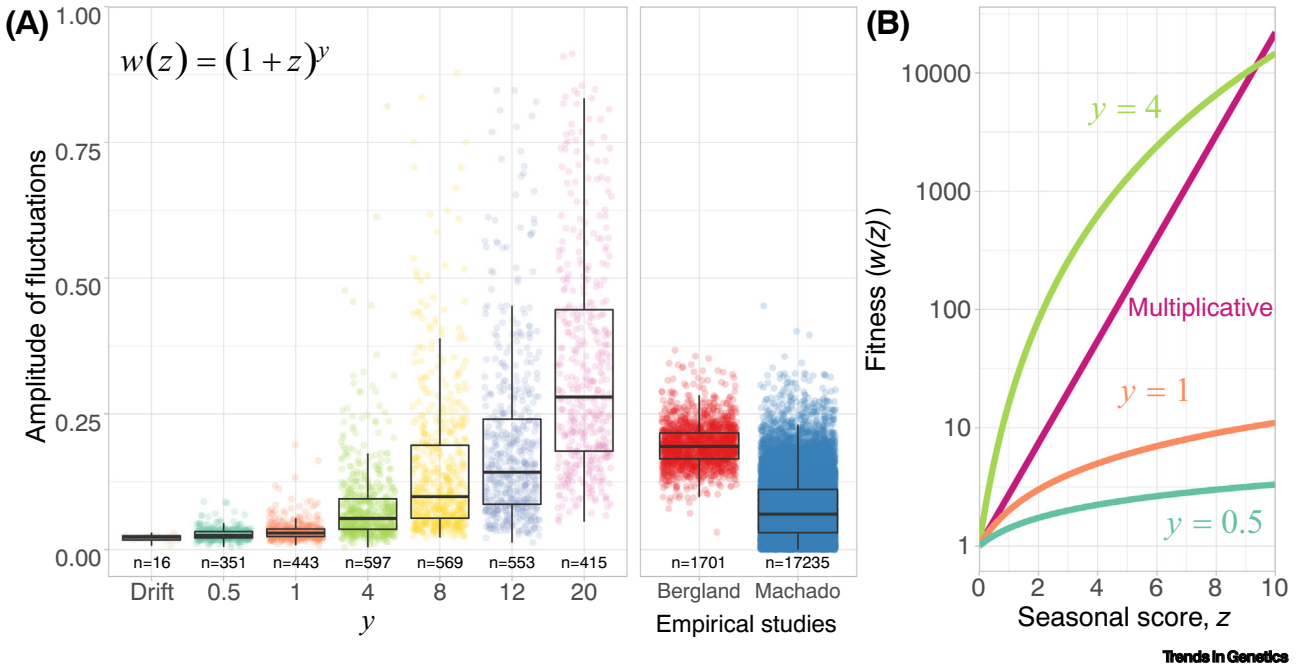

Figure 2. Amplitudes of allele fluctuations from empirical and simulated data. (A) Boxplot of amplitudes of allele frequency fluctuations of unlinked seasonally selected loci under Wittmann and colleagues' complex segregation lift (SL) model [4] with varying epistasis values (y parameter) in a population of 10 000 individuals with ten generations in each season. A total of 1000 loci (ten replicates of 100 loci) were simulated for each y value, with the number of fluctuating loci (i.e., loci still segregating after 90 000 generations) shown beneath each box. All loci have a combined summer and winter dominance greater than 0.5, the critical dominance value for stable fluctuations, which is used to generate the seasonal score [$z = \sum_{l=1}^{L} c_l$, where c_l is the contribution of each locus (i.e., the product of the effect size and the dominance of the locus)]. By varying y, the mean amplitude of the fluctuations can encompass the range of mean amplitudes reported in natural *Drosophila melanogaster* populations by both Bergland *et al.* [2] and Machado *et al.* [3], the distributions of which are shown. X-chromosome SNPs are excluded from the Bergland *et al.* distribution and were not analyzed in the Machado study. (B) Note that, as y increases, epistasis becomes more negative while the strength of per-locus selection increases. This is because log[$w(z)$] is the relevant scale to evaluate epistasis [4].

Box 3. Dominance reversal

The concept of dominance reversal was originally proposed by Sewall Wright in 1915 [97] and has since been discussed primarily in terms of its role in **antagonistic pleiotropy** and sexually antagonistic selection [10,98–104]. Loci characterized under both criteria exhibit fitness trade-offs whereby the fitness effect of an allele switches from positive to negative across environments (with the different sexes being the relevant 'environment' for the latter criterion; Figure I) [98,105]. Dominance reversals can maintain polymorphism at loci exhibiting fitness trade-offs by enabling a net heterozygote advantage; that is, the identity of the beneficial allele alternates across environments but dominance always favors the beneficial allele, sufficiently masking the effects of the deleterious allele in heterozygotes to promote polymorphism [101].

The prevalence of dominance reversal in natural systems remains largely unknown, though it has been observed for polymorphic loci related to salinity tolerance in the copepod *Eurytemora affinis*, with these loci carrying alleles that are simultaneously beneficial and completely dominant in either saltwater or freshwater environments [106]. Dominance reversals have also been observed to impact the expression levels of nearly 1400 different genes in experimental *Drosophila melanogaster* populations evolving under two different temperature regimes, likely as a result of temperature-mediated stress affecting *cis* and *trans* regulation [107]. Around two-thirds of the genes experiencing dominance reversals showed evidence of *trans*-regulatory control, with two of the 13 identified transcription factors also experiencing temperature-dependent dominance reversals themselves [107]. Regulatory mechanisms have also been explored as potential **dominance modifiers** in dominance reversals associated with sexually antagonistic selection, with simulations showing that the regulatory properties of the dominance modifier (in this case, a *cis*-regulatory binding site) induced reverse dominance in allele expression between the sexes [105]. This indicates that dominance reversals are a plausible mechanism in natural populations, although its role in maintaining variation in the presence of fluctuating selection remains to be empirically verified.

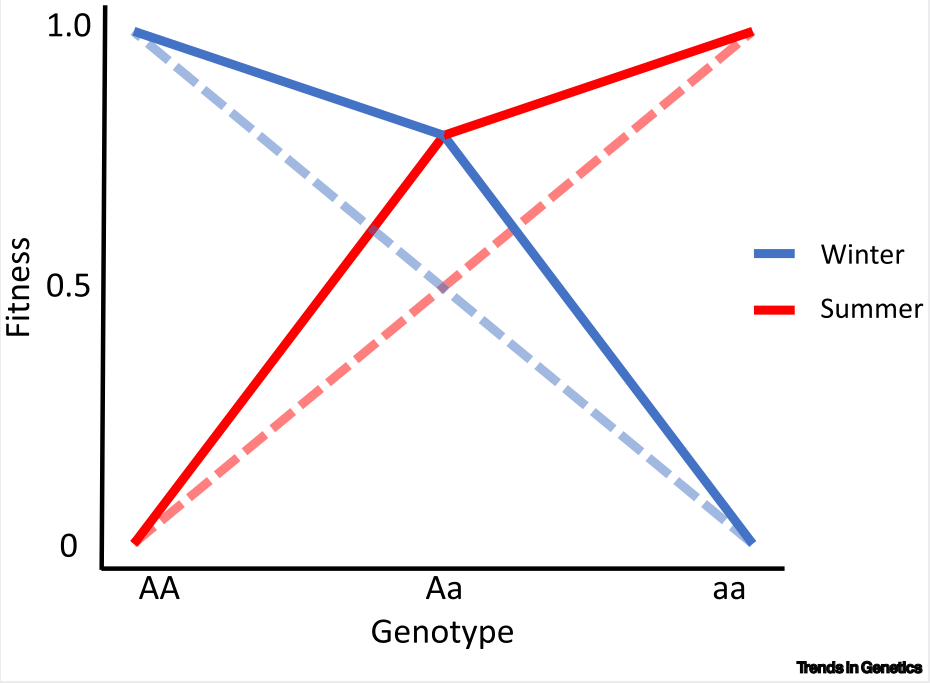

Figure I. Beneficial reversal of dominance in a two-season environment (unbroken lines). The A allele is dominant and beneficial in the winter and becomes recessive and deleterious in the summer. Fitness for the additive case is shown with broken lines. The figure shows symmetrical patterns of dominance across seasons, but it is possible for dominance to be asymmetrical (although the geometric mean fitness across generations of the heterozygote must be larger than that of either homozygote to sustain a polymorphic locus).

across seasons [4]. In this generalized setting, the authors found that stable polymorphisms were possible as long as the arithmetic mean dominance between seasons was greater than 0.5 (i.e., the seasonally favored allele is on average dominant across the two seasons). Accordingly,

the SL model suggests that fluctuating selection can maintain hundreds of polymorphic loci under quite general conditions. Notably, less than 10% of simulated loci were considered detectable (i.e., had shifted 5% in the expected direction in at least half of the evaluated seasons), with these loci typically having the greatest effect size. Even so, by merely varying the epistasis parameter, loci under this model produce allele frequency fluctuations comparable with empirical observations in natural *Drosophila* populations (Figure 2).

Ecological mechanisms for fluctuating selection

Reversal of dominance (Box 3) is fundamental to the SL model: it allows the maintenance of genetic variation without having to assume unrealistically strong selection pressures [6]. Bertram and Masel [6] examined whether ecological mechanisms can also produce balanced polymorphisms in fluctuating environments without having to assume dominance reversal. In conjunction with the genetic mechanism of dominance reversal, they investigated two ecological mechanisms – **boom–bust** demographies and **protection from selection** – both of which are known to lead to low-frequency alleles being favored over high-frequency alleles, a requirement of stable polymorphisms [6]. When modeling the dynamics at a single locus with alleles alternately favored in a binary seasonal environment (i.e., summer and winter), both ecological and genetic mechanisms were capable of stabilizing alleles with strong fitness effects, provided that the effect sizes are relatively similar across seasons (Figure 3). However, only dominance reversal was able to maintain alleles with weak fitness effects. Nonetheless, the authors conclude that both genetic and ecological mechanisms, possibly in combination, may plausibly maintain individual loci exhibiting allele frequency changes consistent with empirical observations in *D. melanogaster* (i.e., where selection pressures are strong). Further, the

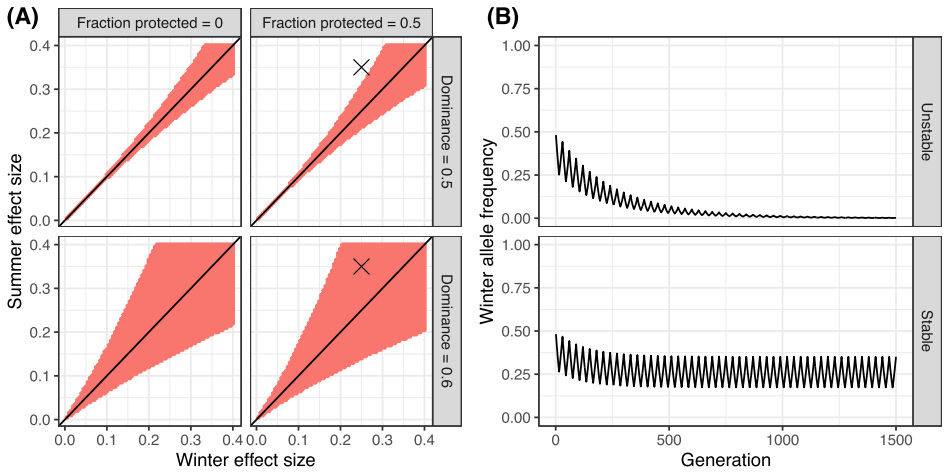

(C)	Summer homozygote	Heterozygote	Winter homozygote
Summer	$\omega_{SS}(S) = 1 + a_s$	$\omega_{SW}(S) = 1 + da_S$	$\omega_{WW}(S) = 1$
Winter	$\omega_{SS}(W) = 1$	$\omega_{SW}(W) = 1 + da_W$	$\omega_{WW}(W) = 1 + a_W$

Trends in Genetics

Figure 3. Protection from selection model. (A) Effect sizes for summer and winter alleles that result in stably fluctuating loci (red region in each subpanel) under different fractions of protection (0, 0.5) and additive (d = 0.5) or reversal of dominance (d = 0.6) models. (B) Allele trajectories when 50% of the population is protected from selection. The black cross in (A) shows the seasonal effect sizes (i.e., both panels: winter = 2.3, summer = 3.5) and dominance values (i.e., top panel = 0.5, bottom panel = 0.6) for the adjacent allele trajectories plotted in (B). (C) Fitness equations used in (A,B), where $a_{s/w}$ represents the fitness benefit of the seasonal allele and d signifies the dominance of the seasonal allele [5,6].

authors suggest that ecological mechanisms widen the scope for temporal variability to balance polymorphism, although the study did not explicitly model multilocus scenarios [6].

The 'protection from selection' mechanism has been extended to the multilocus case in a different study [7] that includes a 'refuge' subpopulation that is protected from cyclically fluctuating selection pressures. This model was shown to maintain a moderate number of selected polymorphisms, but in its current formulation is not able to explain the large number of fluctuating loci observed in North American *Drosophila* [2]. However, it remains to be investigated whether model modifications could promote the maintenance of larger numbers of segregating loci [7], which would demonstrate that dominance reversal is not essential for sustaining hundreds of fluctuating alleles.

Fluctuating selection affects genome-wide diversity

In addition to directly impacting the evolution of selected loci, fluctuating selection may exert considerable influence over surrounding neutral genetic variation. A longstanding debate amongst population geneticists concerns whether the cumulative effects of selection have a major role in determining genome-wide levels of diversity observed within and among different species [56,57]. The genetic hallmarks of **positive** and **background selection** on flanking regions have been well investigated; both selection modes generally reduce levels of linked genetic diversity with the most pronounced reductions occurring in regions with low recombination rates [58,59]. By contrast, classical models of balancing selection lead to an increase in diversity at tightly linked regions but have no effect on diversity in more distant regions [60].

The effect of fluctuating selection on genetic diversity at linked sites is much less well investigated (but see [61–63]). In terms of diversity patterns, fluctuating selection produces signatures consistent with both balancing selection and selective sweeps (i.e., strong positive selection on a single beneficial locus): it increases diversity close to the selected site but decreases diversity further away [5,7,63]. Intriguingly, a fluctuating locus can also diminish genetic variation at unlinked regions (e.g., different chromosomes [5,64]), a consequence of the strong recurrent bottlenecks created by the skewed fitness distribution across individuals after environmental change (whereby the majority of offspring are produced by a small number of individuals [61]). A recent theoretical study suggests that this genome-wide diversity-reducing effect outweighs the increase in diversity in regions tightly linked to the selected sites, predicting a substantial reduction in the diversity in species experiencing strong multilocus fluctuating selection [5]. The scale of this reduction increases with the magnitude of allele frequency fluctuations at the selected loci [5,63], although even small fluctuations can cause large genomic reductions in neutral diversity when their effects aggregate across many loci [5,61].

Importantly, subtle allele frequency fluctuations can be difficult to detect in population genetic data using standard approaches and thus might often be missed or misinterpreted as classical balancing selection. Accordingly, large-sample-size time-series data will be necessary to quantify the abundance and magnitude of fluctuating selection across the genome in various species and to provide insights on the fundamental parameters needed to model its effect on linked neutral diversity. Empirical support for the theoretical predictions comes from an evolve-and-resequence study of *D. melanogaster* populations adapting to either constant or spatially/temporally fluctuating salt and cadmium environments [65]. Among the different regimes, the lowest levels of neutral diversity were found in replicated populations exposed to temporally fluctuating environments, suggesting that the fluctuating regime indeed reduces genome-wide diversity.

In sum, a handful of theoretical and experimental results indicate that fluctuating selection could be a major but currently underappreciated factor shaping levels of genetic diversity in natural

populations. If so, this would have important implications for the resolution of Lewontin's paradox (i.e., the observation that levels of diversity across metazoans vary by only two orders of magnitude while census population sizes vary over several [57,66]). For instance, when exposed to periodically changing environments, species with a large census population size might experience sequential genetic bottlenecks caused by rapid adaptation to changing environments leading to a small local **effective population size (N_e)** (as shown in [18,67] for *Drosophila*), whereas species defined by smaller populations and longer generation times might maintain higher levels of genetic diversity by virtue of being less able to adapt to short-term environmental fluctuations. Therefore, if fluctuating selection is widespread among species, this mechanism could partially resolve Lewontin's paradox by reducing neutral genetic diversity in species in relation to their census population size and generation time [57]. Similarly, fluctuating selection might also contribute to genome-wide levels of linkage disequilibrium (LD) in various species. Indeed, it was suggested that recurrent selection at multiple loci may help to explain the observed excess in long-range LD in natural *D. melanogaster* populations beyond expectations under purely demographic models [68,69].

Concluding remarks and future perspectives

Selection in natural populations is likely to be a dynamic interplay between spatially and temporally varying selection pressures that shape the distribution of functional variation. However, temporally fluctuating selection remains understudied relative to adaptation to spatially heterogeneous environments. Recent results from cosmopolitan *D. melanogaster* populations reporting hundreds to thousands of seasonally selected loci have helped to revive interest in the role of temporally fluctuating selection in adaptation and the maintenance of genetic variation [2,3,13]. Although the concept of fluctuating selection has been around for more than 100 years, only in the past decade have advances in whole-genome sequencing allowed the detection of causal loci and the quantification of their dynamics from genetic time-series data. It is possible that many balanced polymorphisms previously identified in population genetic studies are actually the targets of fluctuating selection rather than examples of classical balanced loci (i.e., where two alleles are maintained at constant frequencies); the similarity of the surrounding genetic footprints left by the two modes of selection is expected to make the two forms difficult to distinguish [5]. Together with evidence of fluctuating selection in a range of species, this suggests that multilocus fluctuating selection may be far more common than previously thought [70]. Accordingly, the development of novel statistical methods to discriminate balanced and fluctuating loci in population genetic studies and the generation of suitable time series datasets for diverse taxa are sorely needed to establish the prevalence and impact of fluctuating selection across the tree of life.

There are still many theoretical and empirical aspects of fluctuating selection and oscillating loci of which we remain largely ignorant (see Outstanding questions). For example, while a significant fraction of fluctuating polymorphisms observed in *D. melanogaster* is shared with sister species *D. simulans* [2], it is plausible that the bulk of these variants are only transient and subject to frequent turnover. This may also explain the lack of overlap in candidate loci between studies of cosmopolitan *D. melanogaster* populations [2,3,13]. Further, the influence of fluctuating selection on genome-wide diversity remains relatively unknown, as previous theoretical and empirical investigations have predominantly focused on the significance of selective sweeps and background selection [59,71]. The recent availability of fast and powerful population genomic simulators [72,73] provides a promising avenue to compare models of fluctuating selection with empirical observations and gain a better understanding of the dynamics at play. In addition, ecological mechanisms remain understudied in the light of recent findings showing that they are a plausible basis for fluctuating loci [6,7], and further investigation is needed to elucidate their role relative to genetic mechanisms like dominance reversal [6].

Outstanding questions

How long are alleles under fluctuating selection typically maintained in natural populations?

How do fluctuating alleles become established? Is it through *de novo* mutation or through introgression from populations in extreme environments?

How prevalent is multilocus fluctuating selection in species other than *Drosophila* and what are the main environmental drivers?

Is there power to discriminate the population genetic signatures of fluctuating selection from those of simple forms of balancing selection or soft selective sweeps?

Is reversal of dominance the main mechanism maintaining alleles under fluctuating selection or do other mechanisms also play a role?

What is the relevance of genes under fluctuating selection for adaptation to massive environmental shifts such as anthropogenic climate change?

To what degree are fluctuating alleles and their environmental pressures shared between species?

Finally, fluctuating selection is potentially an important contributor to genetic variance in fitness. A recent meta-analysis based on an improved statistical approach has proposed that a substantial amount of additive genetic variance in fitness in wild bird and mammal populations had been missed by previous studies, such that additive genetic variance is much larger than previously thought [74]. A substantial fraction of this variance is likely to be maintained by selection [75], with fluctuating selection being a plausible candidate. Ultimately, fluctuating selection might be a major driver of genetic diversity and an important mechanism enabling rapid adaptation to changing climatic conditions and, if so, elucidation of its role will become increasingly relevant for future conservation efforts to protect endangered species [76,77].

Acknowledgments

We thank Meike Wittmann for her helpful comments on the manuscript. C.D.H. was funded by the Australian Research Council's DECRA Fellowship DE180100883, R.T. was funded by Australian Research Council's DECRA Fellowship DE190101069, J.M.S. was funded by the Australian Research Council's Discovery Project DP190103606, and O.L.J. was funded by a Westpac Future Leaders Scholarship and an Australian Government Research Training Program Scholarship.

Declaration of interests

No interests are declared by the authors.

References

1. Clarke, B.C. (1979) The evolution of genetic diversity. *Proc. Biol. Sci.* 205, 453–474
2. Bergland, A.O. *et al.* (2014) Genomic evidence of rapid and stable adaptive oscillations over seasonal time scales in *Drosophila*. *PLoS Genet.* 10, e1004775
3. Machado, H.E. *et al.* (2021) Broad geographic sampling reveals the shared basis and environmental correlates of seasonal adaptation in *Drosophila*. *eLife* 10, e67577
4. Wittmann, M.J. *et al.* (2017) Seasonally fluctuating selection can maintain polymorphism at many loci via segregation lift. *Proc. Natl. Acad. Sci. U. S. A.* 114, E9932–E9941
5. Wittmann, M.J. *et al.* (2022) Modeling the genetic footprint of fluctuating balancing selection: from the local to the genomic scale. *bioRxiv* Published online July 18, 2022. https://doi.org/10.1101/2022.07.15.500223
6. Bertram, J. and Masel, J. (2019) Different mechanisms drive the maintenance of polymorphism at loci subject to strong versus weak fluctuating selection. *Evolution* 73, 883–896
7. Park, Y. and Kim, Y. (2019) Partial protection from cyclical selection generates a high level of polymorphism at multiple non-neutral sites. *Evolution* 73, 1564–1577
8. Bell, G. (2010) Fluctuating selection: the perpetual renewal of adaptation in variable environments. *Philos. Trans. R. Soc. Lond. B Biol. Sci.* 365, 87–97
9. Fisher, R.A. and Ford, E.B. (1947) The spread of a gene in natural conditions in a colony of the moth *Panaxia dominula* L. *Heredity* 1, 143–174
10. Glaser-Schmitt, A. *et al.* (2021) Sexual antagonism, temporally fluctuating selection, and variable dominance affect a regulatory polymorphism in *Drosophila melanogaster*. *Mol. Biol. Evol.* 38, 4891–4907
11. Pfenninger, M. and Foucault, Q. (2022) Population genomic time series data of a natural population suggests adaptive tracking of fluctuating environmental changes. *Integr. Comp. Biol.* 62, 1812–1826
12. Pfenninger, M. *et al.* (2022) Selective effects of a short transient environmental fluctuation on a natural population. *Mol. Ecol.* 32, 335–349
13. Rudman, S.M. *et al.* (2022) Direct observation of adaptive tracking on ecological time scales in *Drosophila*. *Science* 375, eabj7484
14. Tamura, K. *et al.* (2004) Temporal patterns of fruit fly (*Drosophila*) evolution revealed by mutation clocks. *Mol. Biol. Evol.* 21, 36–44
15. Behrman, E.L. *et al.* (2015) Seasonal variation in life history traits in two *Drosophila* species. *J. Evol. Biol.* 28, 1691–1704
16. Kapun, M. and Flatt, T. (2019) The adaptive significance of chromosomal inversion polymorphisms in *Drosophila melanogaster*. *Mol. Ecol.* 28, 1263–1282
17. Kapun, M. *et al.* (2016) Genomic evidence for adaptive inversion clines in *Drosophila melanogaster*. *Mol. Biol. Evol.* 33, 1317–1336
18. Nunez, J.C.B. *et al.* (2022) A cosmopolitan inversion drives seasonal adaptation in overwintering *Drosophila*. *bioRxiv* Published online December 12, 2022. https://doi.org/10.1101/2022.12.09.519676
19. Behrman, E.L. and Schmidt, P. (2022) How predictable is rapid evolution? *bioRxiv* Published online October 28, 2022. https://doi.org/10.1101/2022.10.27.514123
20. Smith, J.M. (1968) "Haldane's dilemma" and the rate of evolution. *Nature* 219, 1114–1116
21. Sved, J.A. (1968) Possible rates of gene substitution in evolution. *Am. Nat.* 102, 283–293
22. Garcia-Elfring, A. *et al.* (2021) Using seasonal genomic changes to understand historical adaptation to new environments: parallel selection on stickleback in highly-variable estuaries. *Mol. Ecol.* 30, 2054–2064
23. Busoms, S. *et al.* (2018) Fluctuating selection on migrant adaptive sodium transporter alleles in coastal *Arabidopsis thaliana*. *Proc. Natl. Acad. Sci. U. S. A.* 115, E12443–E12452
24. Ludwig, A. *et al.* (2015) Twenty-five thousand years of fluctuating selection on leopard complex spotting and congenital night blindness in horses. *Philos. Trans. R. Soc. Lond. Ser. B Biol. Sci.* 370, 20130386
25. Jagoda, E. *et al.* (2018) Disentangling immediate adaptive introgression from selection on standing introgressed variation in humans. *Mol. Biol. Evol.* 35, 623–630
26. Yair, S. *et al.* (2021) The timing of human adaptation from Neanderthal introgression. *Genetics* 218, iyab052
27. Mathieson, S. and Mathieson, I. (2018) FADS1 and the timing of human adaptation to agriculture. *Mol. Biol. Evol.* 35, 2957–2970
28. Mathieson, I. and Terhorst, J. (2022) Direct detection of natural selection in Bronze Age Britain. *Genome Res.* 32, 2057–2067
29. Brown, B.C. *et al.* (2016) Transethnic genetic-correlation estimates from summary statistics. *Am. J. Hum. Genet.* 99, 76–88
30. Galinsky, K.J. *et al.* (2019) Estimating cross-population genetic correlations of causal effect sizes. *Genet. Epidemiol.* 43, 180–188
31. Koch, E.M. and Sunyaev, S.R. (2021) Maintenance of complex trait variation: classic theory and modern data. *Front. Genet.* 12, 763363
32. de Villemereuil, P. *et al.* (2020) Fluctuating optimum and temporally variable selection on breeding date in birds and mammals. *Proc. Natl. Acad. Sci. U. S. A.* 117, 31969–31978

33. Haldane, J.B.S. and Jayakar, S.D. (1963) Polymorphism due to selection of varying direction. *J. Genet.* 58, 237–242
34. Levene, H. (1953) Genetic equilibrium when more than one ecological niche is available. *Am. Nat.* 87, 331–333
35. Hedrick, P.W. *et al.* (1976) Genetic polymorphism in heterogeneous environments. *Annu. Rev. Ecol. Syst.* 7, 1–32
36. Hedrick, P.W. (2006) Genetic polymorphism in heterogeneous environments: the age of genomics. *Annu. Rev. Ecol. Evol. Syst.* 37, 67–93
37. Takahata, N. *et al.* (1975) Effect of temporal fluctuation of selection coefficient on gene frequency in a population. *Proc. Natl. Acad. Sci. U. S. A.* 72, 4541–4545
38. Gillespie, J.H. (1978) A general model to account for enzyme variation in natural populations. V. The SAS-CFF model. *Theor. Popul. Biol.* 14, 1–45
39. Gillespie, J.H. (1979) Molecular evolution and polymorphism in a random environment. *Genetics* 93, 737–754
40. Gillespie, J.H. (1980) The stationary distribution of an asymmetrical model of selection in a random environment. *Theor. Popul. Biol.* 17, 129–140
41. Turelli, M. (1981) Temporally varying selection on multiple alleles: a diffusion analysis. *J. Math. Biol.* 13, 115–129
42. Gillespie, J.H. (1982) A randomized SAS-CFF model of natural selection in a random environment. *Theor. Popul. Biol.* 21, 219–237
43. Gillespie, J.H. (1985) The interaction of genetic drift and mutation with selection in a fluctuating environment. *Theor. Popul. Biol.* 27, 222–237
44. Gillespie, J.H. and Turelli, M. (1989) Genotype–environment interactions and the maintenance of polygenic variation. *Genetics* 121, 129–138
45. Gillespie, J.H. (1994) Substitution processes in molecular evolution. II. Exchangeable models from population genetics. *Evolution* 48, 1101–1113
46. Gillespie, J.H. (1997) Junk ain't what junk does: neutral alleles in a selected context. *Gene* 205, 291–299
47. Gillespie, J.H. (1999) The role of population size in molecular evolution. *Theor. Popul. Biol.* 55, 145–156
48. Schreiber, S.J. (2020) When do factors promoting genetic diversity also promote population persistence? A demographic perspective on Gillespie's SAS-CFF model. *Theor. Popul. Biol.* 133, 141–149
49. Hubby, J.L. and Lewontin, R.C. (1966) A molecular approach to the study of genic heterozygosity in natural populations. I. The number of alleles at different loci in *Drosophila pseudoobscura*. *Genetics* 54, 577–594
50. Agrawal, A.F. and Whitlock, M.C. (2012) Mutation load: the fitness of individuals in populations where deleterious alleles are abundant. *Annu. Rev. Ecol. Evol. Syst.* 43, 115–135
51. Charlesworth, B. (2013) Why we are not dead one hundred times over. *Evolution* 67, 3354–3361
52. Bürger, R. and Gimelfarb, A. (1999) Genetic variation maintained in multilocus models of additive quantitative traits under stabilizing selection. *Genetics* 152, 807–820
53. Chou, H.-H. *et al.* (2011) Diminishing returns epistasis among beneficial mutations decelerates adaptation. *Science* 332, 1190–1192
54. Khan, A.I. *et al.* (2011) Negative epistasis between beneficial mutations in an evolving bacterial population. *Science* 332, 1193–1196
55. Kryazhimskiy, S. *et al.* (2014) Microbial evolution. Global epistasis makes adaptation predictable despite sequence-level stochasticity. *Science* 344, 1519–1522
56. Corbett-Detig, R.B. *et al.* (2015) Natural selection constrains neutral diversity across a wide range of species. *PLoS Biol.* 13, e1002112
57. Buffalo, V. (2021) Quantifying the relationship between genetic diversity and population size suggests natural selection cannot explain Lewontin's paradox. *eLife* 10, e67509
58. Hermisson, J. and Pennings, P.S. (2017) Soft sweeps and beyond: understanding the patterns and probabilities of selection footprints under rapid adaptation. *Methods Ecol. Evol.* 8, 700–716
59. Charlesworth, B. and Jensen, J.D. (2021) Effects of selection at linked sites on patterns of genetic variability. *Annu. Rev. Ecol. Syst.* 52, 177–197
60. Charlesworth, D. (2006) Balancing selection and its effects on sequences in nearby genome regions. *PLoS Genet.* 2, e64
61. Barton, N.H. (2000) Genetic hitchhiking. *Philos. Trans. R. Soc. Lond. B Biol. Sci.* 355, 1553–1562
62. Huerta-Sanchez, E. *et al.* (2008) Population genetics of polymorphism and divergence under fluctuating selection. *Genetics* 178, 325–337
63. Taylor, J.E. (2013) The effect of fluctuating selection on the genealogy at a linked site. *Theor. Popul. Biol.* 87, 34–50
64. Smith, J.M. and Haigh, J. (1974) The hitch-hiking effect of a favourable gene. *Genet. Res.* 23, 23–35
65. Huang, Y. *et al.* (2014) Genome-wide patterns of genetic variation within and among alternative selective regimes. *PLoS Genet.* 10, e1004527
66. Charlesworth, B. and Jensen, J.D. (2022) How can we resolve Lewontin's paradox? *Genome Biol. Evol.* 14, evac096
67. Lange, J.D. *et al.* (2022) A population genomic assessment of three decades of evolution in a natural *Drosophila* population. *Mol. Biol. Evol.* 39, msab368
68. Garud, N.R. *et al.* (2015) Recent selective sweeps in North American *Drosophila melanogaster* show signatures of soft sweeps. *PLoS Genet.* 11, e1005004
69. Garud, N.R. and Petrov, D.A. (2016) Elevated linkage disequilibrium and signatures of soft sweeps are common in *Drosophila melanogaster*. *Genetics* 203, 863–880
70. Messer, P.W. *et al.* (2016) Can population genetics adapt to rapid evolution? *Trends Genet.* 32, 408–418
71. Stephan, W. (2019) Selective sweeps. *Genetics* 211, 5–13
72. Kelleher, J. *et al.* (2018) Efficient pedigree recording for fast population genetics simulation. *PLoS Comput. Biol.* 14, e1006581
73. Haller, B.C. *et al.* (2019) Tree-sequence recording in SliM opens new horizons for forward-time simulation of whole genomes. *Mol. Ecol. Resour.* 19, 552–566
74. Bonnet, T. *et al.* (2022) Genetic variance in fitness indicates rapid contemporary adaptive evolution in wild animals. *Science* 376, 1012–1016
75. Charlesworth, B. (2015) Causes of natural variation in fitness: evidence from studies of *Drosophila* populations. *Proc. Natl. Acad. Sci. U. S. A.* 112, 1662–1669
76. Stern, D.B. and Lee, C.E. (2020) Evolutionary origins of genomic adaptations in an invasive copepod. *Nat. Ecol. Evol.* 4, 1084–1094
77. Teixeira, J.C. and Huber, C.D. (2021) The inflated significance of neutral genetic diversity in conservation genetics. *Proc. Natl. Acad. Sci. U. S. A.* 118, e2015096118
78. Harris, H. (1966) Enzyme polymorphisms in man. *Proc. Biol. Sci.* 164, 298–310
79. Kimura, M. (1968) Evolutionary rate at the molecular level. *Nature* 217, 624–626
80. Kimura, M. (1983) *The neutral theory of molecular evolution*, Cambridge University Press
81. Ohta, T. (1992) The nearly neutral theory of molecular evolution. *Annu. Rev. Ecol. Syst.* 23, 263–286
82. Charlesworth, B. *et al.* (1993) The effect of deleterious mutations on neutral molecular variation. *Genetics* 134, 1289–1303
83. Holderegger, R. *et al.* (2006) Adaptive vs. neutral genetic diversity: implications for landscape genetics. *Landsc. Ecol.* 21, 797–807
84. Kern, A.D. and Hahn, M.W. (2018) The neutral theory in light of natural selection. *Mol. Biol. Evol.* 35, 1366–1371
85. Gillespie, J.H. (1991) *The causes of molecular evolution*, Oxford University Press
86. Fijarczyk, A. and Babik, W. (2015) Detecting balancing selection in genomes: limits and prospects. *Mol. Ecol.* 24, 3529–3545
87. Sellis, D. *et al.* (2011) Heterozygote advantage as a natural consequence of adaptation in diploids. *Proc. Natl. Acad. Sci. U. S. A.* 108, 20666–20671
88. Varpe, Ø. (2017) Life history adaptations to seasonality. *Integr. Comp. Biol.* 57, 943–960
89. Bakker, E.G. *et al.* (2006) A genome-wide survey of R gene polymorphisms in *Arabidopsis*. *Plant Cell* 18, 1803–1818
90. Thomas, J.C. *et al.* (2012) Candidate targets of balancing selection in the genome of *Staphylococcus aureus*. *Mol. Biol. Evol.* 29, 1175–1186

91. Key, F.M. *et al.* (2014) Advantageous diversity maintained by balancing selection in humans. *Curr. Opin. Genet. Dev.* 29, 45–51
92. Hedrick, P.W. (2007) Balancing selection. *Curr. Biol.* 17, R230–R231
93. Siewert, K.M. and Voight, B.F. (2017) Detecting long-term balancing selection using allele frequency correlation. *Mol. Biol. Evol.* 34, 2996–3005
94. Bitarello, B.D. *et al.* (2018) Signatures of long-term balancing selection in human genomes. *Genome Biol. Evol.* 10, 939–955
95. Soni, V. *et al.* (2022) A new test suggests hundreds of amino acid polymorphisms in humans are subject to balancing selection. *PLoS Biol.* 20, e3001645
96. Bull, J.J. (1987) Evolution of phenotypic variance. *Evolution* 41, 303–315
97. Wright, S. (1915) The albino series of allelomorphs in guinea-pigs. *Am. Nat.* 49, 140–148
98. Curtsinger, J.W. *et al.* (1994) Antagonistic pleiotropy, reversal of dominance, and genetic polymorphism. *Am. Nat.* 144, 210–228
99. Barson, N.J. *et al.* (2015) Sex-dependent dominance at a single locus maintains variation in age at maturity in salmon. *Nature* 528, 405–408
100. Grieshop, K. and Arnqvist, G. (2018) Sex-specific dominance reversal of genetic variation for fitness. *PLoS Biol.* 16, e2006810
101. Connallon, T. and Chenoweth, S.F. (2019) Dominance reversals and the maintenance of genetic variation for fitness. *PLoS Biol.* 17, e3000118
102. Ruzicka, F. *et al.* (2019) Genome-wide sexually antagonistic variants reveal long-standing constraints on sexual dimorphism in fruit flies. *PLoS Biol.* 17, e3000244
103. Jardine, M.D. *et al.* (2021) A non-coding indel polymorphism in the fruitless gene of *Drosophila melanogaster* exhibits antagonistically pleiotropic fitness effects. *Proc. Biol. Sci.* 288, 20202958
104. Geeta Arun, M. *et al.* (2021) Experimental evolution reveals sex-specific dominance for surviving bacterial infection in laboratory populations of *Drosophila melanogaster*. *Evol. Lett.* 5, 657–671
105. Grieshop, K. *et al.* (2021) Dominance reversals, antagonistic pleiotropy, and the maintenance of genetic variation. *arXiv* Published online September 3, 2021. https://doi.org/10.48550/arXiv.2109.01571
106. Posavi, M. *et al.* (2014) Testing for beneficial reversal of dominance during salinity shifts in the invasive copepod *Eurytemora affinis*, and implications for the maintenance of genetic variation. *Evolution* 68, 3166–3183
107. Chen, J. *et al.* (2015) Temperature stress mediates decanalization and dominance of gene expression in *Drosophila melanogaster*. *PLoS Genet.* 11, e1004883
108. Buffalo, V. and Coop, G. (2020) Estimating the genome-wide contribution of selection to temporal allele frequency change. *Proc. Natl. Acad. Sci. U. S. A.* 117, 20672–20680

Chapter 2

Population genetic simulation: Benchmarking frameworks for non-standard models of natural selection

Statement of Authorship

Title of Paper	Population genetic simulation: Benchmarking frameworks for non-standard models of natural selection
Publication Status	☐ Published ☒ Accepted for Publication ☐ Submitted for Publication ☐ Unpublished and Unsubmitted w ork w ritten in manuscript style
Publication Details	In press at Molecular Ecology Resources

Principal Author

Name of Principal Author (Candidate)	Olivia Johnson
Contribution to the Paper	Designed the simulation and benchmarking framework, set up and ran the simulations, conducted the analysis of the results, interpreted results, and wrote the manuscript.
Overall percentage (%)	80%
Certification:	This paper reports on original research I conducted during the period of my Higher Degree by Research candidature and is not subject to any obligations or contractual agreements with a third party that would constrain its inclusion in this thesis. I am the primary author of this paper.
Signature	Date 10/01/24

Co-Author Contributions

By signing the Statement of Authorship, each author certifies that:

i. the candidate's stated contribution to the publication is accurate (as detailed above);

ii. permission is granted for the candidate in include the publication in the thesis; and

iii. the sum of all co-author contributions is equal to 100% less the candidate's stated contribution.

Name of Co-Author	Christian Huber
Contribution to the Paper	Designed the simulation and benchmarking framework, conducted the analysis of the results, interpreted results, contributed to writing the manuscript, and acted as corresponding author.
Signature	Date 08/01/2024

Name of Co-Author	Raymond Tobler
Contribution to the Paper	Designed the simulation and benchmarking framework, interpreted results, and contributed to writing the manuscript.
Signature	Date 08/01/24

Name of Co-Author	Joshua M. Schmidt
Contribution to the Paper	Designed the simulation and benchmarking framework, interpreted results, and contributed to writing the manuscript.
Signature	Date 09/01/24

Abstract

Population genetic simulation has emerged as a common tool for investigating increasingly complex evolutionary and demographic models. Software capable of handling high-level model complexity has recently been developed, and the advancement of tree sequence recording now allows simulations to merge the efficiency and genealogical insight of coalescent simulations with the flexibility of forward simulations. However, frameworks utilising these features have not yet been compared and benchmarked. Here we evaluate various simulation workflows using the coalescent simulator msprime and the forward simulator SLiM, to assess resource efficiency and determine an optimal simulation framework. Three aspects were evaluated: 1) the burn-in, to establish an equilibrium level of neutral diversity in the population; 2) the forward simulation, in which temporally fluctuating selection is acting; and 3) the final computation of summary statistics. We provide typical memory and computation time requirements for each step. We find that the fastest framework, a combination of coalescent and forward simulation with tree sequence recording, increases simulation speed by over twenty times compared to classical forward simulations without tree sequence recording, though it does require six times more memory. Overall, using efficient simulation workflows can lead to a substantial improvement when modelling complex evolutionary scenarios – though the optimal framework ultimately depends on the available computational resources.

Introduction

Evolutionary and demographic processes have long been explored using theoretical models [1–3]. While these models have been predominantly examined using analytical methods, simulation approaches have recently become a common companion to such methods and have facilitated the exploration of evolutionary genetic contexts that are not tractable using

conventional analytic approaches [4–7]. Over the last few decades, simulation software has been developed and enhanced to the point that they are now, in principle, easily adaptable to arbitrarily complex population and evolutionary genetic scenarios [8–13]. Although realism is still restricted by the time and memory (random-access memory, RAM) required to simulate a given model, recent advances have increased the capability of simulation software and enabled more efficient use of resources. In the following sections, we provide a brief overview of the two principled means of simulating population genetic models – namely, coalescent simulations and forward simulations [12,14,15] – then introduce the tree sequence data structure [16,17], a recent advance in data recording that allows for the combination of coalescent and forward simulation in a single framework.

Simulation types

There are three main types of numerical approaches available for population genetic studies: forward, coalescent, and resampling [18]. A description of resampling simulations is omitted as it requires empirical data from existing samples, likely to contain non-neutral regions and an unknown selection regime, from which the simulated data is generated. Given that the general aim of simulation in evolutionary genomics is to model specific modes of selection and their effect on the linked neutral background [19–23], this work will instead focus on coalescent and forward simulations.

Forward simulations model population genetic change across successive generations as it advances forward in time. This allows for the exploration of complex events with high levels of ecological and evolutionary realism throughout the simulation, as demographic and selective events can vary across time and space and act heterogeneously across the genome [24]. As forward simulations simulate all individuals across successive generations they can be both time and memory-intensive, particularly because not all individuals contribute to the

subsequent generation and, consequently, most simulated individuals/genomes are not ancestral to those sampled in the present [8,24]. In contrast, coalescent simulations actively reduce computational burden by working backwards in time and only model the genetic ancestry of individuals directly ancestral to a fixed set of individuals sampled in the present. Thus, coalescent simulations start from the sampled individuals and build genealogical trees backwards in time, connecting individual DNA sequences with ancestral lineages until all branches have coalesced to form a single root sequence, which signifies the most recent common genetic ancestor of all sampled individuals [14]. While coalescent models did not accommodate recombination initially, the ancestral recombination graph (ARG) is a form of the coalescent model that includes recombination by allowing for standard ancestry coalescence (i.e. two homologous sequences meeting at a common ancestor) but also recombination-based coalescence (i.e. two contiguous genetic sequences annealing onto a common ancestral background) [25,26]. This results in multiple different genealogies across large DNA sequences, such as chromosomes, each of which represents the ancestry of a distinct recombined segment [14,15,25,26]. This method of genealogical back-tracking means that coalescent simulations are faster and often more efficient than those that move forward in time, as they use an idealised population model to generate the genetic ancestry of individuals that does not require simulating the genetic history of whole populations across all generations [15,18]. Coalescent models also generally assume that new mutations arise independently of the underlying genealogies, which allows mutations to be overlaid once the genealogy has been generated [14,17]. However, while this replicates the expected behaviour of neutral mutations, it is not the case for those that are under selection [27–29]. Accordingly, while it is possible to simulate selection in the coalescent framework, the available models are limited in complexity, with most coalescent simulators only considering selection at a single locus (e.g. [13,30–32]).

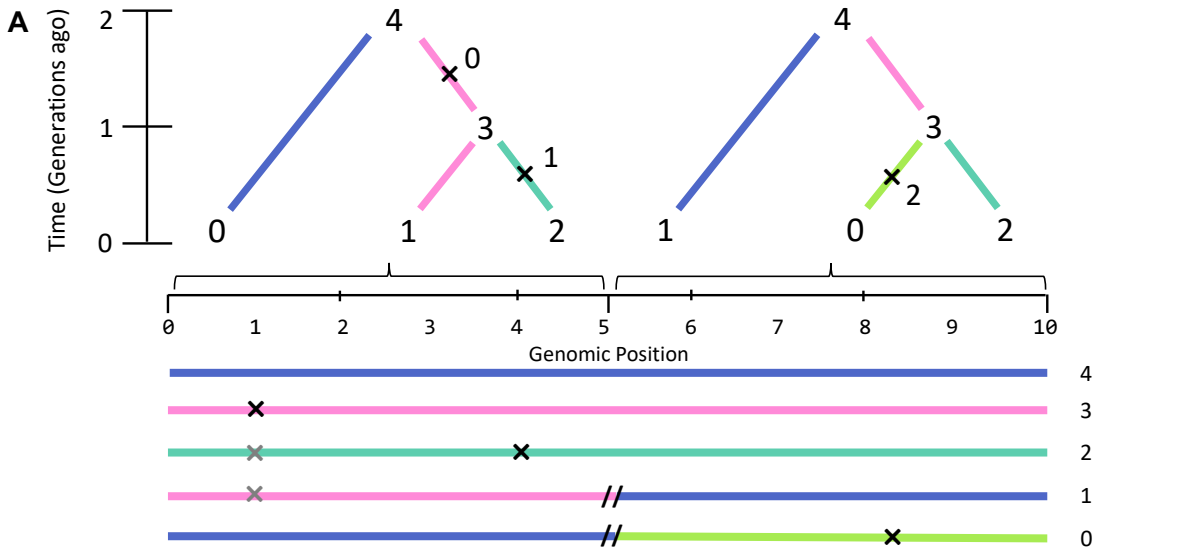

B

Node Table

ID	Time
0	0
1	0
2	0
3	1
4	2

Edge Table

Left	Right	Parent	Child
0	5	4	0
5	10	3	0
0	5	3	1
5	10	4	1
0	10	3	2
0	10	4	3

Site Table

ID	Position	Ancestral State
0	1	A
1	4	C
2	8	T

Mutation Table

ID	Site	Node	Derived State
0	0	3	T
1	1	2	G
2	2	0	A

C

```
#OUT: 3 3 SS p1 3
Mutations:
0  0  m2  1  1  0.6  p1  1  3
1  1  m1  4  0  0.5  p1  2  1
2  2  m1  8  0  0.5  p1  2  1
Individuals:
p1:i0  H  p1:0   p1:3
p1:i1  H  p1:1   p1:4
p1:i2  H  p1:2   p1:4
Genomes:
p1:0  A  2
p1:1  A  0
p1:2  A  0  2
p1:3  A  0
p1:4  A
```

Figure 1. Diagram of genealogy with associated output tree sequence and non-genealogical data.

A Genealogies across a genomic sequence and through time, with time units on the y-axis in generations and branches coloured by the ancestry of the numbered nodes. Mutations are shown by crosses (x) and labelled with their associated ID found in the subsequent tables. Each genealogy derives from a contiguous segment of the genome, with the corresponding genomic coordinates shown on the x-axis. The haploid genomes of each node are shown below, with segments coloured according to their branch. Each node is labelled on the right-hand side of the segment. New mutations introduced to that node are shown in black, whereas inherited mutations are shown in grey. Recombination events are also depicted (//). **B** The tree sequence output consists of a node table, edge table, site table, and mutation table. The values included in these tables correspond to the illustrated genealogy in **A**. This data structure is coloured red or purple throughout the study, depending on the incorporation of neutral mutation. Panel **A** and **B** adapted from Kelleher *et al.* 2018 [17]. **C** An example of non-genealogical output in the form of standard *SLiM* output. This data structure is

coloured in turquoise throughout the study. The header contains information about the output, these values are (left to right): the time (tick and cycle) that the output corresponds to, whether it is an output of the full population (A) or just a sample (SS), the population sampled, and the number of individuals. This is followed by mutation information. Each line is a unique mutation with the associated values being (left to right): a within-file numeric identifier, mutation ID, mutation type, position, selection coefficient, dominance coefficient, the population the mutation arose in, the time it arose and a frequency count. In this example, mutation 0 is under selection, while the others are neutral. The mutation section is followed by information on sampled individuals. This includes the individual ID, the sex if enabled (in this case H for hermaphrodite), and the identifier for the two haploid genomes of the individual. Finally, the genome section contains the genome ID, followed by the chromosome type (A for autosomal), and the identifiers of the mutations in the genome.

The tree sequence

The "succinct tree sequence" is a data structure that captures the genealogy of individuals and recombination events (shown in Figure 1), similar to an Ancestral Recombination Graph (ARG) [15,16]. It can be used in both coalescent and forward simulations and is an efficient way to simulate, store, and analyse genealogical and genetic variation data [15–17,33]. Several simulators use this data structure [10,13,16,34], notably the widely-used coalescent simulator *msprime* [13] and forward simulator *SLiM* [10].

The tree sequence data structure consists of four tables (Figure 1B): a node table, which contains haploid genome information including ID and age; an edge table, that records the branches between distinct ancestor and child nodes (haploid genomes); a site table, which records the ancestral state of sites in the simulated sequence; and a mutation table, which records the position, the derived state, and the first node to inherit each mutation that occurs during the simulation. The tree sequence tables are filled backwards in time in coalescent simulations [15] and chronologically for forward simulations, iterating over all individuals in each generation [17]. For forward simulations, the tree sequence is simplified periodically, removing records of branches that terminate prematurely; this eliminates redundant node and edge information, improving memory efficiency and ensuring the final tree sequence only

contains information relevant to the final population. The efficiency can be further enhanced by delaying the storage of neutral sequence data in the tree sequence. When filling the tree sequence tables using simulations, only non-neutral mutations that will affect the resulting genealogy need to be accounted for, as neutral mutations do not affect genealogical relationships and thus would only slow the simulation with additional data recording and storage burden. Neutral diversity can be added onto the final tree sequence conditional on the local genealogy (i.e. neutral mutations drawn onto branches of the tree after it has been formed) [16,17]. Additionally, summary statistics are efficiently calculable over the tree sequence and these calculations – which utilise the topology and branch lengths of the tree sequence – are often faster than those using allele frequencies [13,15,16]. The tree sequence approach stands in contrast to standard forward simulations, which do not retain genealogical relationship information for sampled individuals [30,35,36]. An example of this non-genealogical format is shown in Figure 1C.

In this study, simulations were run using both coalescent and forwards-in-time simulators to evaluate the efficiency of these methods and their use of tree sequence recording compared to standard simulation practices. Five methods were compared in the generation of a burn-in to establish equilibrium levels and patterns of neutral diversity (see Figure 2); the burn-in was then used as the initial population data for the forward simulation of selection. The primary aim of these simulations is to examine the temporal impact of evolutionary processes on the neutral diversity within a population, necessitating the sampling of individuals at multiple timepoints throughout the forward simulation. As a test model, we implement both single- and multi-locus models of fluctuating selection – a dynamic selection model wherein selection pressures vary over time. This model is challenging to execute with standard simulation software and is introduced as the evolutionary process of interest in these forward simulations (Figure 2). Each aspect of the simulation framework was compared using tree

sequence recording and classical non-genealogical (i.e., sequence-based) methods of simulating data, which simulate neutral mutations in real time rather than overlaying them onto the genealogy after the simulation is complete. Further, the calculation of population genetic statistics using functions that utilise the tree sequence data structure was compared to those that require allele frequency information. Finally, the complete simulation framework was evaluated by benchmarking the time and memory usage across various combinations of simulation programs, data types, and summary statistic calculations. While the classical and tree sequence approaches have been benchmarked previously [16], hybrid approaches using a coalescent burn-in and forward simulation with selection have not yet been compared.

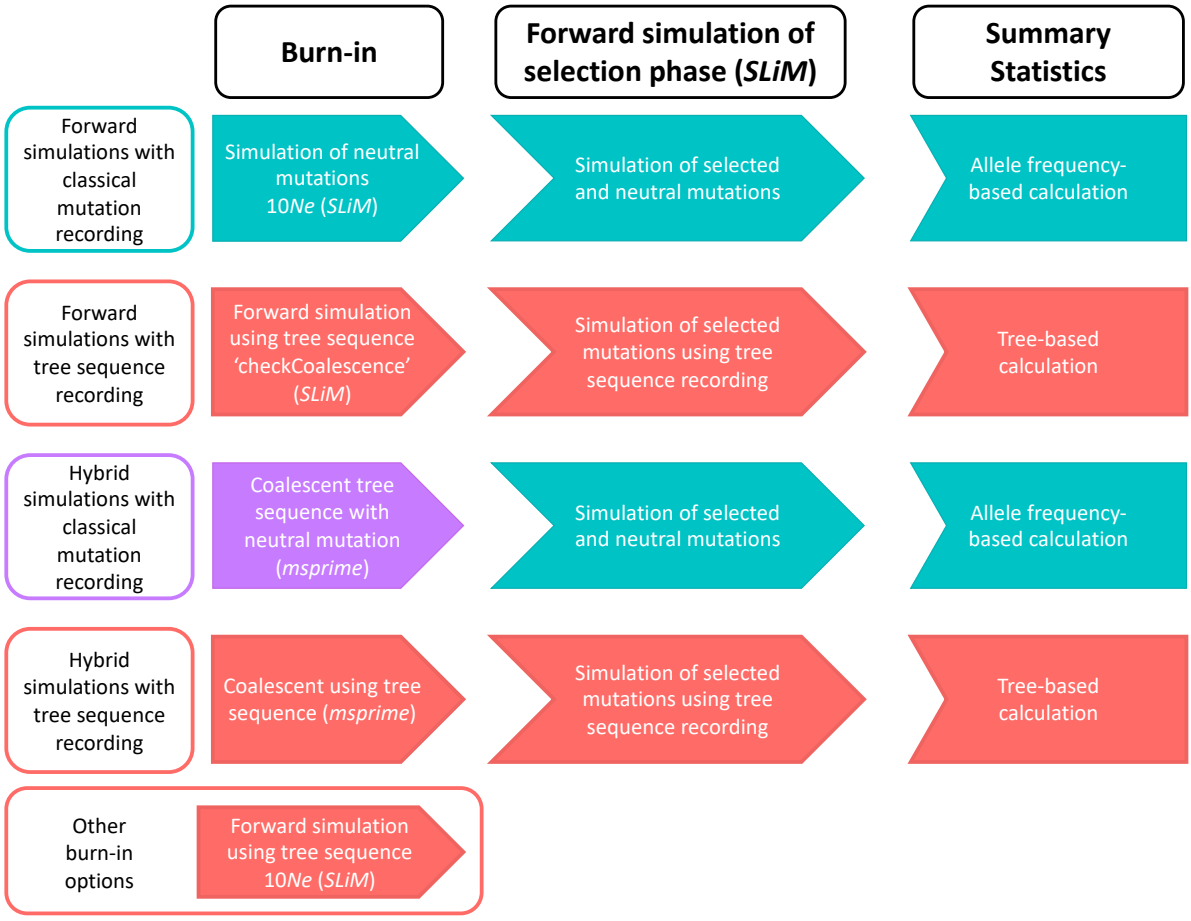

Figure 2. Workflow of the benchmarking tests.

Four primary workflows were examined: The first workflow entailed a classical forward simulation, encompassing a burn-in phase followed by a selection simulation where both neutral and non-neutral mutations were generated. Summary statistics were subsequently derived from the resulting allele frequency data. The second workflow, akin to the first, employed forward simulation for both the burn-in and selection simulation phases; however, tree sequence recording was utilized and only non-neutral mutations were simulated. This allowed the use of the 'checkCoalescence' option in *SLiM* for the burn-in, which guarantees coalescence of all local genealogies across the genome. All simulations in these two workflows were executed solely in *SLiM*. The third and fourth workflows adopted a hybrid approach, commencing with a coalescent burn-in conducted in *msprime*. In the third workflow, neutral mutations were overlaid on the resulting trees and then used to initiate a classical forward simulation. The fourth approach followed the coalescent burn-in with a forward simulation in *SLiM* utilizing tree sequence recording. Summary statistics were calculated using both tree sequence and allele frequency-based calculations. Additionally, a burn-in comprising a forward simulation with tree sequence recording for $10N_e$ generations, where N_e is the effective population size, was also conducted to directly compare the classical and tree sequence approach under the widely used $10N_e$ criterion. The delineated boxes are color-coded based on the data type employed: turquoise for non-genealogical data format, red for the tree sequence data structure, and purple for the tree sequence accompanied by neutral mutation information.

Methods

All simulations were conducted on a MacBook Pro (2.4 GHz 8-Core Intel Core i9 with 64 GB of RAM), using python 3.8.12.

Simulated population context

For all simulations, a 1 megabase (Mb) chromosomal region was simulated, with evolutionary and population genetic parameters reflecting those of a wild *Drosophila melanogaster* population. *D. melanogaster* was chosen because *Drosophilids* have been the focal taxon of research into the population genetics of many different types of selection [37], including temporally fluctuating selection [38–42], a form of selection that displays complex dynamics not easily implemented using standard population genetic simulation software. As *D. melanogaster* has a very large estimated effective population size (N_e), on the order of 1 million individuals [43], population parameters were downscaled in the simulations, and recombination rate (r) and mutation rate (μ) parameters proportionately upscaled. This conserves key compound parameters (e.g. $2N_e r$ and $4N_e \mu$) while expediting run times by avoiding simulating and storing genetic data of 1 million individuals each generation. Accordingly, rescaled population sizes of 10,000 individuals, r of 10^{-6}, and μ of 10^{-7} were simulated to model a *Drosophila* population with a N_e equal to 1 million, r of 10^{-8} [44] and μ of 10^{-9} [45,46], respectively. When scaling population parameters, the selection coefficient must also be appropriately scaled. Hence, we use a scaled selection coefficient of 1 that is equivalent to a selection pressure two orders of magnitude weaker in a natural population (i.e. unscaled $s = 0.01$).

Simulation workflows

Three different aspects of a typical population genetic simulation project were evaluated (Figure 2): 1) the burn-in, to establish an equilibrium level of neutral diversity in the population; 2) the forward simulation, in which selection is acting; and 3) the computation of summary statistics. This study utilises the coalescent simulator *msprime* (v. 1.2.0; [13]) and the forward simulator *SLiM* (v. 4.0.1; [10]) in conjunction with the python programming libraries: *pySLiM* (v. 1.0), to process the tree sequences; and *tskit* (v. 0.5.2), to analyse the tree sequences [13,17,47]. *SLiM* was chosen due to its flexibility, which allows users to customise the simulation by scripting specific evolutionary and demographic events using a range of functions that target these aspects. Similarly, *msprime*, *PySLiM*, and *tskit* are used as they also work with tree sequences and have been integrated with *SLiM*.

To conduct benchmarking, the memory and time requirements of *msprime* and *SLiM* are compared, as well as the efficiency of using the tree sequence data structure compared to the classical forward approach. Memory usage was measured using the python package *tracemalloc*. As this package cannot measure the memory usage of *SLiM*, the peak RAM usage of *SLiM* simulations was measured using an internal function, 'usage(peak = T)', in the software. Following the *SLiM* tree sequence recording benchmarks presented in Haller et al. [16], we conducted 10 replicates of each simulation. Examination of the results revealed that the inter-replicate variance was sufficiently small relative to the absolute values to provide adequately robust estimates (Table S1, S2, S3).

Burn-in

Burn-in simulations are commonly employed in population genetic models to establish equilibrium levels of neutral population genetic diversity prior to the commencement of the phase of empirical interest (e.g. the fluctuating selection phase in the present study). The

difference in resource usage was compared for five different burn-in scenarios that combined the two types of simulations – i.e. the *msprime* coalescent simulator or *SLiM* forward simulations – and two recording scenarios – i.e. with neutral mutations being directly recorded throughout the simulations or tree sequence recording used instead (see Figure 2).

When running burn-ins in *SLiM*, classical forward simulations (i.e. those utilising in-time neutral mutation recording) were run for 100,000 generations, since the number of generations required to achieve sequence-wide coalescence and stable levels of neutral diversity is approximately 10 times the effective population size (N_e) [14,48]. However, recent work suggests that simulating for $10N_e$ generations is not sufficient to ensure coalescence [16,35] and, accordingly, *SLiM* has introduced an option (*checkCoalescence=T*) to check if all lineages have coalesced across the full length of the simulated sequence. Hence, *SLiM* simulated burn-ins that used tree sequence recording were run by either simulating for $10N_e$ generations or until all lineages had confirmed coalescence. Each burn-in approach was replicated 10 times.

Diversity was measured for all burn-in simulations to evaluate if the levels of neutral population genetic variation match theoretical expectations [14]; i.e. $\frac{\theta}{1+\theta}$ where θ is $4N_e\mu$, and μ is the per-generation mutation rate. For *msprime* simulations and *SLiM* tree sequence output, *tskit's* diversity function was used to calculate nucleotide diversity. For the classical simulation approach, diversity was calculated directly in *SLiM* based on allele frequency data using the 'calcHeterozygosity' function. The normality of the diversity distributions for each simulation type was examined using the Shapiro-Wilk test. Because the diversity distribution of some simulation types was not strictly Gaussian, we conducted both t-test and the nonparametric Mann-Whitney U-test to examine if the mean significantly deviates from the neutral expectation. Relative diversity, calculated by dividing the diversity value by the

neutral theoretical expectation ($\frac{\theta}{1+\theta}$), was then compared between the different simulation approaches.

Forward simulation selection models

Next, we evaluated the resource usage of *SLiM* simulations of a complex selection regime – namely, a stable population of 10,000 individuals experiencing a fluctuating selection pressure that oscillates across two seasons, with 10 generations per season – comparing the same two recording options that were used in the burn-ins (i.e. either tree sequence recording or the classical in-time mutation recording).

We explored two models of fluctuating selection, in which selection targeted either a single locus or multiple loci. Both models were replicated 10 times for each data recording method. To simulate single locus selection, we implemented the model proposed by Wittmann and colleagues, who derived fitness equations for genotypes at a seasonal locus (Table 1; [7]). For all simulations conducted using this model, we set the selection coefficient to 1 and the dominance value to 0.6 across both seasons.

Table 1. Fitness equations from Wittmann et al. 2023 used to simulate seasonally fluctuating selection at a single locus.

A fitness equation was used to calculate an individual's fitness (ω) depending on the season (either summer or winter) and the genotype at the seasonal locus (i.e. either WW, SW, or SS, where W denotes the winter-adapted allele and S the summer-adapted allele), by assuming a selection coefficient (s) and a dominance coefficient (h) for each seasonal allele.

Season	ω_{WW}	ω_{SW}	ω_{SS}
Winter	$1 + s_w$	$1 + h_w s_w$	1
Summer	1	$1 + h_s s_s$	$1 + s_s$

For our simulations of multilocus fluctuating selection, we used the following two-part fitness function [38]:

$$z_x = n_x + d_x \times n_{het} \quad [1]$$

$$\omega(z) = (1 + z)^y \quad [2]$$

The first equation is a score (z) that combines the effects of favoured alleles at seasonal loci in a given season (the x subscript in eq. 1 indicates that the season could be either summer or winter). This score comprises the number of loci homozygous for the seasonal allele (n_x) plus the product of the number of sites that are heterozygous for the seasonal allele (n_{het}) and the dominance of that allele (d_x). This score is then incorporated in a fitness function ($\omega(z)$; eq. 2), where y is a coefficient that accounts for epistasis between seasonal loci. For this model, 10 seasonal loci are simulated, each with a dominance value of 0.6 and a y value of 4 for both seasons as this was shown to lead to stable polymorphism [38].

For simulated selection models using a specific recording type (i.e. classical mutation recording or tree sequencing recording), the final population from the burn-in step was used as the initial population for the selection phase. All forward simulations of fluctuating selection were run in *SLiM* for $4N_e$ (40,000) generations, as this provided sufficient time for allele frequencies to reach stable oscillations and is the time required for the stabilisation of genome-wide patterns of neutral diversity under the influence of fluctuating selection [7]. To observe changes in genetic variation over time as selection exerts its effect on linked diversity, 100 individuals were sampled in the first generation after the burn-in, and then every 10,000 generations throughout the simulation. In the final generation, the whole population was sampled. For simulations using tree sequence recording, resource usage calculations also included importing the final tree sequence into python and overlaying

neutral mutations with *msprime*, resulting in neutral and non-neutral mutation information at the conclusion of both simulation workflows.

Calculation of summary statistics

The resource usage involved in the calculation of summary statistics was also tested, with comparisons of functions that either utilise the tree sequence data structure or those that use allele frequency information for estimation. Calculations were performed using *tskit* (v. 0.5.2) [13,17,47] functions on tree sequence data and the python package *scikit-allel* (v. 1.3.5) [49] on allele frequency data from the 10 replicates of each selection model and data recording combination. Tajima's D and nucleotide diversity statistics were calculated using both *tskit* and *scikit-allel,* as both packages have functions to calculate these statistics. The peak memory usage and time required for the calculation of each statistic were recorded as well as the total time, including necessary reformatting steps.

Results

Population genomic simulation is an important tool for exploring and testing the dynamics and consequences of complex evolutionary phenomena. Given the large number of simulations typically required for robust quantification and testing, efficient simulation frameworks are key. Here, a combination of modern simulation approaches are compared to benchmark workflows for population genetic studies of non-standard forms of natural selection.

Burn-in to establish neutral diversity

When comparing the computational efficiency of *msprime* and *SLiM* to run a neutral burn-in, the former was considerably faster than when using either tree sequence recording ($10N_e$ generations or until coalescence is confirmed) or the classical mutation recording approach in

SLiM. *msprime* burn-ins were 40 times faster than those conducted in *SLiM* when simulating for $10N_e$ generations and using tree sequence recording (Figure 3A; Table S1). Overlaying neutral mutations had a negligible impact on runtime, with *msprime* being able to generate ~260,000 mutations in less than a second, including file input and output [13]. The runtime difference between *msprime* and *SLiM* approaches increased to almost 114 times when using the 'checkCoalescence' option for tree sequence recording in *SLiM,* which ensures that all lineages have coalesced across the simulated sequence. In this case, simulations ran for an average of 283,840.5 generations, and coalescence was reached in no fewer than 240,189 generations. Notably, this is substantially more (~180% increase) than the value of $10N_e$ that is typically recommended for reaching an equilibrium state in burn-in simulations [35], suggesting that the coalescence checking option should be used to ensure robust burn-ins in *SLiM*. *msprime* was over 220 times faster than *SLiM w*hen using the classical in-time mutation recording approach, consistent with previous benchmarking results showing that forward approaches only outcompete *msprime* when extremely long sequences (i.e. 10^{10} nucleotides) are simulated [16].

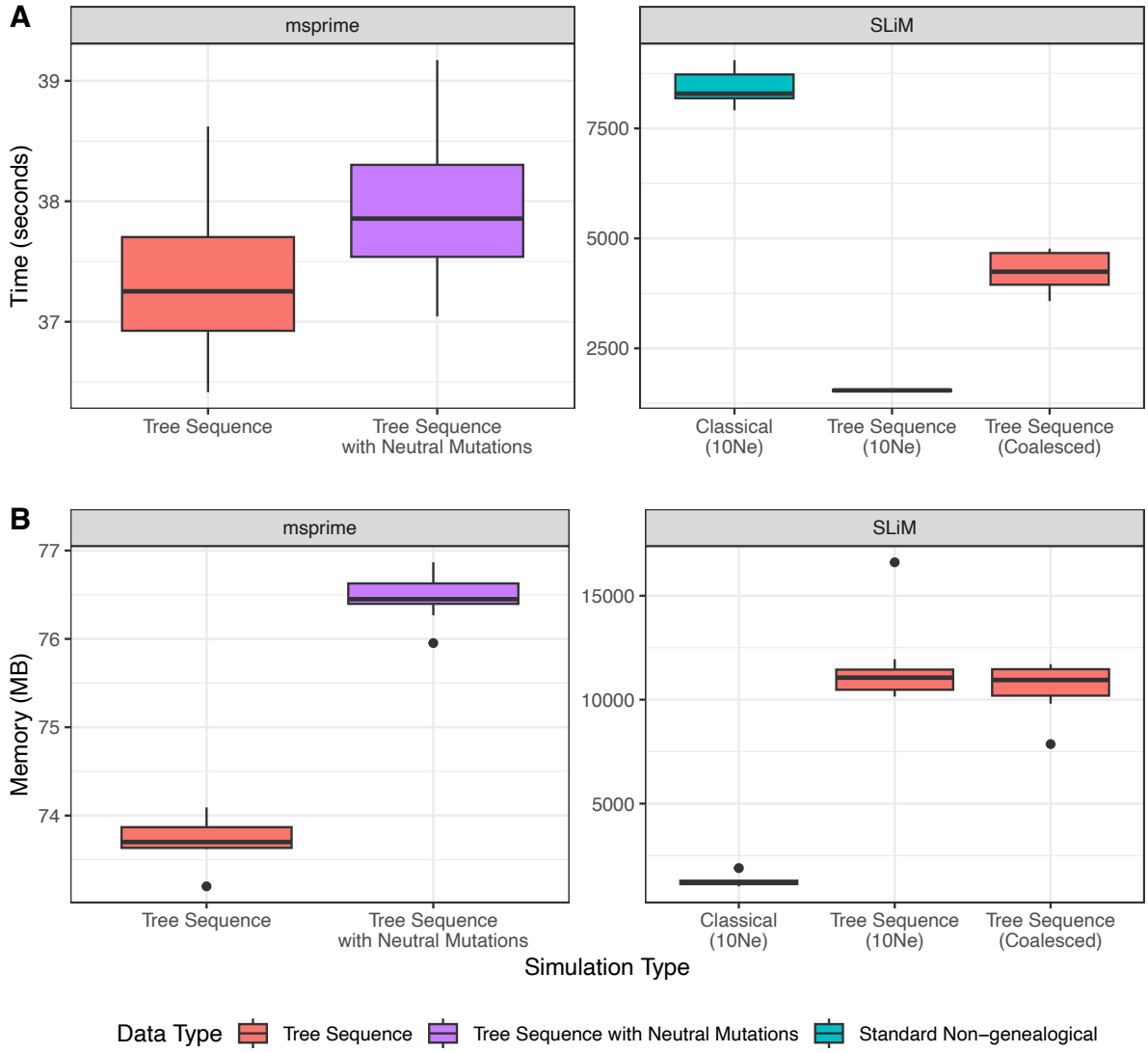

Figure 3. Resource usage for burn-in simulations.

Simulations that use standard non-genealogical output are shown in turquoise, red signifies simulations that output a tree sequence, and purple are simulations resulting in a tree sequence that is overlaid with neutral mutations. Each approach was replicated 10 times. A Time in seconds for simulations to complete, comparing the use of the tree sequence data structure, in msprime with and without overlaid neutral mutations as well as in SLiM run for 10Ne generations and until coalescence is ensured, and using the classical approach. B Memory usage in megabytes (MB) for these same simulations.

The memory required for *msprime* simulations was also significantly lower compared to simulating forwards in time with *SLiM* (Figure 3B), irrespective of the recording method used. *msprime* had a peak memory consumption of about 76 MB when running a burn-in and overlaying neutral mutations. This was almost 140 times lower than the mean peak memory

of the *SLiM* burn-in using tree sequence recording, which required an average of about 10.6 GB whether the 'checkCoalescence' option was activated or not. The use of in-time mutation recording resulted in significant reductions in memory burden relative to tree sequence recording, requiring around 1.3 GB, though this is still 16x more memory than that consumed by *msprime* using in-time mutation recording. This difference in memory consumption was also found when the tree sequence recording method was first proposed [17]. However, the initial benchmarking found that tree sequence recording consumed less memory compared to the classical mutation recording approach [16]. This disparity is potentially due to less frequent usage of tree simplification in the current study, as there is a trade-off between the frequency of simplification events and resource usage (i.e. increasing the frequency of simplification events leads to greater computational time but lower memory consumption [16]).

When comparing levels of diversity (Figure 4), the coalescent simulations in *msprime* resulted in levels of neutral diversity close to the theoretical expectation (relative diversity = 0.996; *p*: Shapiro-Wilk < 0.05, t-test > 0.05, Mann-Whitney U-test > 0.05). Forwards simulations in *SLiM* result in slightly decreased levels of diversity when 'checkCoalescence' is not implemented, such that the mean levels of neutral diversity when simulating for $10N_e$ generations with tree sequence recording (0.966; *p*: Shapiro-Wilk < 0.05, t-test < 0.001, Mann-Whitney U-test < 0.01) and using the classical mutational recording approach (0.994; *p*: Shapiro-Wilk > 0.05, t-test < 0.05) were significantly less than the neutral expectation. However, using tree sequence recording and conditioning on coalescence results in a mean diversity that is similar to the neutral expectation (0.999; *p*: Shapiro-Wilk > 0.05, t-test > 0.05). This reinforces the importance of ensuring coalescence when running burn-ins with tree sequence recording in *SLiM*. Notably, coalescent approaches such as *msprime* guarantee coalescence across the full simulated sequence, which together with the minimal resource

usage makes it the preferred method for producing burn-ins to establish neutral diversity. However, should a non-neutral burn-in be required, e.g. to evaluate changing selection pressures or continuously introduced deleterious mutations, then forward simulations are required and users need to decide between the time-efficient but memory-heavy tree sequence recording (confirming coalescence) or the slower but more memory-efficient classical mutation reporting approach.

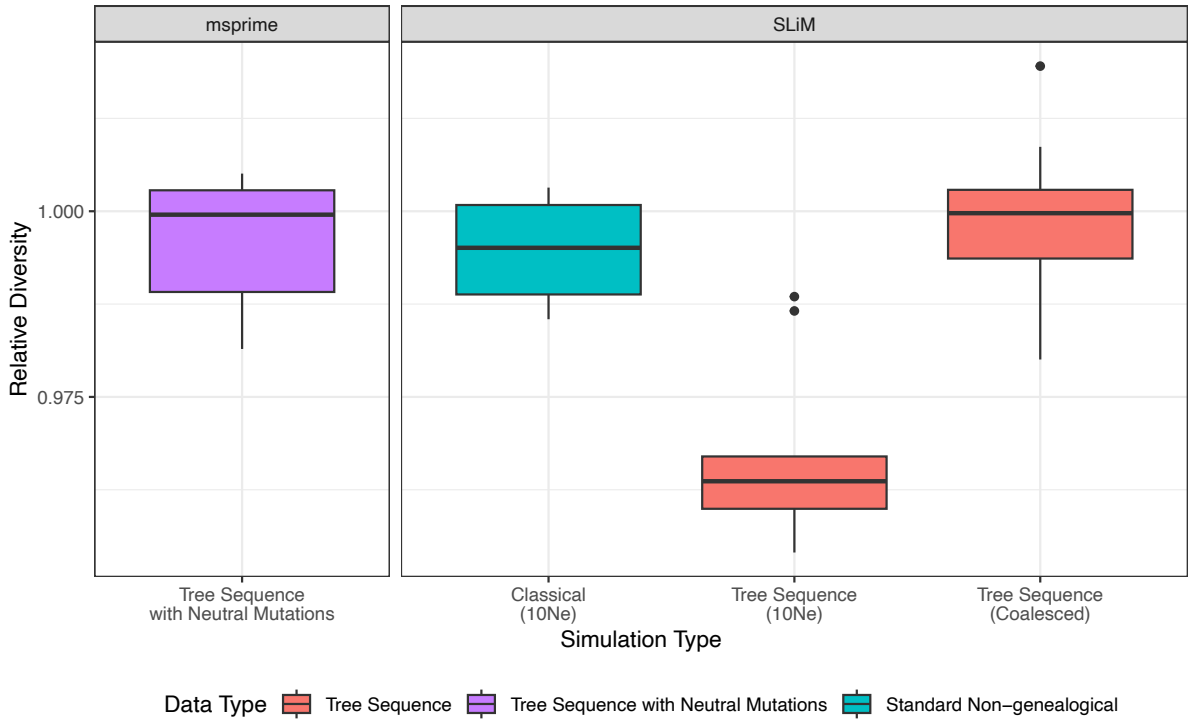

Figure 4. Relative diversity of burn-in simulations.

Relative diversity was calculated to compare the levels of neutral diversity at the end of each burn-in simulation with expected diversity levels for the simulated population under neutral evolution (expectation is equal to $\frac{\theta}{1+\theta}$). Coalescent simulations generated in *msprime* were compared with forward simulations that were generated in *SLiM*.

Forward simulation of fluctuating selection

Following the benchmarking of the burn-in methods, the resource usage of the forward simulation of fluctuating selection in SLiM was tested. Here, classical forward simulations utilising in-time mutation reporting and forward simulation with recently developed tree

sequence recording methods are compared, and both the single locus and multilocus models were implemented.

For the forward simulations of the single locus selection model, the classical approach took over 12 times longer (approximately 2 hours and 43 minutes; Table S2; Figure 5A) than using tree sequence recording and overlaying neutral mutations afterwards (~13.5 minutes). The runtime of the classical approach decreased when simulating multilocus selection, taking an average of 1 hour and 23 minutes versus approximately 18 minutes when using tree sequence recording. This time improvement provided by tree sequence recording does come with an increase in memory burden (Figure 5B), requiring approximately six times more memory (12.1 and 8.8 GB for single locus and multilocus models, respectively) than forward simulations employing in-time mutation reporting (1.9 and 1.4 GB). The developers of tree sequence recording do note that it can be more memory intensive and thus is not always advisable [16,17]. However, when the required RAM is available, the reduction in the time required for the simulation to run, combined with the additional data captured in the tree sequence data structure, can make tree sequence recording more desirable than classical forward simulations.

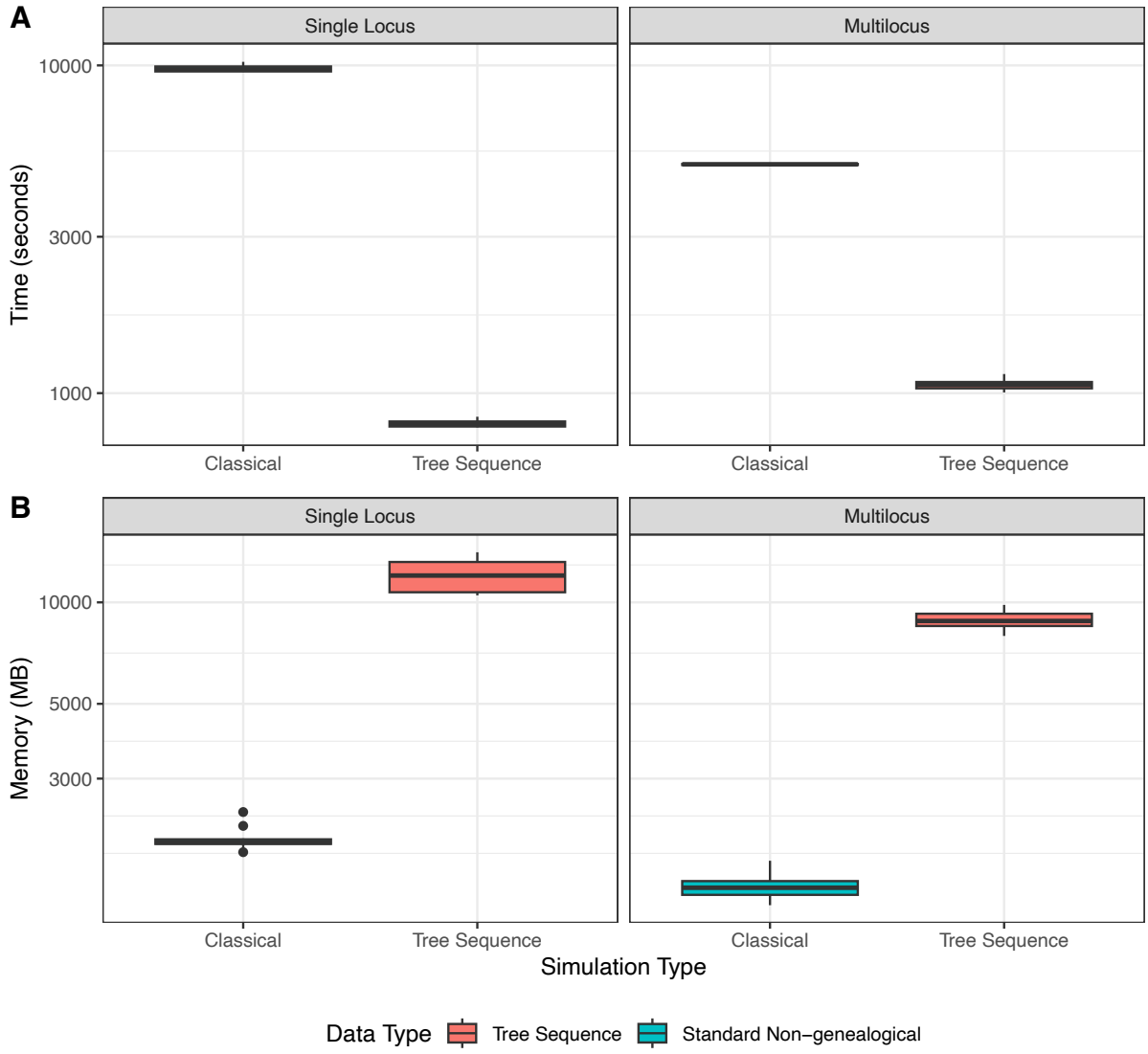

Figure 5. Resource usage for forward simulations modelling selection.

A Time and **B** memory requirements for forward simulations in *SLiM* on a log scale. Two models of fluctuating selection, a single locus and a multilocus model, are compared, along with the use of the tree sequence recording (red) compared to classical forward simulation (i.e. using in-time mutational reporting; turquoise).

Summary statistics

Given the benchmarking results reported in the previous sections, a simulation set-up that utilised a coalescent burn-in in *msprime* and forward simulation of selection using tree sequence recording was determined to be the fastest approach. Previous studies indicate that the use of the tree sequence data structure can also facilitate the rapid calculation of

population genetic statistics [13,17]. Accordingly, we performed tree- or allele-based calculations on the relevant outputs of our simulated fluctuating selection regime and compared computation times and memory usage (Table S3). The tree-based statistics required less memory than the allele-based calculations, exhibiting an 80% average reduction in RAM usage for the single locus selection model, and a 50% average reduction for the multilocus selection model (Figure 6A). In contrast, the tree-based calculations had the longest mean compute time, ranging from 0.3 to 1.2 s for the four combinations of statistics and selection models (Figure 6B). The allele-based calculations were significantly faster, taking less than a hundredth of a second. However, this calculation time does not take into account the time required to manipulate that data into the form required by the statistical function. The tree-based calculation can be applied directly to the tree sequence resulting from the forward simulation, whereas the allele-based statistics require a specific array of allele counts and a separate vector of variant positions. When the time taken to prepare these data formats is included, allele- and tree-based calculations have similar compute times (Figure 6C).

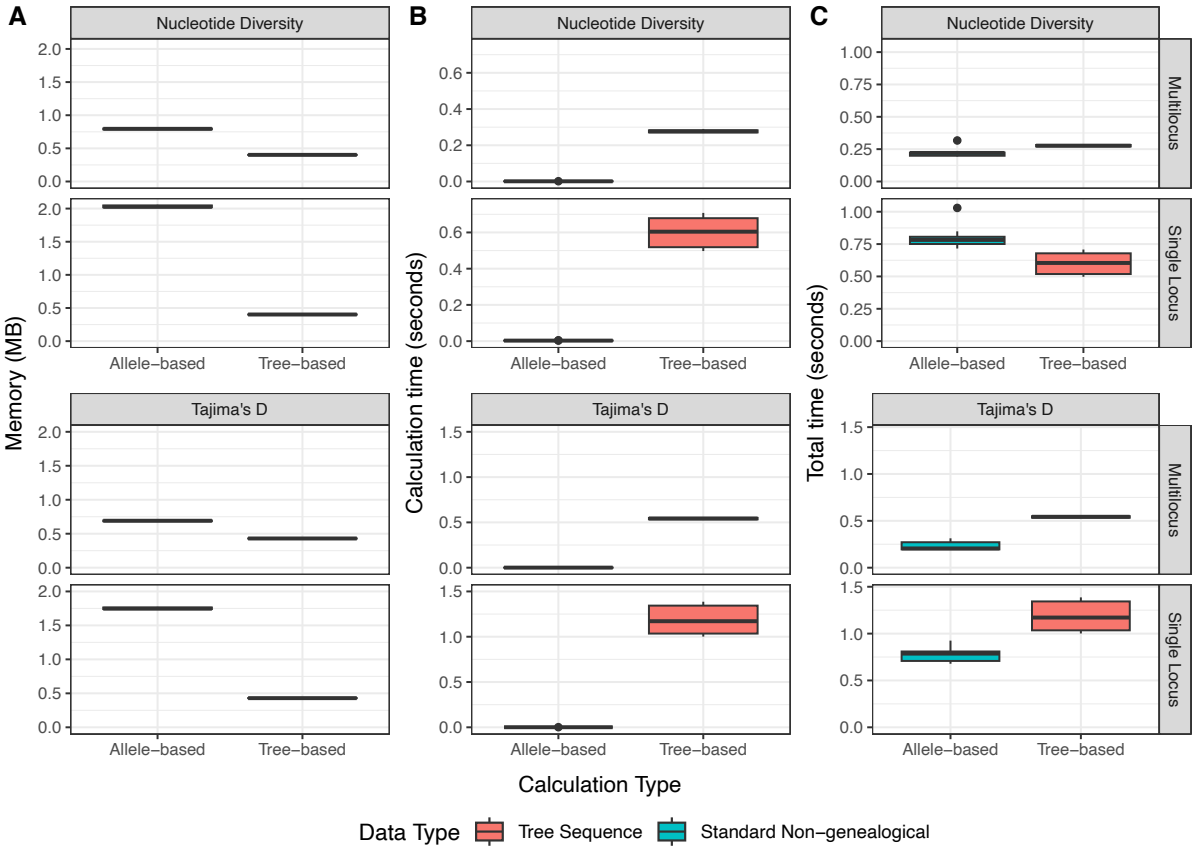

Figure 6. Resource requirements for analysis of simulated data.

Comparisons of **A** memory, **B** calculation time and **C** total time taken including data manipulation for combinations of models of selection and calculation type for two common population genetic statistics, nucleotide diversity, and Tajima's D.

The complete simulation framework

We combined the outcomes of the burn-in, selection phase (single allele model), and summary statistic calculations (nucleotide diversity), to obtain benchmarks for the four tested simulation frameworks (Figure 2; Table S4): 1, classical forward simulations using in-time mutation recording during the burn-in and selection phases with allele-based calculations; 2, forward simulations using tree sequence recording in the burn-in (generating a robust burn-in using the check coalescent option to ensure coalescence of lineages) and selection phase with tree-based calculations; 3, a coalescent burn-in overlaid with neutral mutations followed by a selection phase with in-time mutation recording and allele-based calculations; and 4, a coalescent burn-in followed by a selection phase using tree sequence recording with tree-

based calculations of summary statistics. Notably, the complete framework values for the multilocus method are similar and can be found in Table S4. In contrast, single locus selection models displayed considerable differences with approaches that utilised classical methods taking the longest time to complete, having an average computation time of approximately 5 hours when in-time mutation reporting was used for both burn-in and selection phase and taking 2 hours and 43 minutes when it was only used in the selection phase. Significant gains were made by frameworks that used tree sequence recording, with run times decreasing to 85 minutes when this was employed in the selection phase and only 14 minutes when employed in both the burn-in and selection phase. These gains in computation incur a trade-off with memory consumption, with frameworks employing tree sequencing recording in at least one step having a maximum memory burden of ~12 GB versus ~2 GB for frameworks where this recording type was not used.

Discussion

SLiM is a powerful population genetic simulation tool that implements tree sequence reporting within a forward simulation structure, which has made the evaluation of arbitrarily complex evolutionary scenarios feasible. Previous studies benchmarking *SLiM* simulations have all employed *msprime's* recapitation function, where lineages that remain uncoalesced at the end of the simulation are joined in post-simulation data processing [16]. Accordingly, population-wide levels of neutral diversity are not fixed at a specific value at the onset of the simulation, making this method unsuitable for research that aims to investigate how the effect of selection on linked neutral variation builds up over time.

In our study, we have explored four options for generating appropriate population-wide patterns of neutral diversity in a pre-simulation burn-in phase, followed by *SLiM* forward simulations of a complex fluctuating selection scenario. Our benchmarks show that a hybrid

workflow employing a *msprime* coalescent burn-in phase and conducting the selection phase using *SLiM's* tree reporting procedure provides appropriate levels of initial population genetic diversity as well as delivering rapid simulations. This hybrid framework is between 6-21 times faster than the other three options. While the tree sequence reporting format does impose higher memory burdens than simulations that employ in-time mutation reporting, these RAM levels are feasible for modern computing environments (~12 GB in the present study). Similarly, summary statistic calculations on tree-based outputs are slightly slower than allele-based methods, though this comprises a small proportion of the overall run time and is not sufficient to offset the time savings created by the usage of tree recording (in place of in-time mutation recording) throughout the simulation.

Another important consideration arising from our study is that the coalescence of neutrally evolving lineages is not guaranteed to occur within $10N_e$ generations, a criterion that is often used in population genetic simulations. While this is not an issue when using coalescent simulators like *msprime*, which ensure genome-wide lineage coalescence, for users choosing to work solely in *SLiM*, we strongly encourage the use of the 'checkCoalescence' option to generate appropriate population levels of neutral diversity at the onset of the simulations.

Taken together our benchmarks demonstrate the hybrid tree sequence workflow – which combines an *msprime* coalescent burn-in with the core simulation conducted in *SLiM* – is an effective framework for the simulation of non-standard evolutionary processes due to the rich information provided by the tree sequence data structure and the potential for greatly reduced computational run times compared to workflows adopting in-time mutation recording. As shown in this study, however, the improved run times afforded by tree sequence recording also come with higher memory requirements, and this trade-off depends on the population genetic model being simulated. Accordingly, the optimal simulation framework for each

evolutionary genetic study will ultimately depend on both the simulated population genetic model and resources available in the local computational environment.

Acknowledgements

C.D.H. was funded by the National Institute of Health under award number R35GM146886, R.T. was funded by Australian Research Council's DECRA Fellowship DE190101069, J.M.S. was funded by the Australian Research Council's Discovery Project DP190103606, and O.L.J. was funded by a Westpac Future Leaders Scholarship and an Australian Government Research Training Program Scholarship. Thank you to the Australian Centre for Ancient DNA's Thesis Writing Group for providing feedback on an early version of this manuscript.

References

1. Haldane JBS. A mathematical theory of natural and artificial selection. Math Proc Cambridge Philos Soc. 1926;23: 363–372. doi:10.1017/S0305004100015176

2. Wright S. The evolution of dominance. Am Nat. 1929;63: 556–561. doi:10.1086/280290

3. Fisher RA. The genetical theory of natural selection. Oxford: The Clarendon Press; 1930.

4. Matheson J, Masel J. Background selection from unlinked sites causes non-independent evolution of deleterious mutations. bioRxiv. 2023. p. 2022.01.11.475913. doi:10.1101/2022.01.11.475913

5. Korfmann K, Temple-Boyer M, Sellinger T, Tellier A. Determinants of rapid adaptation in species with large variance in offspring production. Mol Ecol. 2023. doi:10.1111/mec.16982

6. Isildak U, Stella A, Fumagalli M. Distinguishing between recent balancing selection and incomplete sweep using deep neural networks. Mol Ecol Resour. 2021;21: 2706–2718. doi:10.1111/1755-0998.13379

7. Wittmann MJ, Mousset S, Hermisson J. Modeling the genetic footprint of fluctuating balancing selection: From the local to the genomic scale. Genetics. 2023;223. doi:10.1093/genetics/iyad022

8. Hoban S, Bertorelle G, Gaggiotti OE. Computer simulations: Tools for population and evolutionary genetics. Nat Rev Genet. 2012;13: 110–122. doi:10.1038/nrg3130

9. Adrion JR, Cole CB, Dukler N, Galloway JG, Gladstein AL, Gower G, et al. A community-maintained standard library of population genetic models. Elife. 2020;9. doi:10.7554/eLife.54967

10. Haller BC, Messer PW. SLiM 4: Multispecies eco-evolutionary modeling. Am Nat. 2023;201: E127–E139. doi:10.1086/723601

11. Haller BC, Messer PW. SLiM 3: Forward genetic simulations beyond the Wright–Fisher model. Hernandez R, editor. Mol Biol Evol. 2019;36: 632–637. doi:10.1093/molbev/msy228

12. Haller BC, Messer PW. SLiM 2: Flexible, interactive forward genetic simulations. Mol Biol Evol. 2017;34: 230–240. doi:10.1093/molbev/msw211

13. Baumdicker F, Bisschop G, Goldstein D, Gower G, Ragsdale AP, Tsambos G, et al. Efficient ancestry and mutation simulation with msprime 1.0. Genetics. 2022;220. doi:10.1093/genetics/iyab229

14. Wakeley J. Coalescent Theory: An Introduction. Roberts & Company; 2009.

15. Kelleher J, Etheridge AM, McVean G. Efficient coalescent simulation and genealogical analysis for large sample sizes. PLoS Comput Biol. 2016;12: e1004842. doi:10.1371/journal.pcbi.1004842

16. Haller BC, Galloway J, Kelleher J, Messer PW, Ralph PL. Tree-sequence recording in SLiM opens new horizons for forward-time simulation of whole genomes. Mol Ecol Resour. 2019;19: 552–566. doi:10.1111/1755-0998.12968

17. Kelleher J, Thornton KR, Ashander J, Ralph PL. Efficient pedigree recording for fast population genetics simulation. PLoS Comput Biol. 2018;14: e1006581. doi:10.1371/journal.pcbi.1006581

18. Yuan X, Miller DJ, Zhang J, Herrington D, Wang Y. An overview of population genetic data simulation. J Comput Biol. 2012;19: 42–54. doi:10.1089/cmb.2010.0188

19. Kaushik S. Effect of beneficial sweeps and background selection on genetic diversity in changing environments. J Theor Biol. 2023;562: 111431. doi:10.1016/j.jtbi.2023.111431

20. Charlesworth B, Jensen JD. Effects of selection at linked sites on patterns of genetic variability. Annu Rev Ecol Syst. 2021;52: 177–197. doi:10.1146/annurev-ecolsys-010621-044528

21. Barton NH. Genetic hitchhiking. Phil Trans R Soc Lond B. 2000;355: 1553–1562.

22. Smith JM, Haigh J. The hitch-hiking effect of a favourable gene. Genet Res. 1974;23: 23–35. doi:10.1017/S0016672300014634

23. Charlesworth D. Balancing selection and its effects on sequences in nearby genome regions. PLoS Genet. 2006;2: e64. doi:10.1371/journal.pgen.0020064

24. Bank C, Ewing GB, Ferrer-Admettla A, Foll M, Jensen JD. Thinking too positive? Revisiting current methods of population genetic selection inference. Trends Genet. 2014;30: 540–546. doi:10.1016/j.tig.2014.09.010

25. Griffiths RC. The two-locus ancestral graph. Lect Notes Monogr Ser. 1991;18: 100–117. Available: http://www.jstor.org/stable/4355649

26. Griffiths RC, Marjoram P. An ancestral recombination graph. Progress in population genetics and human evolution. Springer; 1997. pp. 257–270. Available: https://ui.adsabs.harvard.edu/abs/1997IMA....87..257G

27. Kaplan NL, Darden T, Hudson RR. The coalescent process in models with selection. Genetics. 1988;120: 819–829. doi:10.1093/genetics/120.3.819

28. Hudson RR, Kaplan NL. The coalescent process in models with selection and recombination. Genetics. 1988;120: 831–840. doi:10.1093/genetics/120.3.831

29. Braverman JM, Hudson RR, Kaplan NL, Langley CH, Stephan W. The hitchhiking effect on the site frequency spectrum of DNA polymorphisms. Genetics. 1995;140: 783–796. doi:10.1093/genetics/140.2.783

30. Kern AD, Schrider DR. Discoal: Flexible coalescent simulations with selection. Bioinformatics. 2016;32: 3839–3841. doi:10.1093/bioinformatics/btw556

31. Shlyakhter I, Sabeti PC, Schaffner SF. Cosi2: An efficient simulator of exact and approximate coalescent with selection. Bioinformatics. 2014;30: 3427–3429. doi:10.1093/bioinformatics/btu562

32. Ewing G, Hermisson J. MSMS: A coalescent simulation program including recombination, demographic structure and selection at a single locus. Bioinformatics. 2010;26: 2064–2065. doi:10.1093/bioinformatics/btq322

33. Kelleher J, Wong Y, Wohns AW, Fadil C, Albers PK, McVean G. Inferring whole-genome histories in large population datasets. Nat Genet. 2019;51: 1330–1338. doi:10.1038/s41588-019-0483-y

34. Thornton KR. A C++ template library for efficient forward-time population genetic simulation of large populations. Genetics. 2014;198: 157–166. doi:10.1534/genetics.114.165019

35. Haller BC, Messer PW. SLiM: An evolutionary simulation framework. Cornell University; 2022 Sep. Available: https://github.com/MesserLab/SLiM/releases/download/v4.0.1/SLiM_Manual.pdf

36. Hudson RR. Generating samples under a Wright-Fisher neutral model of genetic variation. Bioinformatics. 2002;18: 337–338. doi:10.1093/bioinformatics/18.2.337

37. Sella G, Petrov DA, Przeworski M, Andolfatto P. Pervasive natural selection in the *Drosophila* genome? PLoS Genet. 2009;5: e1000495. doi:10.1371/journal.pgen.1000495

38. Wittmann MJ, Bergland AO, Feldman MW, Schmidt PS, Petrov DA. Seasonally fluctuating selection can maintain polymorphism at many loci via segregation lift. Proc Natl Acad Sci USA. 2017;114: E9932–E9941. doi:10.1073/pnas.1702994114

39. Rudman SM, Greenblum SI, Rajpurohit S, Betancourt NJ, Hanna J, Tilk S, et al. Direct observation of adaptive tracking on ecological time scales in *Drosophila*. Science. 2022;375: eabj7484. doi:10.1126/science.abj7484

40. Machado HE, Bergland AO, Taylor R, Tilk S, Behrman E, Dyer K, et al. Broad geographic sampling reveals the shared basis and environmental correlates of seasonal adaptation in *Drosophila*. eLife. 2021;10: e67577. doi:10.7554/eLife.67577

41. Behrman EL, Schmidt P. How predictable is rapid evolution? bioRxiv. 2022. p. 2022.10.27.514123. doi:10.1101/2022.10.27.514123

42. Nunez JCB, Lenhart BA, Bangerter A, Murray CS, Yu Y, Nystrom TL, et al. A cosmopolitan inversion drives seasonal adaptation in overwintering *Drosophila*. bioRxiv. 2022. p. 2022.12.09.519676. doi:10.1101/2022.12.09.519676

43. Sprengelmeyer QD, Mansourian S, Lange JD, Matute DR, Cooper BS, Jirle EV, et al. Recurrent collection of *Drosophila melanogaster* from wild African environments and genomic insights into species history. Mol Biol Evol. 2020;37: 627–638. doi:10.1093/molbev/msz271

44. Comeron JM, Ratnappan R, Bailin S. The many landscapes of recombination in *Drosophila melanogaster*. PLoS Genet. 2012;8: e1002905. doi:10.1371/journal.pgen.1002905

45. Schrider DR, Houle D, Lynch M, Hahn MW. Rates and genomic consequences of spontaneous mutational events in *Drosophila melanogaster*. Genetics. 2013;194: 937–954. doi:10.1534/genetics.113.151670

46. Keightley PD, Ness RW, Halligan DL, Haddrill PR. Estimation of the spontaneous mutation rate per nucleotide site in a *Drosophila melanogaster* full-sib family. Genetics. 2014;196: 313–320. doi:10.1534/genetics.113.158758

47. Ralph P, Thornton K, Kelleher J. Efficiently summarizing relationships in large samples: A general duality between statistics of genealogies and genomes. Genetics. 2020;215: 779–797. doi:10.1534/genetics.120.303253

48. Messer PW. SLiM: Simulating evolution with selection and linkage. Genetics. 2013;194: 1037–1039. doi:10.1534/genetics.113.152181

49. Miles A, Bot P io, R. M, Ralph P, Harding N, Pisupati R, et al. cggh/scikit-allel: v1.3.3. 2021. doi:10.5281/zenodo.4759368

Data Accessibility and Benefit-Sharing

Data Accessibility Statement

Code to replicate this benchmarking can be found at github.com/olivia-johnson/2023_popgen_benchmarking.git.

Benefit-Sharing Statement

This study was conducted in accordance with the principles of the Nagoya Protocol on Access to Genetic Resources and the Fair and Equitable Sharing of Benefits Arising from their Utilization.

Author Contributions

All authors designed the simulation and benchmarking framework. O.L.J. set up the simulations. O.L.J. and C.D.H. conducted the analysis of the results. All authors contributed to writing the manuscript.

Supplementary Information

Table S1. Summary values for resource usage, diversity, and the final generation of burn-in simulations.

Simulator	Data Type	Resource	Mean	Variance	Minimum	Maximum
msprime	Tree Sequence	Time (s)	37.366637	0.42374342	36.41605	38.62125
msprime	Tree Sequence with Neutral Mutations	Time (s)	37.963179	0.39716497	37.04375	39.17149
SLiM	Tree Sequence ($10N_e$)	Time (s)	1543.8	506.622222	1506	1583
SLiM	Tree Sequence (Coalesced)	Time (s)	4256.4	185244.267	3575	4768
SLiM	Classical ($10N_e$)	Time (s)	8426.9	161730.544	7913	9053
msprime	Tree Sequence	Memory (MB)	73.719385	0.05721054	73.19834	74.09223
msprime	Tree Sequence with Neutral Mutations	Memory (MB)	76.466541	0.06223297	75.95247	76.8672
SLiM	Tree Sequence ($10N_e$)	Memory (MB)	11490.49	3554020.55	10149.5	16608
SLiM	Tree Sequence (Coalesced)	Memory (MB)	10612.379	1.35E+06	7863.87	11708.8
SLiM	Classical ($10N_e$)	Memory (MB)	1253.42	6.05E+04	1020.63	1898.95
msprime	Tree Sequence with Neutral Mutations	Diversity	0.0039687	1.21E-09	0.00391	0.004004
SLiM	Tree Sequence ($10N_e$)	Diversity	0.003852	2.17E-09	0.003801	0.003938
SLiM	Tree Sequence (Coalesced)	Diversity	0.0039807	1.82E-09	0.003905	0.004062
SLiM	Classical ($10N_e$)	Diversity	0.003963	7.06E-10	0.003926	0.003997
msprime	Tree Sequence & Tree Sequence with Neutral Mutations	Final Generation	N/A	N/A	N/A	N/A
SLiM	Tree Sequence ($10N_e$) & Classical ($10N_e$)	Final Generation	100000	0	100000	100000
SLiM	Tree Sequence (Coalesced)	Final Generation	283840.5	848881820	240189	322276

Table S2. Summary values for forward simulations of selection phase.

Simulator	Selection Model	Resource	Mean	Variance	Minimum	Maximum
Classical	Multilocus	Time (s)	4985.737735	527.9862688	4948.706671	5009.905124
Classical	Single Locus	Time (s)	9784.142022	55038.2371	9558.260197	10251.72032
Tree Sequence	Multilocus	Time (s)	1065.124218	1779.645299	1005.015845	1143.515013
Tree Sequence	Single Locus	Time (s)	809.140324	497.9385517	786.5171781	847.118891
Classical	Multilocus	Memory (MB)	1434.322	15351.50888	1263.54	1711.59
Classical	Single Locus	Memory (MB)	1990.348	28251.41591	1815.12	2387.28
Tree Sequence	Multilocus	Memory (MB)	8837.154	348108.16	7951.19	9825.66
Tree Sequence	Single Locus	Memory (MB)	12082.54	2185613.069	10490.5	14080.6

Table S3. Summary values for analysis of simulation data with allele-based and tree-based calculations.

Input Data Type	Calculation Type	Selection Model	Statistic	Resource	Mean	Variance	Minimum	Maximum
Tree Sequence	Tree-based	Single Locus	Nucleotide Diversity	Memory (MB)	0.401701	3.83E-07	0.400564	0.402675
Tree Sequence	Tree-based	Single Locus	Tajima's D	Memory (MB)	0.429567	1.59E-07	0.429004	0.430196
Tree Sequence	Allele-based	Single Locus	Nucleotide Diversity	Memory (MB)	6.700995	0.483635	6.006624	7.387836
Tree Sequence	Allele-based	Single Locus	Tajima's D	Memory (MB)	6.069129	0.395609	5.441	6.690508
Classical	Allele-based	Single Locus	Nucleotide Diversity	Memory (MB)	2.03	0.00028	2.008968	2.057128
Classical	Allele-based	Single Locus	Tajima's D	Memory (MB)	1.750968	0.0002	1.731624	1.772904
Tree Sequence	Tree-based	Multilocus	Nucleotide Diversity	Memory (MB)	0.401888	2.08E-07	0.401332	0.402531
Tree Sequence	Tree-based	Multilocus	Tajima's D	Memory (MB)	0.42972	1.09E-07	0.42908	0.430056
Tree Sequence	Allele-based	Multilocus	Nucleotide Diversity	Memory (MB)	3.394773	0.000311	3.357887	3.419015
Tree Sequence	Allele-based	Multilocus	Tajima's D	Memory (MB)	3.024864	0.000247	2.991728	3.045936
Classical	Allele-based	Multilocus	Nucleotide Diversity	Memory (MB)	0.792682	0.000105	0.774896	0.809112
Classical	Allele-based	Multilocus	Tajima's D	Memory (MB)	0.689093	7.74E-05	0.673848	0.703176
Tree Sequence	Tree-based	Single Locus	Nucleotide Diversity	Calculation Time (s)	6.01E-01	0.007784	0.49732	0.707807
Tree Sequence	Tree-based	Single Locus	Tajima's D	Calculation Time (s)	1.185142	0.029352	1.001424	1.386468
Tree Sequence	Allele-based	Single Locus	Nucleotide Diversity	Calculation Time (s)	0.008996	1.96E-06	0.007031	0.011153
Tree Sequence	Allele-based	Single Locus	Tajima's D	Calculation Time (s)	0.007064	1.62E-06	0.005917	0.009892
Classical	Allele-based	Single Locus	Nucleotide Diversity	Calculation Time (s)	0.003102	2.15E-07	0.00277	0.004277
Classical	Allele-based	Single Locus	Tajima's D	Calculation Time (s)	0.001074	2.63E-08	0.000889	0.001491
Tree Sequence	Tree-based	Multilocus	Nucleotide Diversity	Calculation Time (s)	0.277023	5.42E-05	0.267461	0.289421
Tree Sequence	Tree-based	Multilocus	Tajima's D	Calculation Time (s)	0.542382	8.20E-05	0.529961	0.554457
Tree Sequence	Allele-based	Multilocus	Nucleotide Diversity	Calculation Time (s)	0.004918	3.69E-07	0.004363	0.006341

Tree Sequence	Allele-based	Multilocus	Tajima's D	Calculation Time (s)	0.004039	6.71E-07	0.00346	0.006273
Classical	Allele-based	Multilocus	Nucleotide Diversity	Calculation Time (s)	0.001236	3.48E-08	0.001026	0.001601
Classical	Allele-based	Multilocus	Tajima's D	Calculation Time (s)	0.000611	7.26E-09	0.000516	0.000705
Tree Sequence	Tree-based	Single Locus	Nucleotide Diversity	Total Time (s)	0.601318	0.007784	0.497325	0.707812
Tree Sequence	Tree-based	Single Locus	Tajima's D	Total Time (s)	1.185142	0.029352	1.001425	1.386468
Tree Sequence	Allele-based	Single Locus	Nucleotide Diversity	Total Time (s)	12.11231	2.625862	10.39819	13.84901
Tree Sequence	Allele-based	Single Locus	Tajima's D	Total Time (s)	12.27627	3.272729	10.39801	15.15988
Classical	Allele-based	Single Locus	Nucleotide Diversity	Total Time (s)	0.801595	0.007893	0.715683	1.029525
Classical	Allele-based	Single Locus	Tajima's D	Total Time (s)	0.772711	0.005633	0.678232	0.925132
Tree Sequence	Tree-based	Multilocus	Nucleotide Diversity	Total Time (s)	0.277026	5.42E-05	0.267463	0.289425
Tree Sequence	Tree-based	Multilocus	Tajima's D	Total Time (s)	0.542382	8.20E-05	0.529962	0.554457
Tree Sequence	Allele-based	Multilocus	Nucleotide Diversity	Total Time (s)	6.47338	0.042623	6.22972	6.767085
Tree Sequence	Allele-based	Multilocus	Tajima's D	Total Time (s)	6.279504	0.013452	6.135808	6.547757
Classical	Allele-based	Multilocus	Nucleotide Diversity	Total Time (s)	0.223205	0.001295	0.193988	0.317061
Classical	Allele-based	Multilocus	Tajima's D	Total Time (s)	0.23141	0.002209	0.190004	0.313396

Table S4. Summary of resource usage for the four complete simulation frameworks examined.

Framework	Selection Model	Mean Time (s)	Peak Mean Memory (MB)
1 - Forward simulation with classical mutation recording and allele-based calculation	Single locus	18211.84362	1990.348
2 - Forward simulation with tree sequence recording and tree-based calculation	Single locus	5066.141642	12082.54
3 - Hybrid simulation with classical mutation recording and allele-based calculation	Single locus	9822.906796	1990.348
4 - Hybrid simulation with tree sequence recording and tree-based calculation	Single locus	847.1082791	12082.54
1 - Forward simulation with classical mutation recording and allele-based calculation	Multilocus	13412.86094	1434.322
2 - Forward simulation with tree sequence recording and tree-based calculation	Multilocus	5321.801244	10612.379
3 - Hybrid simulation with classical mutation recording and allele-based calculation	Multilocus	5023.924119	1434.322
4 - Hybrid simulation with tree sequence recording and tree-based calculation	Multilocus	1102.767881	8837.154

Chapter 3

Discerning the genetic footprints of seasonal fluctuating selection: A comparison with established selection forms

Statement of Authorship

Title of Paper	Discerning the Genetic Footprints of Seasonal Fluctuating Selection: A Comparison with Established Selection Forms
Publication Status	☐ Published ☐ Accepted for Publication ☐ Submitted for Publication ☒ Unpublished and Unsubmitted work written in manuscript style
Publication Details	Formatted for Genome Biology and Evolution.

Principal Author

Name of Principal Author (Candidate)	Olivia Johnson		
Contribution to the Paper	Conceptualisation, developed and ran simulations, data analysis, interpretation, wrote the manuscript.		
Overall percentage (%)	75%		
Certification:	This paper reports on original research I conducted during the period of my Higher Degree by Research candidature and is not subject to any obligations or contractual agreements with a third party that would constrain its inclusion in this thesis. I am the primary author of this paper.		
Signature		Date	08/01/2024

Co-Author Contributions

By signing the Statement of Authorship, each author certifies that:

i. the candidate's stated contribution to the publication is accurate (as detailed above);

ii. permission is granted for the candidate in include the publication in the thesis; and

iii. the sum of all co-author contributions is equal to 100% less the candidate's stated contribution.

Name of Co-Author	Christian Huber		
Contribution to the Paper	Conceptualisation, developed simulations, data analysis, interpretation, wrote the manuscript.		
Signature		Date	08/01/2024

Name of Co-Author	Raymond Tobler		
Contribution to the Paper	Conceptualisation, developed simulations, data analysis, interpretation, wrote the manuscript.		
Signature		Date	08/01/24

Name of Co-Author	Joshua Schmidt		
Contribution to the Paper	Conceptualisation, developed simulations, data analysis, interpretation, wrote the manuscript.		
Signature		Date	09/01/24

Abstract

Fluctuating selection is frequently studied in natural populations by observing allele frequency trajectories over brief or contemporary timeframes and through theoretical analyses of frequency dynamics. However, little is known of its effect on linked neutral diversity. Here, we simulate single locus seasonally fluctuating selection and characterise its genomic footprint using diversity, site-frequency spectrum (SFS), and haplotype-based statistics. Notably, fluctuating selection exhibited distinct signals depending on when in the seasonal cycle the population was sampled. Differences were also observed between recently established fluctuating selection and selection that has fluctuated over an extended period of time. Compared to other types of selection, fluctuating selection showed distinguishing signatures compared to both hard and soft selective sweeps but overlapped considerably with balancing selection. Leveraging linear discriminant analysis, we identified a combination of statistics that most effectively distinguishes fluctuating selection from positive and balancing selection. Our findings shed light on the distinct genomic signatures of fluctuating selection, paving the way for in-depth analyses of the long-term dynamics of loci pinpointed in contemporary studies.

Significance

This research sheds light on the unique genomic patterns of fluctuating selection in natural populations. By simulating and analysing its impact on linked neutral diversity, we reveal how it differs from other established selection forms, and how it varies across different stages of the seasonal cycle. Our findings enhance our understanding of the intricacies of fluctuating selection and introduce effective statistical tools for distinguishing it in population genetic studies. Importantly, our research facilitates population genetic analyses of loci previously

identified as fluctuating over a short time frame to better understand their long-term dynamics.

Introduction

It has long been understood that genetic selection can have a significant impact on surrounding neutral genetic variation (Smith & Haigh 1974; Clarke 1979; Holderegger et al. 2006; Kern & Hahn 2018; Charlesworth & Jensen 2021). This impact can be characterised and used to identify genomic loci that have been under selection. Such distortions of neutral genetic variation can be identified in several ways using different statistics and aspects of genomic variation; these include measures of diversity, haplotype frequencies, and changes to the site frequency spectrum (Watterson 1975; Tajima 1983, 1989; Garud & Rosenberg 2015; Bitarello et al. 2018). The effects of positive and balancing selection on these statistics are well-documented. Positive selection is characterised by a significant decrease in diversity surrounding the selected site (Smith & Haigh 1974; Braverman et al. 1995), an excess of rare variants (Tajima 1989), and an increase in haplotype homozygosity (Smith & Haigh 1974; Tajima 1989; Braverman et al. 1995; Garud & Rosenberg 2015). In contrast, an increase in diversity and an excess of intermediate frequency variants are a hallmark of balancing selection (Charlesworth 2006).

Fluctuating selection, defined by variation in strength or direction of selection over time, is a form of balancing selection whose genomic impact is much less well explored (Gillespie 1997; Barton 2000; Huerta-Sanchez et al. 2008; Taylor 2013; Wittmann et al. 2023). It has previously been studied from phenotype observations alone until recent advances in next-generation sequencing allowed the examination of allele frequency fluctuations across time (Bell 2010). Genetic evidence of fluctuating selection is now observed across a wide range of diverse species (Ludwig et al. 2015; Garcia-Elfring et al. 2021; Kelly 2022; Pfenninger &

Foucault 2022; Lynch et al. 2023; and reviewed in Johnson et al. 2023) but is particularly strong in *Drosophila melanogaster* with studies finding tens to thousands of alleles fluctuating between 4 - 20% across seasonal cycles (Bergland et al. 2014; Machado et al. 2021; Glaser-Schmitt et al. 2021; Behrman & Schmidt 2022; Rudman et al. 2022; Nunez et al. 2023). In addition to these empirical studies, a number of theoretical models have been developed to better understand the dynamics and mechanisms of fluctuating selection (Haldane & Jayakar 1963; Takahata et al. 1975; Gillespie 1978, 1997; Barton 2000; Taylor 2013; Wittmann et al. 2017; Bertram & Masel 2019; Park & Kim 2019; Wittmann et al. 2023; Kim 2023; reviewed in Johnson et al. 2023). While this work has largely aimed to add ecological realism and explain the abundant number of fluctuating SNPs observed in certain species (Bergland et al. 2014; Machado et al. 2021; Kelly 2022; Pfenninger et al. 2022; Pfenninger & Foucault 2022; Rudman et al. 2022; Bitter et al. 2023), few studies have contributed to our knowledge of the indirect effects of fluctuating selection on surrounding neutral genetic variation (Huerta-Sanchez et al. 2008; Wittmann et al. 2023). As a form of balancing selection, fluctuating selection maintains genetic diversity directly at, and very closely linked to, selected sites; however, recent analytical analysis has suggested that regions less strongly linked and unlinked to the selected sites decrease in diversity, which on a genome-wide level overwhelms the increase close to the selected loci (Wittmann et al. 2023). This effect has been confirmed in a temporal study of *Daphnia pulex*, where the authors show that temporal variation in selection coefficients is reducing levels of genome-wide diversity (Lynch et al. 2023). The effect of fluctuating selection on the site frequency spectrum (SFS) has been explored using diffusion approximations and simulation to obtain the SFS following random, autocorrelated environmental fluctuations (Huerta-Sanchez et al. 2008). Fluctuating selection was seen to distort the SFS, with fewer rare and intermediate alleles and more high-frequency alleles than expected under neutrality. While this distortion is evident in the

unfolded SFS, it is less pronounced in the folded SFS. Consequently, SFS-based statistics that are derived from the folded spectrum, like Tajima's D (Tajima 1989), remain largely unaffected. There is also limited power to discriminate fluctuating selection from positive selection, using likelihood-ratio tests, when the temporal variance in the selection coefficient is small (Huerta-Sanchez et al. 2008). Additionally, fluctuating selection leads to a greater fixation rate for selected sites, resulting in increased divergence compared to polymorphism akin to the effects of positive selection (Huerta-Sanchez et al. 2008; Gossmann et al. 2014). While these findings are vital in our understanding of the influence of fluctuating selection on genetic variation and population genetic inference, the effect of regular oscillations, such as those seen in *Drosophila,* remain largely unexplored. Moreover, fluctuating selection has yet to be characterised in the context of haplotype-based statistics which may provide further understanding of the dynamics of loci and the surrounding genetic variation under this type of selection.

Here, we investigate the effect of fluctuating selection on linked neutral variation. We conducted fast and efficient simulations, using tree sequence recording, of a seasonally fluctuating allele originating from a single *de novo* mutation. We then contrasted these with simulations of positive selection, in the form of hard and soft selective sweeps, and balancing selection represented by heterozygote advantage. To this end, we employed common diversity and SFS-based population genetic statistics along with measures based on haplotype frequencies, calculated in windows across the simulated region. These were then used in linear discriminant analysis (LDA) to identify a combination of statistics that best discriminate fluctuating selection from the other types of selection examined. We find fluctuating selection to be distinct from all forms of positive selection at the central window containing the selected site. In contrast, the signatures of balancing and fluctuating selection largely overlap across most metrics, but they can be differentiated using haplotype statistics.

Importantly, the signals from seasonally fluctuating selection varied depending on its sampling time during the cycle. This distinction could improve our capacity to differentiate it from other selection types that do not vary across seasons when data sampling covers multiple time points.

Results

We simulated a diploid, randomly mating population with constant population size and recombination rate and mutation rates reflecting the *Drosophila melanogaster* species (Comeron et al. 2012; Schrider et al. 2013; Keightley et al. 2014). We assume a binary two-season environment with 10 generations per season (Wittmann et al. 2023). Three types of selection were modelled: fluctuating selection (Wittmann et al. 2023); balancing selection, in the form of heterozygote advantage (Charlesworth et al. 1997); and positive selection, in the form of both hard and soft selective sweeps (Garud & Rosenberg 2015).

Hard selective sweeps were simulated by introducing a single beneficial mutation in the center of the simulated sequence, whereas soft selective sweeps were simulated by introducing multiple beneficial mutations via a high beneficial mutation rate (see Methods). These modes of selection were chosen as fluctuating selection has been suggested to reflect aspects of both balancing and positive selection (Barton 2000; Huerta-Sanchez et al. 2008; Taylor 2013; Wittmann et al. 2023). From these simulations, we then characterised the effect of each form of selection in 10 kb windows over a 5 Mb region.

Fluctuating allele frequency trajectories

Fluctuating selection was simulated using a seasonal single locus model, starting from a single *de novo* summer-favoured mutation introduced at the beginning of the summer season. We used the fitness model presented by Wittmann and colleagues (Table 1; Wittmann et al.

2023) and tested three selection coefficients (*s*; 1, 0.5, 0.1) and two dominance coefficients (*d*; 0.5, 0.6). The seasonal allele was seen to fluctuate in frequency immediately after introduction, with the trajectory oscillating around an average frequency that increased until a stable oscillation around an equilibrium frequency was reached (Figure 1). For most simulations, the seasonal allele was maintained in the population until the simulation terminated at 100,000 generations. However, for weak selection ($s < 0.1$) and dominance of 0.5, seasonal alleles were often either lost or reached fixation before the end of the simulation. The following analysis only considers simulations where the selected allele was segregating until the end of the simulation, i.e. in some cases this required the simulation to restart if the selected locus was fixed or lost (Appendix 1). In general, greater selection coefficients conferred fluctuations with a larger amplitude and less variance in the allele frequencies at any given time. The different dominance coefficients also affect seasonal allele frequency trajectories, with $d = 0.6$ leading to more stable fluctuations than $d = 0.5$ (Figure 1; Wittmann et al. 2017, 2023).

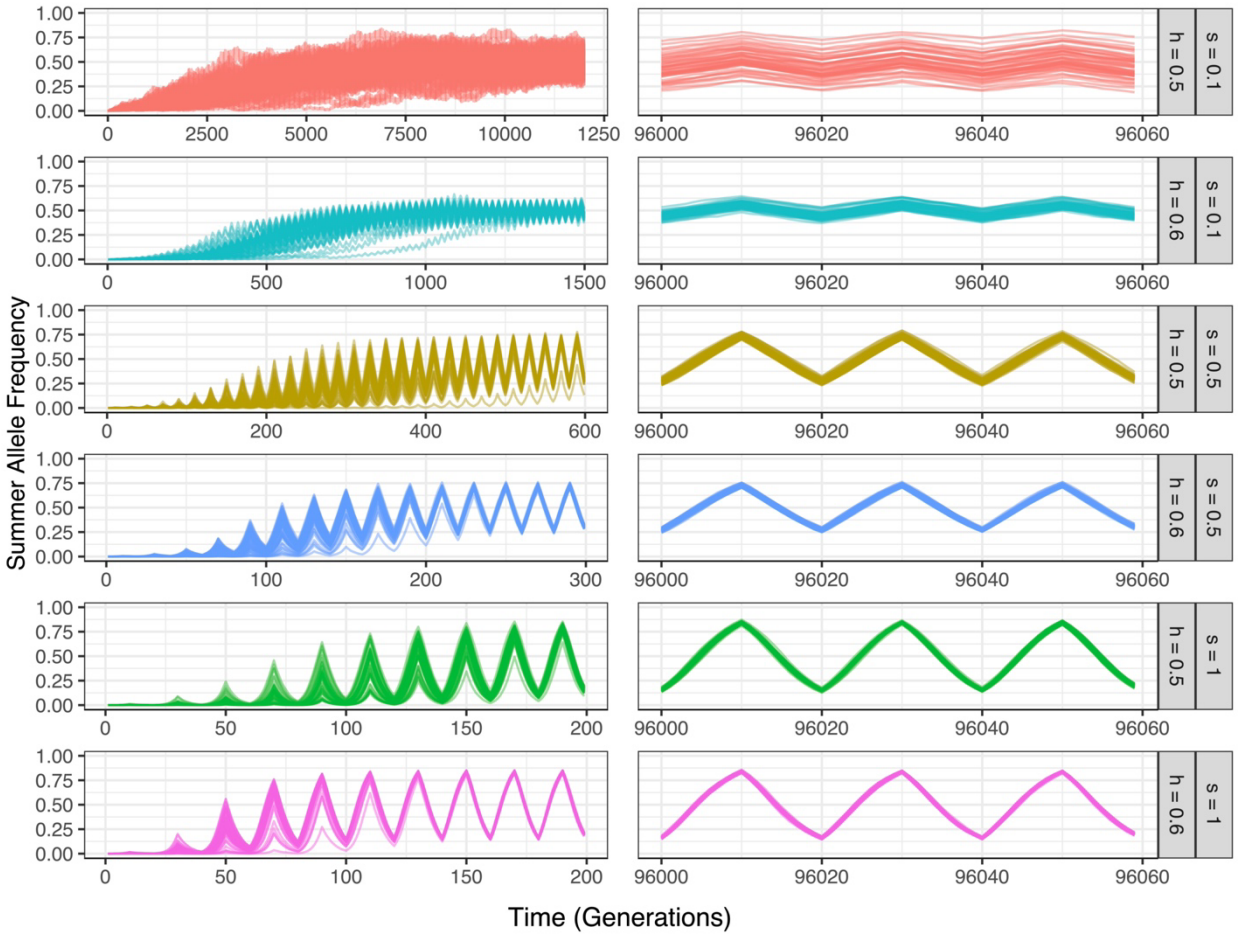

Figure 1. Allele frequency trajectories of fluctuating selection for different selection and dominance coefficients.

Three different selection coefficients (s; 0.1, 0.5, 1) and two dominance coefficients (h; 0.5, 0.6) are shown, labelled on the right-hand side of each row of panels to which it corresponds. Left-hand panels show the increase in the frequency of the summer-favoured allele from a single mutation until the allele is stably oscillating around the equilibrium frequency. The right-hand panels show the fluctuations after 96,000 generations over three consecutive seasonal cycles.

Characterising the signatures of fluctuating selection.

The influence of fluctuating selection was characterised across a 5 Mb simulated region using a range of population genetic statistics and averaging the values of statistics, calculated in 10 kb windows, across 50 replicates. These include measures of diversity, statistics based on the site frequency spectrum (SFS), and haplotype statistics. We compare fluctuating selection immediately after it reaches a stable oscillation around an equilibrium frequency (early

equilibrium) and after it has been at equilibrium for approximately 96,000 generations (long-term). The use of these two timepoints allow the characterisation of the signatures of selection at varying timepoints during which the allele frequency trajectories are stable. This provides the opportunity to determine how the signature of selection differs from when selection is first clearly identifiable with allele frequency data to when the allele has been stably segregating for extended periods of time and the genomic region surrounding the site is at equilibrium. We again simulate under three values of s (0.1, 0.5, 1), but use a constant dominance coefficient of 0.6 as it resulted in more stable trajectories. Samples are taken from the final generation of summer where we expect the most distinction from neutrality due to the extreme allele frequency at this time point.

When looking at measures of diversity, such as nucleotide diversity (π) and Watterson's theta (Figure 2), at early equilibrium, fluctuating selection demonstrates a narrow decrease at the selected site which is less negative with lower selection coefficients. However, long-term a broad decrease can be seen greater than 1 Mb away from the selected site, with a small increase in diversity right at the selected locus. This broad decrease lessens with decreasing strength of selection such that it is not noticeable when $s = 0.1$. Tajima's D demonstrates a decrease at the selected site with slightly positive shoulders when fluctuation selection is at early equilibrium; however, this becomes a small and narrow positive peak once selection has been stable long-term.

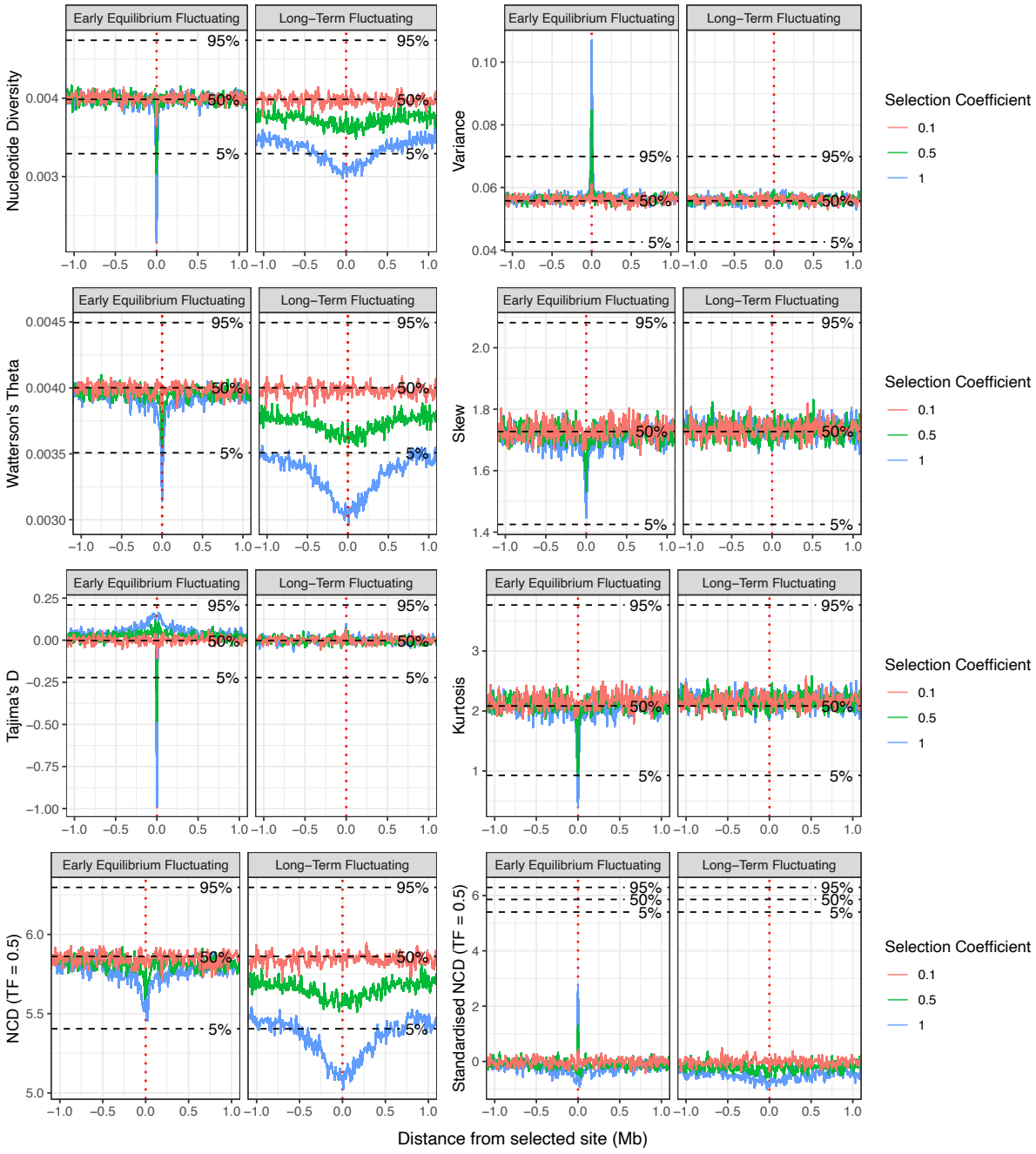

Figure 2. Footprints of fluctuating selection across time using SFS-based statistics.

Signature of fluctuating selection at early equilibrium and long-term for nucleotide diversity, Watterson's theta, Tajima's D, and the variance, skew, and kurtosis of the SFS, as well as non-central deviation (NCD) with a target frequency of 0.5 in both its unstandardised and standardised forms. Statistics were calculated in 10 kb windows across the simulated region and were averaged across 50 replicates for three selection coefficients: 1, in blue; 0.5, shown in green; and 0.1, in red. A dashed red line signifies the position of the selected site. Dashed black lines illustrate the 5%, 50% and 95% quartiles for simulations without selection, lines are labelled with the relevant quartiles.

We also examined the moments of the unfolded SFS to identify if fluctuating selection had any unique effects on the distribution of allele frequencies surrounding a seasonally selected site (Figure 2). A narrow peak in variance, that increases with greater selection coefficients, is visible at early equilibrium. This suggests that fluctuating selection increases the variance in allele frequencies around the selected site. For the skew and kurtosis of the SFS, we see a narrow negative peak together with a subtle broader decrease surrounding the central peak. A more negative central peak and more pronounced broader decrease is correlated with a greater selection coefficient. The decrease in skew and kurtosis around the selected site suggests the SFS has a broader, less skewed distribution of allele frequencies (e.g., fewer rare variants and more intermediate and high-frequency variants) compared to surrounding regions. Huerta-Sanchez and colleagues observed a similar effect on the SFS under randomly fluctuating selection (Huerta-Sanchez et al. 2008). However, they found fewer intermediate variants than we observe under seasonally fluctuating selection where there are equally elevated levels of intermediate and high-frequency variants (Figure S1). This increase in intermediate variants contradicts the negative peak we see in Tajima's D at the central window (Figure 2), however, fluctuating selection appears to decrease in singletons while maintaining, and potentially increasing, other low-frequency variants along with the increase in more common variants which likely contributes to the negative values of Tajima's D (Figure S1). When we look further away from the selected site, we find the distribution to be skewed towards rare variants, potentially as a result of the recurrent sweep-like manner of seasonally fluctuating selection (Coop & Ralph 2012). Long-term fluctuating selection at the central window does not show the same pattern in the moments of the SFS (Figure 2), however when looking at the site frequency spectrum, we see the increase in intermediate and high-frequency variants is still visible at this time point (Figure S1).

Non-central deviation (NCD) is a statistic designed to identify balancing selection that quantifies how the SFS deviates from the expected balanced equilibrium frequency i.e. the target frequency (TF; Bitarello et al. 2018). Here, we use a version of NCD (NCD1) that does not require outgroup information, and we use it with three target frequencies (0.5, 0.4, 0.3). As recommended, we standardised NCD based on the number of segregating sites in each window to control for potential confounding (Bitarello et al. 2018). Fluctuating selection has similar overall influences on NCD at all three target frequencies and when NCD is standardised (Figure 2; Figure S2). When fluctuating selection has reached early equilibrium, NCD is characterised by a large increase at the selected locus, specifically for standardised measures of NCD but also as the target frequency decreases. This central positive peak is located within a broader negative peak. For long-term fluctuating selection, the broader negative peak becomes more pronounced whereas the central positive peak disappears. As the selection coefficient decreases, this signature becomes less apparent such that when $s = 0.1$, it is not visible anymore.

Fluctuating selection also has a visible impact on haplotype-based statistics (Figure 3). We calculated Garud's H statistics which are a range of statistics that measure shifts in the haplotype frequency distributions to identify positive selection and discriminate hard and soft sweeps. For Garud's H1, H12 and H123, a large narrow peak is seen at the selected site for selection coefficients equal to 0.5 and 1 when fluctuating selection has just reached early equilibrium. The peak becomes an order of magnitude smaller when selection has been stable and at long-term equilibrium, and is effectively inverted for Garud's H2/H1, used to classify soft sweeps. The significant peak in H1, H12, and H123, suggests there is a small number of haplotypes at high frequencies surrounding the selected site, similar to a selective sweep. This signature is more pronounced for higher selection coefficients which is to be expected as the fluctuations are quicker to reach a stable oscillation. This leaves little time for

recombination and mutation to deteriorate the haplotype initially linked to the novel summer-beneficial mutation, thus resembling a hard selective sweep. Moreover, high values of H12 and H2/H1 are also indicative of a soft sweep (Garud & Rosenberg 2015); at early equilibrium, fluctuating selection demonstrates a high H12 but low H2/H1 at the selected site. However, by the long-term timepoint H2/H1 has increased, while H12 remains elevated, suggesting the sweep pattern softens over time.

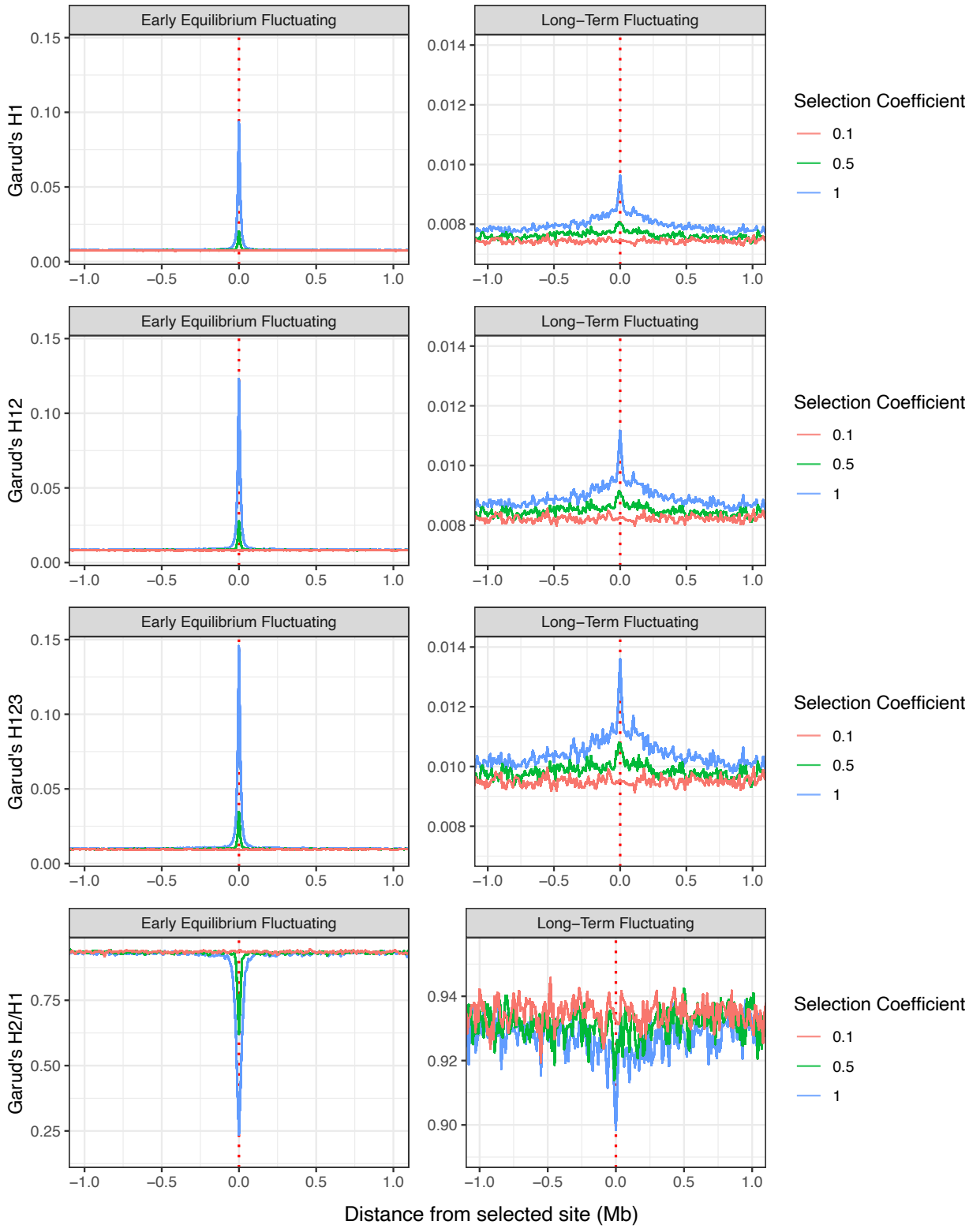

Figure 3. Signatures of fluctuating selection in haplotype statistics.

Garud's H statistics calculated in 10 kb windows across a 2 Mb region with the selected site at the centre for early equilibrium and long-term fluctuating selection. Three selection coefficients were considered, $s = 1$ in blue, $s = 0.5$ in green, and $s = 0.1$ in red.

Signatures of fluctuating selection change across the seasonal cycle

While these statistics show that fluctuating selection has a distinctive footprint when sampled at the end of summer, the signature can change when sampling at different stages throughout the seasonal cycle. Nucleotide diversity, Watterson's theta, Tajima's D, haplotype statistics, NCD, and the variance, skew, and kurtosis of the SFS all demonstrate differences between the different sampling times in each season, i.e. in the middle or end of either summer or winter, particularly right after reaching early equilibrium (Early Equilibrium Fluctuating). For diversity measures, NCD, moments of the SFS, and Tajima's D, signals are most pronounced at the end of summer, where it is distinct from the weaker pattern seen in the middle of summer or winter (Figure 4). The end of winter shows the weakest signal, looking almost neutral. This is also seen for haplotype-based statistics when fluctuating selection reaches early equilibrium (Figure 4). At long-term time points differences in patterns between winter and summer are not observed. However, an additional pattern is observed at long-term sampling points whereby features are present at the end of seasons but are not visible in the middle of seasons. Haplotype-based statistics and Tajima's D demonstrate this pattern at long-term fluctuating selection (Long-Term Fluctuating; Figure 4). In contrast, statistics such as NCD and diversity measures demonstrate a constant Long-Term Fluctuating signature across the season (Figure 4). Together, this suggests that there are optimum times at which natural populations should be sampled to detect signatures of fluctuating selection.

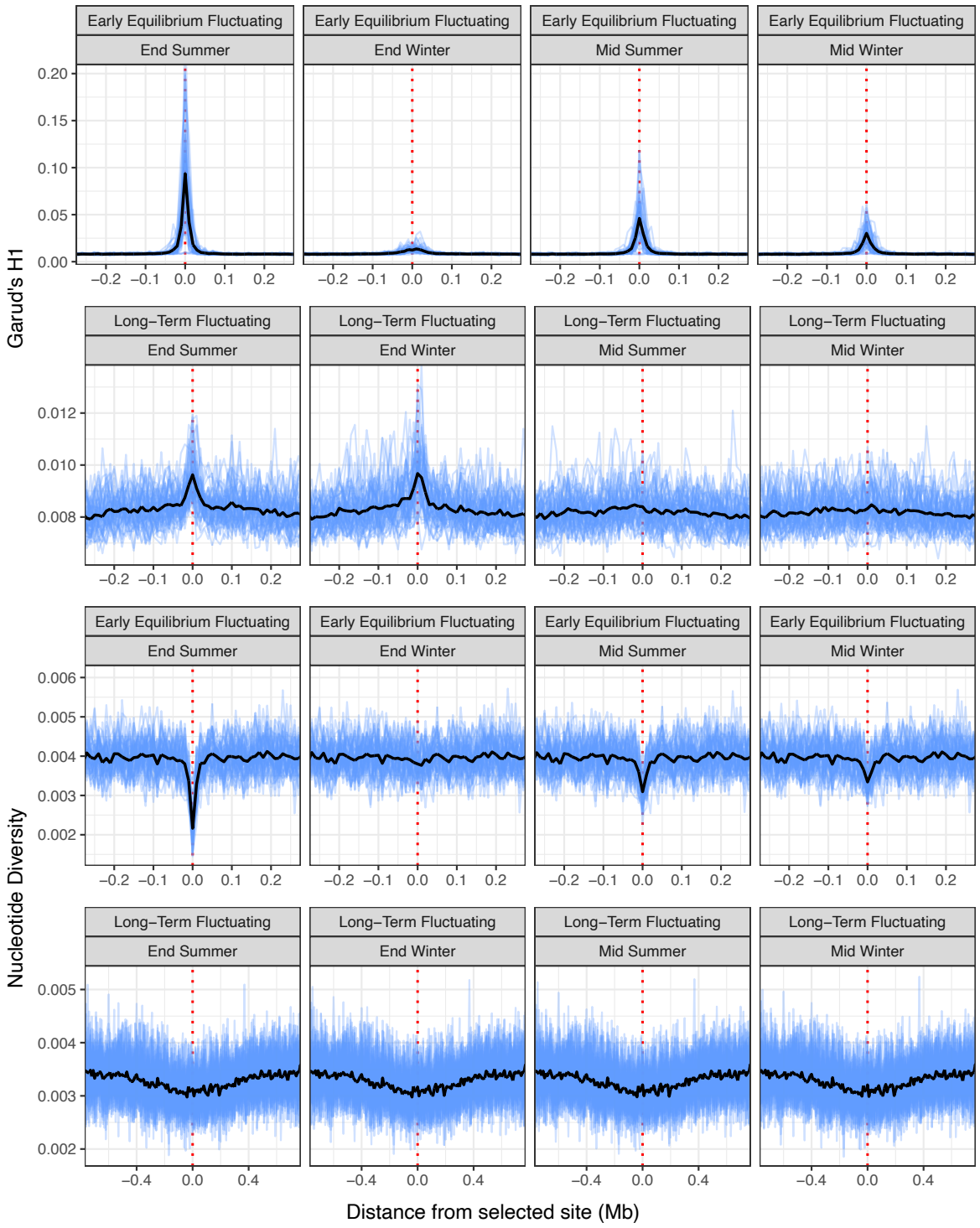

Figure 4. Signatures of fluctuating selection differ at different points of the seasonal cycle.

Garud's H1 and nucleotide diversity values for early equilibrium and long-term fluctuating selection are plotted at the middle and end of summer and winter across a single seasonal cycle. Data simulated with a selection coefficient of 1 is shown as it gives the clearest patterns, which are less pronounced as the selection coefficient decreases. There are a few different patterns seen across the seasonal cycle in a number of statistics tested in this study but shown here for Garud's H1 and nucleotide diversity. The first, visualised in both statistics when fluctuating selection reaches early equilibrium, when there

is a single motif that is more or less pronounced at different points; the second a presence/absence of signatures depending on when individuals are sampled, is observed in Garud's H1 at Long-Term Fluctuating between the middle and ends of the season. Nucleotide diversity demonstrates a consistent signal across the whole of the seasonal cycle for Long-Term Fluctuating.

Distinguishing fluctuating selection from other forms of selection

After characterising the signatures of fluctuating selection, we compared them to the footprints of more traditional forms of selection, such as positive and balancing selection. We aimed to ascertain if fluctuating selection has unique features that can be leveraged to discriminate it from other types of selection in empirical data. Our simulations of balancing and fluctuating selection as well as positive hard sweeps, start from a single *de novo* mutation (Figure S3). However, in the case of positive soft selective sweeps, we consider a beneficial trait conferred by multiple mutations. This was implemented using an increased mutation rate at the site of the selection which introduced multiple beneficial mutations in a short time. Balancing selection was simulated as symmetrical overdominance. All forms of selection were simulated with a selection coefficient of 0.1. Fluctuating and positive selection were also simulated with selection coefficients of 0.5 and 1. Particularly in the case of fluctuating selection, estimates of s from empirical data have spanned this range (Bergland et al. 2014; Machado et al. 2021; Rudman et al. 2022; Bitter et al. 2023). Balancing selection was not simulated at these strengths due to its unrealistic effects on fitness which lead to large proportions of (heterozygous) individuals not contributing any offspring each generation. The dominance coefficient was 0.6 for fluctuating selection as it gives stable trajectories while it was 0.5 for positive and balancing selection (Figure 1).

For hard sweeps, data was sampled immediately after fixation of the selected allele. For soft sweeps, data was sampled immediately after fixation of the beneficial trait, i.e. when each individual has at least two beneficial alleles either from the same or different mutational

origins. Balancing and fluctuating selection were sampled immediately after the alleles reached their stable fluctuations or early equilibrium frequency (Early Equilibrium Balancing/Fluctuating) and in the final sampling year of the simulation (~96,000 generations; Long-Term Balancing/Fluctuating). In all cases, we sampled the population over a full seasonal cycle, i.e. for each of 20 generations.

Population genetic statistics were then calculated in 10 kb windows across the simulated sequence. We first contrasted signatures of the different forms of selection at the focal window, which is centred over the selected site. We used samples taken at the end of summer where we expect the strongest distinction between different selection models.

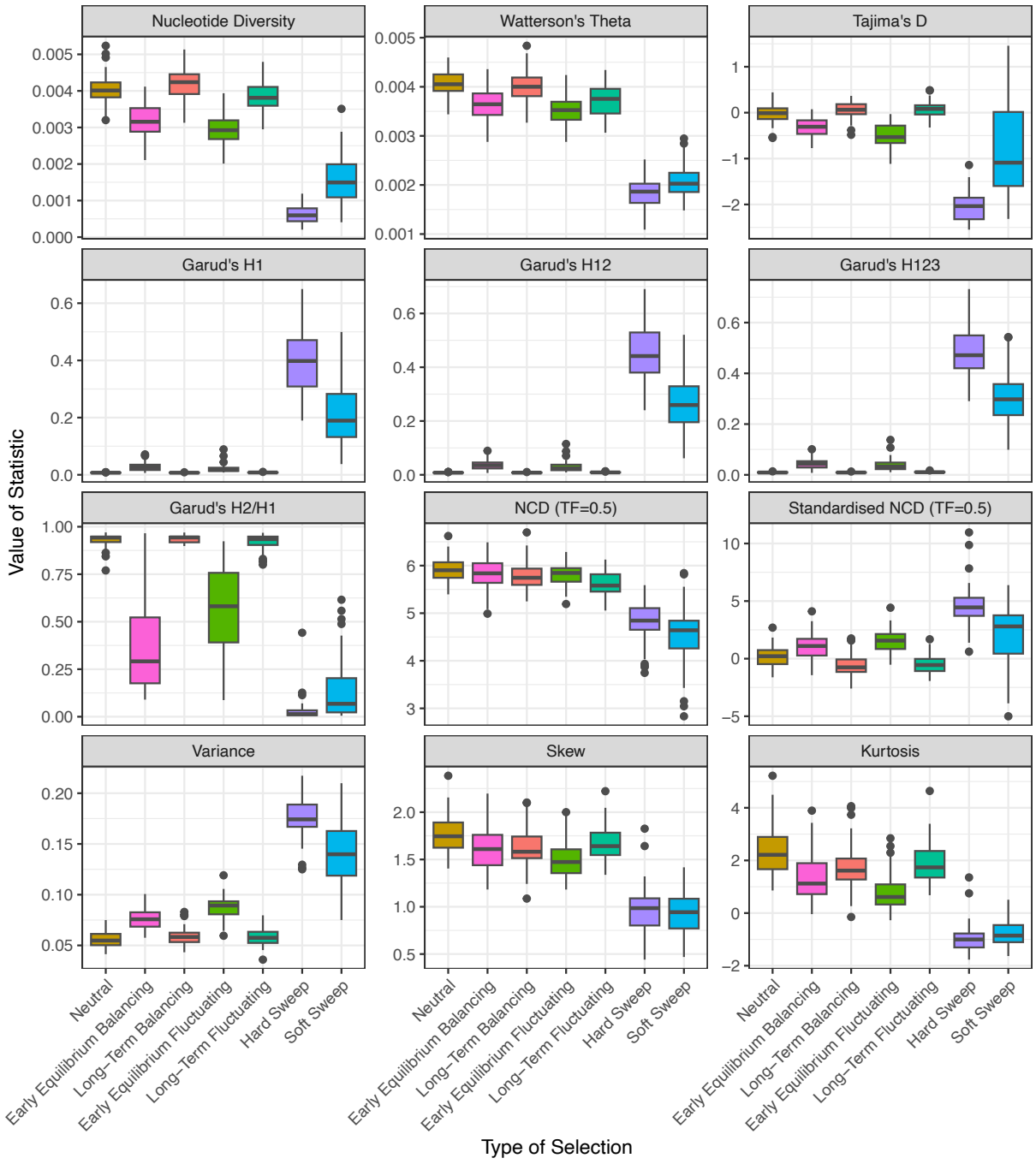

Figure 5. Population genetic statistics at the 10 kb window centred over the selected site for different types of selection.

Boxplots show the distribution of values for each statistic, labelled at the top of each facet, from 50 replicates of each form of selection (s = 0.5). Positive selection in the form of hard (purple) and soft (blue) selective sweeps often cluster together and away from Early Equilibrium and Long-Term Balancing (red and pink) and Fluctuating selection (turquoise and green) and neutral evolution (mustard) for most statistics.

Signals of positive selection are distinct from those of fluctuating selection.

We compared fluctuating selection to other forms of selection using multiple-testing corrected t-tests (Figure S4, S5, S6), starting with the weakest strength of simulated selection ($s = 0.1$). Overall, hard and soft sweep patterns were significantly different ($p < 0.05$; Figure S4) from fluctuating selection at both its early equilibrium and long-term sampling for all statistics excluding comparisons of standardised NCD in comparison with soft sweeps and unstandardised NCD (TF = 0.3) in comparison with hard selective sweeps. We calculated Cohen's D (Cohen 1988), as a means to evaluate the degree of overlap in the distribution of statistics (Grice & Barrett 2014).

Pairwise comparisons of Early Equilibrium Fluctuating and hard selective sweeps for nucleotide diversity, Watterson's theta and variance in SFS ($p < 0.001$) had no more than 5% overlap between the distributions of the two types of selection (Figure S4, S7; Grice & Barrett 2014). This was also seen for Tajima's D ($p < 0.01$) which showed considerably more overlap with soft sweeps (75%) than with hard sweeps (13%). Haplotype-based statistics also follow this trend with 25-40% overlap with hard sweeps and 40-70% overlap with soft sweeps. This suggests that overall, fluctuating selection shows more similarity with soft sweeps than with hard sweeps. However, the skew and kurtosis of the SFS ($p < 0.001$) demonstrated similar levels of overlap with both forms of positive selection, with 20-35% for hard sweep comparisons and 21-25% for soft sweep comparisons, suggesting that these aspects of the SFS are equally similar to hard and soft selective sweeps. Unstandardised NCD with target frequencies of 0.4 and 0.5 were the only two measures that overlap more with hard sweeps (40-70%) than with soft sweeps (32-45%).

When comparing positive selection with Long-Term Fluctuating selection, again most statistics were significantly different ($p < 0.05$) except for the comparison with hard sweeps

for unstandardised NCD (TF = 0.4). Similar to Early Equilibrium Fluctuating selection, Long-Term Fluctuating selection is more distinct from hard selective sweeps than soft selective sweeps for all significant comparisons, with 0-65% and 15-76% overlap respectively across all statistics (Figure S5).

These trends in the overlap between fluctuating selection and hard and soft sweeps continue to be seen with stronger selection (s = 0.5 and s = 1; see Figure 5, S5, S6 and S8). In particular, comparisons of standardised NCD becomes non-significant ($p > 0.05$) between Early Equilibrium Fluctuating and soft selective sweeps for selection coefficients of both 0.5 and 1, as this measure increases to levels that are seen for positive selection. However, this is not true for Long-Term Fluctuating, which consistently shows negative standardised NCD values. A similar behaviour is observed for Tajima's D, which is also indistinct between Early Equilibrium Fluctuating and soft selective sweeps when selection is strong (s = 1), but which is consistently distinct when compared with Long-Term Fluctuating selection. This suggests that shortly after the introduction of the selected allele fluctuating selection SFS patterns are similar to soft selective sweeps (positive standardised NCD, negative Tajima's D), whereas long-term signals become similar to balancing selection (negative standardised NCD, positive Tajima's D). Moreover, all other statistics show significantly distinct distributions between fluctuating and positive selection (Figure S6, S7), although for certain statistics weak positive selection could mimic strong fluctuating selection. For example, when fluctuating selection has a strength of 1 and positive selection has a selection coefficient of 0.1, we find nucleotide diversity is not significantly different between soft positive selection and fluctuating selection at early equilibrium, and comparisons of the variance and kurtosis of the SFS are non-significant between fluctuating selection and hard sweeps at this same time point.

Finally, it should be noted that while fluctuating selection is distinct from positive selection for many statistics, it frequently did not differ from neutral evolution in our analysis. At Early

Equilibrium Fluctuating and $s = 0.1$, fluctuating selection significantly differed from neutral simulations only for nucleotide diversity, Watterson's theta, and variance in the SFS ($p < 0.01$). At Long-Term Fluctuating and $s = 0.1$, Tajima's D, unstandardised NCD of all target frequencies and standardised NCD (TF=0.4 and 0.5) were significantly distinct from neutral evolution ($p < 0.05$). This suggests that while fluctuating selection is distinguishable from positive selection, at least for the central window, differentiating it from neutrality proved to be significantly more challenging.

Next, we focus on discriminating balancing selection from fluctuating selection, which demonstrated more similarity at the central window than positive selection.

Fluctuating selection shows distinct but subtle differences from balancing selection.

Fluctuating selection was next compared to balancing selection. Three selection strengths for fluctuating selection were tested. Both fluctuating and balancing selection were sampled at two time points and only equivalent time points were compared. At early equilibrium when $s = 0.1$, only unstandardised NCD and the skew of the SFS were non-significant between balancing and fluctuating selection ($p > 0.05$). However, at the long-term sampling point, there were no statistics that demonstrated a significant difference between the two forms. Maximum divergence at early equilibrium is seen in Garud's haplotype statistics where overlap between the two selection forms is between 13% and 35% (Figure S9). The variance in the SFS also shows lower levels of overlap (~45%) than the other statistics which share between 61-80% of their distribution.

The number of statistics where the two selection forms significantly differ is at its lowest when the fluctuating selection coefficient is 0.5 (Figure 6). At early equilibrium, this was only H2/H1, the variance and kurtosis of the SFS, and Tajima's D ($p < 0.01$). At the long-

term sampling point, haplotype-based statistics, nucleotide diversity, unstandardised NCD (TF = 0.5) and Watterson's theta showed significance ($p < 0.05$). These comparisons all showed considerable overlap, falling between 51% and 80%. At this selection strength, equilibrium is reached, from a *de novo* frequency, in a similar time frame for both balancing and fluctuating selection (an average of 140 generations for balancing, and 160 generations for fluctuating selection) resulting in similar patterns at this early time point (explored further below).

The most significant differences occur when the strength of fluctuating selection is 1. At early equilibrium, all statistics but unstandardised NCD (TF = 0.4 and 0.5) are significant ($p < 0.05$). Whereas at long-term, only comparisons of haplotype statistics, nucleotide diversity, unstandardised NCD and Watterson's theta are significant.

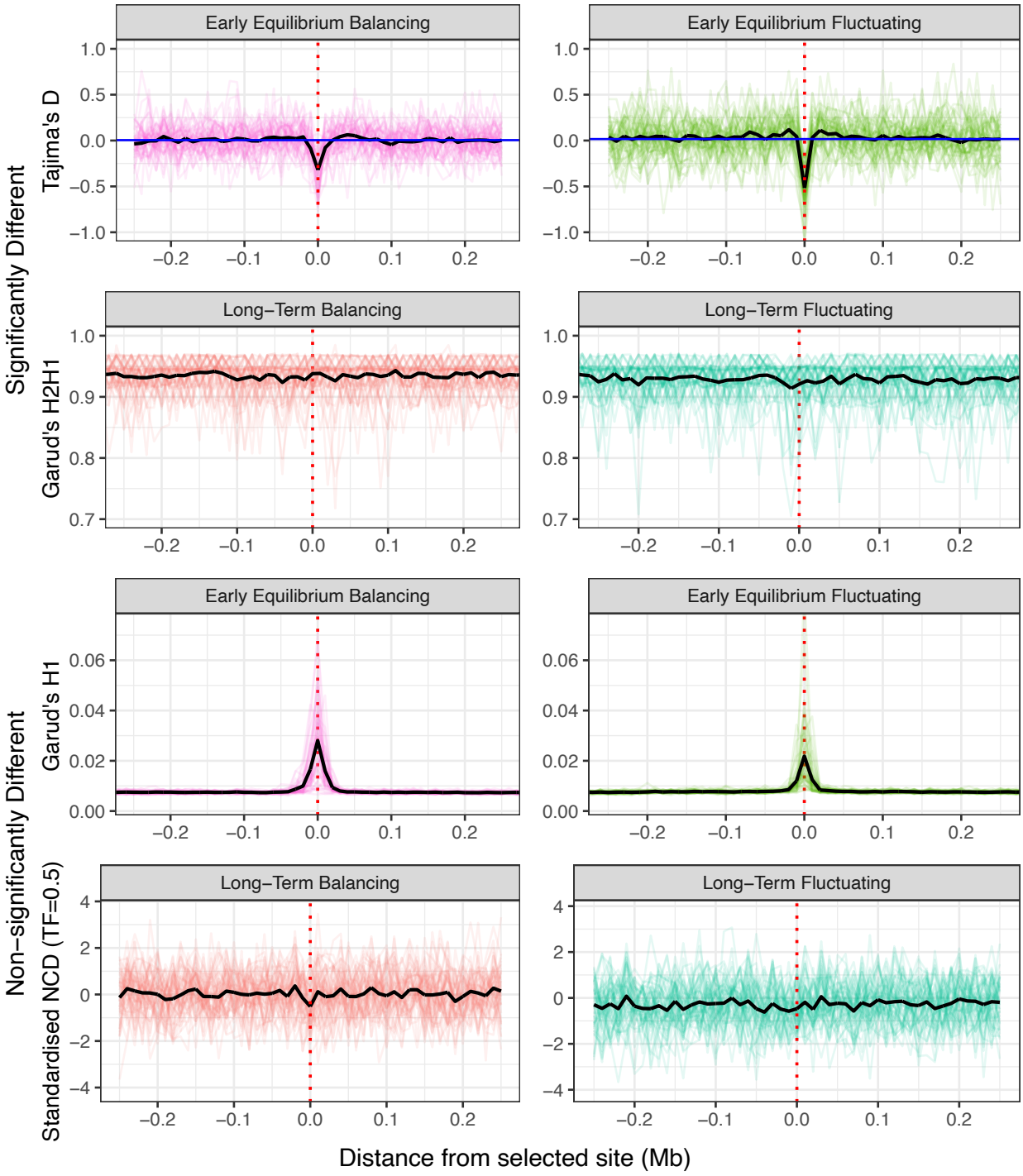

Figure 6. Comparisons between equilibrium balancing and fluctuating selection.

The values of the statistics for comparisons of fluctuating selection (s = 0.5) and balancing selection (s = 0.1). The coloured lines are the values of the replicates, while the black line shows the average value at each window. Both early equilibrium and long-term timepoints are shown. The top two rows show statistics that are significantly different at the central window, while the bottom rows show statistics that demonstrate a non-significant difference. The dashed red line shows the position of the selected site.

If we consider the broader simulated region and when the selection strength is equal between balancing (s = 0.1) and fluctuating selection (s = 0.5), early equilibrium balancing and fluctuating selection show similar signals (Figure 6). The signal looks similar to a partial sweep, which is expected as the selected mutation starts from a *de novo* frequency of $1/2N_e$ and is sampled immediately after the allele frequency becomes stable. For balancing selection this is after an average of 140 generations into the simulation, and 160 generations, with an increased selection coefficient, for fluctuating selection. What is slightly unexpected is the difference in this partial sweep signal between balancing and fluctuating selection. Given the allele frequency trajectory, one would expect fluctuating selection to have a greater partial signal sweep as the selected allele reaches greater frequencies than under balancing selection. However, this is not always the case, with Garud's H1 at early equilibrium showing a smaller peak than balancing selection (Figure 6). Similar distinctions in the signal are seen even when sampling at the same time for both fluctuating and balancing selection (Figure S10) with fluctuating selection showing consistently smaller signals than balancing selection. The initial difference in time to reach equilibrium allele frequency, combined with the fluctuating allele trajectory, is likely causing these observations. The shorter time to reach a stable equilibrium under balancing selection means less recombination occurs, resulting in a greater loss of diversity around the selected site that is maintained until later in the simulation when recombination can break up the haplotype that the selected allele is found on. In addition, balancing selection maintains this signal for longer than fluctuating selection, where it deteriorates faster due to the constant change in the direction of the allele frequency. This partial sweep signal weakens as the selection coefficient decreases and the alleles take more time to reach a balanced equilibrium (Figure S11).

Linear Discriminant Analysis (LDA)

We conducted LDA analysis, using the 'lda' function of the R package *MASS*, to determine if a combination of the summary statistics tested above could be used to discriminate early equilibrium and long-term fluctuating selection from balancing selection and neutral evolution. Multiple aspects of the dataset were examined to see if there is an optimal combination of variables that can best differentiate fluctuating selection both from balancing selection and at different time points (i.e. early equilibrium and long-term). We consider just the central window both at the end of summer and combinations of either the ends of both seasons or the middle and end of summer. We also examined if using multiple windows to capture the signal of selection in flanking regions could improve our ability to discriminate fluctuating selection. As there are a large number of statistics to be considered and not all may significantly contribute to discriminating the different forms of selection, we used a stepwise approach to first determine a set of statistics that allow for the most separation between selection types. The approach utilised the 'greedy.wilks' function (of the *klaR* package) to determine which statistics contribute significantly to discriminating the different selection types and sampling points. This function utilises Wilks' lambda, a measure of how well groups can be separated based on dependent variables and aims to minimise this value to determine which statistics will provide the best discriminatory ability (Wilks 1932). We first conducted stepwise forward variable selection on the training dataset of 30 (out of 50) replicates of each selection type and sampling point. This returned a formula of variables to be used in the subsequent LDA (supplementary tables). The resulting model was then used to predict the type and time point of selection using a cross validation approach on the remaining 20 replicates to determine the accuracy of the model. We compared the accuracy between each type of selection and each time point to determine the ability to distinguish fluctuating selection using different aspects of the data (Figure 7). We tested four different

approaches. The first used only the central window over the selected site sampled at the end of summer. We then tested if using multiple windows improved discrimination, using the central window, the window directly adjacent and a window 250 kb away from the selected site, in the hope of using patterns that extend further into the flanking region to discriminate the forms of selection. The final two approaches utilise multiple sampling points within a seasonal cycle, being either the ends of both summer and winter or the middle and end of summer. Overall, accuracy of prediction increases with increasing strength of fluctuating selection.

We focus on the model using balancing selection with a selection coefficient of 0.1 and fluctuating selection with a strength of 0.5 as these selection strengths were the least differentiated when comparing individual statistics (Figure 7). We find that using multiple time points leads to the most accurate distinction of Early Equilibrium Fluctuating selection, with the use of the data from the end of each season leading to 90% correct classification when classifying this form of selection. In contrast, using a single time point and multiple windows had the most accuracy when predicting Long-Term Fluctuating selection, with 85% of cases correctly classified. This multi-window approach had the highest overall accuracy for all forms of selection and all strengths of fluctuating selection (Figure S12, S13). Together, these results demonstrate that there is still power to distinguish fluctuating selection from other forms of selection even in cases where there are few individual statistics that can differentiate these forms.

Figure 7. Confusion matrix of LDA accuracy.

Confusion matrices show LDA model accuracy for a fluctuating selection coefficient of 0.5 and balancing selection strength of 0.1. The predicted selection type and sampling point is labelled on the x-axis with the model's true classification on the y-axis. The proportion of calls for each combination is shown on the respective tile.

Discussion

Fluctuating selection has been largely examined in the context of allele frequency trajectories over time. While the signature of fluctuating selection on diversity and the SFS at linked neutral sites have been previously elucidated, this study expands this current understanding to haplotype-based statistics as well as statistics developed to identify balancing selection. Moreover, this study focuses on regular fluctuations (i.e. seasonally fluctuating selection) due to the mounting empirical evidence in *Drosophila* and other species (Bergland et al. 2014; Machado et al. 2021; Behrman & Schmidt 2022; Pfenninger & Foucault 2022; Rudman et al.

2022; Bitter et al. 2023; Nunez et al. 2023) while most previous studies have considered only random fluctuations (Haldane & Jayakar 1963; Takahata et al. 1975; Gillespie 1997; Barton 2000; Huerta-Sanchez et al. 2008; Taylor 2013).

The signatures of fluctuating selection in diversity and SFS measures have been previously studied. Wittmann and colleagues found that diversity generally decreases at neutral sites linked to the site under fluctuating selection. However, diversity very closely linked to the selected sites is slowly increasing after the start of selection, leading to a peak within a broader depression of diversity, a specific signature of fluctuating selection that is distinct from either positive or balancing selection. This signature is partly captured in this study, with samples at early equilibrium showing a substantial decrease linked to the selected site. However, even at the long-term sampling point, diversity at our central 10 kb window was never significantly exceeding expected neutral levels (Figure 2). Wittmann et al. note that the width of the peak in diversity around the selected site decreases with increasing amplitude, as it is largely dependent on the harmonic mean allele frequency (Wittmann et al. 2023). Further, in their study the peak only appears below a recombination rate of 10^{-4}. Given the recombination rate used in our study, we would expect the peak to be only about 100 bp in width, which is unlikely to be visible in the 10 kb windows used. Wittmann and colleagues also highlight that this signature may be difficult to identify in empirical data due to its narrow width.

While the signature in the SFS observed here generally supports the findings of Huerta-Sanchez et al. (Huerta-Sanchez et al. 2008) with a decrease in singletons and an increase in high frequency variants, we observe an increase in intermediate variants that was not seen in previous analysis. We also found fluctuating selection to be distinct from positive selection when using the moments of the unfolded SFS, observing decreased variance and increased skew and kurtosis. Fluctuating selection was also seen to affect Tajima's D at early

equilibrium, causing a substantial negative peak at the central window; this is likely due to fluctuating selection only decreasing singletons while increasing intermediate and high-frequency variants.

Fluctuating selection demonstrates visible differences in signal between different points in the seasonal cycle for many of the population genetic statistics tested. This was also seen in Wittmann et al's investigation of long-term diversity signatures of fluctuating selection (Wittmann et al. 2023), where they suggested that the peak in diversity centred on the selected site is expected to be greatest in the middle of the season. However, their long-range effects (i.e. further away from the selected sites) were found to be constant across the seasonal cycle which is consistent with our observations of constant diversity values across the season for Long-Term Fluctuating (Figure 4). Wittmann et al's observed short-range effects seemingly contradict our results, as we identified the end of summer to be where the most distinct signal and the most extreme values for statistics can be observed. However, this is because the summer-favoured allele is introduced as a single mutation in our study, leading to a transient partial sweep signal shortly after due to the summer-allele being largely on a single genetic background while the winter-allele is found on numerous backgrounds. This contrasts to the setup of Wittmann et al, where the seasonal allele is introduced already at 50% frequency and is only sampled at long-term time points. The effect of our choice of model implementation, introducing the selected allele as *de novo* mutation, is also visible in a number of statistics including haplotype-based statistics (Figure 4). Shortly after the introduction of the summer-beneficial mutation, at the end of summer when the allele is at its highest frequency, we see a decrease in diversity and an increase in H1 (haplotype homozygosity) around the selected site. In the middle of the season, this summer allele and its associated haplotype is at an intermediate frequency leading to intermediate signals at these time points. H1 decreases further at the end of winter when the summer allele has

decreased such that its genetic background is less likely to be captured when sampling the population. In addition, we also see a seasonal signature in H1 at the long-term sampling point, whereby we observe a peak around the selected site at the end of each season. This suggests that the end of seasons would be the optimal time to sample populations to capture the signals of fluctuating selection. Moreover, this temporal dependence of signatures could be used to discriminate seasonal selection from constant forms of selection, such as classical balancing selection or selective sweeps, where selection signals are not expected to change over short seasonal timeframes. For example, we show a substantial increase in power in our Linear Discriminant Analysis (LDA) when samples from the end of each season (instead of just the end of summer season) were used for classification. Moreover, by capturing the presence of the signal in the middle of the season, and its absence at the end of the sampled season, one might be able to infer that the allele is favoured towards the opposite season. We have tested reasonably strong levels of selection for positive selection, weaker positive selection may also require this temporal sampling.

It has previously been suggested that fluctuating selection shows signatures of recurrent partial sweeps (Coop & Ralph 2012). As a generalised model Coop & Ralph suggest that as the rate of recurrent sweeps increases, the SFS is further skewed towards rare variants and loses intermediate variants, with high frequency variants increasing but becoming fixed with subsequent sweeps (Coop & Ralph 2012). Our results have similarities and differences with these findings. At the central window we see a general increase in intermediate and high-frequency alleles, and a loss of singletons which contradicts these results. But when we look at linked neutral sites further away from the selected site, we observe this predicted skew towards rare variants (Figure S1).

For lower selection coefficients fluctuating selection is not significantly different from neutral evolution for a number of statistics. Estimates of selection strength of fluctuating alleles from

empirical data range from 0.1 to 1 (Bergland et al. 2014; Machado et al. 2021; Rudman et al. 2022; Bitter et al. 2023) suggesting that signals seen in this study are plausible. Using linear discriminant analysis, we are able to distinguish between fluctuating and balancing selection at all tested selection coefficients with varying degrees of accuracy. The approach used to train the LDA did affect the accuracy of prediction, with models leveraging information from across seasonal cycles having the greatest accuracy for Early Equilibrium Fluctuating but using multiple windows having greater overall accuracy and classification of Long-Term Fluctuating. This highlights the use of different sampling frameworks to leverage this information in future studies. The LDA models consistently included haplotype statistics, particularly H1 and H2/H1, and variance of the SFS suggesting these statistics form the basis on which balancing and fluctuating selection is distinguished.

It is difficult to know how the signatures observed in this study are affected by other forces experienced in a natural environment. Hence, the field will benefit from the exploration of fluctuating selection signals with additional ecological realism such as realistic demographic models with bottlenecks and admixture, rapid boom-bust demography within a seasonal cycle, or combined with other forms of selection such as background selection, or multilocus selection.

Conclusion

Overall, fluctuating selection impacts linked genetic variation as early as when the allele frequency has reached a stable equilibrium. These signatures are distinct from positive selection and change between different points in the seasonal cycle. We find that fluctuating selection can be distinguished from balancing selection, at both its early equilibrium and long-term sampling points and for all tested selection coefficients, when information in seasonal patterns and the genomic pattern around the selected site are leveraged.

Methods

Simulations

All simulations were of a 5 Mb segment with a selected locus at its centre. Four forms of selection were simulated: positive selection in the form of soft and hard selective sweeps, balancing selection, and seasonally fluctuating selection. Positive selection was simulated with the selection pressure acting from the start of the simulation. For hard selective sweeps, a single mutation was added in the first generation at a frequency of $1/2N_e$. To establish multiple mutations for the soft selective sweep, an increased beneficial mutation rate was implemented to establish multiple beneficial mutations at the selected locus early in the simulation, imitating a multiple-origin soft sweep. Balancing selection was simulated from a single mutation with the fitness of individuals dictated by the genotype at the selected site. Individuals with a heterozygous genotype at the selected site had a fitness of 1, and homozygote fitness being 1 minus the selection coefficient (s) of the alternate allele. Similarly, fluctuating selection was simulated from a single mutation in a binary two-season environment with the selection pressure implemented using a fitness model presented by Wittmann and colleagues (Wittmann et al. 2023). The model comprises seasonal selection and dominance coefficients (s and h respectively). Individual fitness depends on the genotype and the season (summer/winter), shown in Table 1. In the simulations, the selection and dominance coefficients were equal between seasons which were each 10 generations in length.

Table 1. Fitness equations from Wittmann et al. 2023 and used to simulate seasonally fluctuating selection. The fitness equation used to calculate an individual's fitness depends on the season they are in and the genotype at the seasonal locus.

Season	ω_{ww}	ω_{sw}	ω_{ss}
Winter	$1 + s_w$	$1 + h_w s_w$	1
Summer	1	$1 + h_s s_s$	$1 + s_s$

As models of fluctuating selection have been developed for *Drosophila melanogaster* populations, we use downscaled population parameters to increase the efficiency of the simulations while capturing the genetic changes expected in the natural population. To simulate a population equivalent to a natural population with an effective population size of 1 million individuals, a recombination rate of 10^{-8} (Comeron et al. 2012), and a mutation rate of 10^{-9} (Schrider et al. 2013; Keightley et al. 2014), we use a population size of 10,000, a recombination rate of 10^{-6} and mutation rate of 10^{-7}. In accordance, the selection coefficient must also be scaled such that $s = 0.01$ in a natural population corresponds to an s of 1 in the downscaled, simulated population. For these simulations, we maintained a constant population size between seasons.

The simulations were comprised of three parts, using a method benchmarked in Chapter 2. Firstly, a coalescent burn-in was simulated using *msprime* (v. 1.2.0; Baumdicker et al. 2022) to establish neutral diversity and ensure coalescence of the lineages of the population in which selection was simulated. The tree sequence of the burn-in (Haller et al. 2019) was then read into the forward simulator, *SLiM* (v. 4.0.1; Haller & Messer 2023), as the starting population. The selected mutation/s were drawn into a genome in the starting population (as described above given the form of selection being simulated) and the simulation was run for

100,000 generations in a binary two-season environment. If the mutation was lost prior to the completion of the forward simulation, the simulation was restarted, reading in the coalescent burn-in population. The number of restarts was recorded (Appendix 1). Tree sequence recording was used to sample 100 individuals for 60 consecutive generations (three seasonal cycles) at various time points throughout the simulation. For positive selection, this also included immediately after the selected allele became fixed in the population. For fluctuating and balancing selection, populations were also sampled after the allele frequency trajectory was at equilibrium for a whole seasonal cycle (early equilibrium). This provided high resolutions at some time points as well as the ability to watch the patterns of selection develop through time. The allele frequency of the selected allele was also recorded (Kelleher et al. 2016, 2018; Haller et al. 2019).

The tree sequence resulting from the forward simulation consisted of the coalescent burn-in as well as the forwards in time simulation in which selection was acting. Neutral mutations were then overlaid onto the tree sequence using msprime. The *pySLiM* (v. 1.0) and *tskit* (v. 0.5.2) libraries (Kelleher et al. 2018; Ralph et al. 2020; Baumdicker et al. 2022) were also used in the processing of the tree sequence throughout the simulation workflow.

Calculation of summary statistics

Subsequent analysis of the tree sequence was conducted using *tskit* (v. 0.5.2), *PySLiM* (1.0), and *scikit-allel* (v. 1.3.5; Miles et al. 2021). Statistics were calculated in 10 kb windows across the simulated segment. A number of summary statistics were calculated. Tajima's D (Tajima 1989) and nucleotide diversity (Tajima 1983), and the number of segregating sites were calculated with *tskit*. Tajima's D was also calculated using *scikit-allel* (v. 1.3.5) which was used to calculate Watterson's theta (Watterson 1975), Garud's H1, H2, H2/H1, and H123 (Garud & Rosenberg 2015). In addition to these statistical functions, we also calculated the

balancing selection statistic NCD (Bitarello et al. 2018). This statistic was calculated in python, using eq. 1.

$$NCD = \sqrt{\frac{\sum_{i=1}^{n}(p_i - TF)^2}{n}} \qquad [1]$$

The NCD statistic uses the minor allele frequencies of mutations in a window and compares them to a target frequency (TF). We used three values for the TF, 0.5, 0.4 and 0.3. As NCD can be correlated to the number of segregating sites in the window, we standardised the NCD values by binning each window by the number of segregating sites. Bins increasing by increments of 25 were used. We then calculated the mean and standard deviation of NCD at each TF under neutral evolution. NCD was then standardised (Z_{NCD}) using eq. 2.

$$Z_{NCD} = \frac{NCD - mean_{neutral}}{sd_{neutral}} \qquad [2]$$

Variance, skew, and kurtosis of the distribution of allele frequencies in each window were also captured, the variance was calculated with the Python library *statistics*, while skew and kurtosis were calculated using the *SciPy* package (v. 1.9.0; Virtanen et al. 2020).

Comparing forms of selection

Pairwise comparisons to obtain values of significance were calculated with a t-test using the 'compare_means' function of *ggpubr* (v. 0.6.0) with the Hochberg correction. The different selection types were compared at the window over the selected site for each statistic investigated. Cohen's D was also calculated for each comparison (Cohen 1988; Grice & Barrett 2014) using the *lsr* R package (v. 0.5.2) to evaluate the difference between means for statistics that returned a significant *p*-value.

Linear Discriminant Analysis (LDA)

Linear Discriminant Analysis was conducted using a stepwise approach, by first determining which statistics separate the groups best and using this tailored subset to determine the formula for the LDA. Analysis was conducted without positive selection to ensure the model was tailored to distinguishing early equilibrium and long-term balancing and fluctuating selection. We used four approaches, the first used only the values of each statistic at the central window from the final generation of summer as the relevant time point in the simulation. The second utilised values from the central window, the adjacent window, and a window 250 kb away from the selected site for each statistic. The third, used only the central windows but values sampled from the end of each season in the relevant seasonal cycles, and the final approach used values from the central window sampled at the middle and end of summer. The model was developed and trained on 30 (out of 50) replicates and then tested on the remaining 20 replicates. The 'greedy.wilks' function, from the R package *klaR* (v. 1.7), was run over all the statistics to determine which variables best separated the different selection types. The level for the F-test decision ('*niveau*' argument of function) was set to 0.05 (i.e. the maximum *p*-value of difference between the previous model and the model with the additional variable). This function conducts a stepwise forward variable selection, testing different combinations of variables to determine the one that confers the most separation and returns a formula for subsequent LDA analysis. The LDA was conducted using the R package *MASS* and its 'lda' function. This formula was used to train the model on the 30 replicates. It was then tested on the remaining 20 replicates using a cross validation approach and the accuracy of prediction of the model for each form and time point of selection was calculated and recorded.

References

Barton NH. 2000. Genetic hitchhiking. Phil. Trans. R. Soc. Lond. B. 355:1553–1562. doi: 10.1098/rstb.2000.0716.

Baumdicker F et al. 2022. Efficient ancestry and mutation simulation with msprime 1.0. Genetics. 220. doi: 10.1093/genetics/iyab229.

Behrman EL, Schmidt P. 2022. How predictable is rapid evolution? bioRxiv. 2022.10.27.514123. doi: 10.1101/2022.10.27.514123.

Bell G. 2010. Fluctuating selection: The perpetual renewal of adaptation in variable environments. Philos. Trans. R. Soc. Lond. B Biol. Sci. 365:87–97. doi: 10.1098/rstb.2009.0150.

Bergland AO, Behrman EL, O'Brien KR, Schmidt PS, Petrov DA. 2014. Genomic evidence of rapid and stable adaptive oscillations over seasonal time scales in *Drosophila*. PLoS Genet. 10:e1004775. doi: 10.1371/journal.pgen.1004775.

Bertram J, Masel J. 2019. Different mechanisms drive the maintenance of polymorphism at loci subject to strong versus weak fluctuating selection. Evolution. 73:883–896. doi: 10.1111/evo.13719.

Bitarello BD et al. 2018. Signatures of long-term balancing selection in human genomes. Genome Biol. Evol. 10:939–955. doi: 10.1093/gbe/evy054.

Bitter MC et al. 2023. Continuously fluctuating selection reveals extreme granularity and parallelism of adaptive tracking. bioRxiv. 2023.10.16.562586. doi: 10.1101/2023.10.16.562586.

Braverman JM, Hudson RR, Kaplan NL, Langley CH, Stephan W. 1995. The hitchhiking effect on the site frequency spectrum of DNA polymorphisms. Genetics. 140:783–796. doi: 10.1093/genetics/140.2.783.

Charlesworth B, Jensen JD. 2021. Effects of selection at linked sites on patterns of genetic variability. Annu. Rev. Ecol. Syst. 52:177–197. doi: 10.1146/annurev-ecolsys-010621-044528.

Charlesworth B, Nordborg M, Charlesworth D. 1997. The effects of local selection, balanced polymorphism and background selection on equilibrium patterns of genetic diversity in subdivided populations. Genet. Res. 70:155–174. doi: 10.1017/s0016672397002954.

Charlesworth D. 2006. Balancing selection and its effects on sequences in nearby genome regions. PLoS Genet. 2:e64. doi: 10.1371/journal.pgen.0020064.

Clarke BC. 1979. The evolution of genetic diversity. Proc. R. Soc. Lond. B Biol. Sci. 205:453–474. doi: 10.1098/rspb.1979.0079.

Cohen J. 1988. *Statistical power analysis for the behavioral sciences*. 2nd ed. Routledge: London, England doi: 10.4324/9780203771587.

Comeron JM, Ratnappan R, Bailin S. 2012. The many landscapes of recombination in *Drosophila melanogaster*. PLoS Genet. 8:e1002905. doi: 10.1371/journal.pgen.1002905.

Coop G, Ralph P. 2012. Patterns of neutral diversity under general models of selective sweeps. Genetics. 192:205–224. doi: 10.1534/genetics.112.141861.

Garcia-Elfring A et al. 2021. Using seasonal genomic changes to understand historical adaptation to new environments: Parallel selection on stickleback in highly-variable estuaries. Mol. Ecol. 30:2054–2064. doi: 10.1111/mec.15879.

Garud NR, Rosenberg NA. 2015. Enhancing the mathematical properties of new haplotype homozygosity statistics for the detection of selective sweeps. Theor. Popul. Biol. 102:94–101. doi: 10.1016/j.tpb.2015.04.001.

Gillespie JH. 1978. A general model to account for enzyme variation in natural populations. V. The SAS-CFF model. Theor. Popul. Biol. 14:1–45. doi: 10.1016/0040-5809(78)90002-3.

Gillespie JH. 1997. Junk ain't what junk does: Neutral alleles in a selected context. Gene. 205:291–299. doi: 10.1016/s0378-1119(97)00470-8.

Glaser-Schmitt A, Wittmann MJ, Ramnarine TJS, Parsch J. 2021. Sexual antagonism, temporally fluctuating selection, and variable dominance affect a regulatory polymorphism in *Drosophila melanogaster*. Mol. Biol. Evol. 38:4891–4907. doi: 10.1093/molbev/msab215.

Gossmann TI, Waxman D, Eyre-Walker A. 2014. Fluctuating selection models and McDonald-Kreitman type analyses. PLoS One. 9:e84540. doi: 10.1371/journal.pone.0084540.

Grice JW, Barrett PT. 2014. A note on Cohen's overlapping proportions of normal distributions. Psychol. Rep. 115:741–747. doi: 10.2466/03.PR0.115c29z4.

Haldane JBS, Jayakar SD. 1963. Polymorphism due to selection of varying direction. J. Genet. 58:237–242. doi: 10.1007/BF02986143.

Haller BC, Galloway J, Kelleher J, Messer PW, Ralph PL. 2019. Tree-sequence recording in SLiM opens new horizons for forward-time simulation of whole genomes. Mol. Ecol. Resour. 19:552–566. doi: 10.1111/1755-0998.12968.

Haller BC, Messer PW. 2023. SLiM 4: Multispecies eco-evolutionary modeling. Am. Nat. 201:E127–E139. doi: 10.1086/723601.

Holderegger R, Kamm U, Gugerli F. 2006. Adaptive vs. neutral genetic diversity: Implications for landscape genetics. Landsc. Ecol. 21:797–807. doi: 10.1007/s10980-005-5245-9.

Huerta-Sanchez E, Durrett R, Bustamante CD. 2008. Population genetics of polymorphism and divergence under fluctuating selection. Genetics. 178:325–337. doi: 10.1534/genetics.107.073361.

Johnson OL, Tobler R, Schmidt JM, Huber CD. 2023. Fluctuating selection and the determinants of genetic variation. Trends Genet. 39:491–504. doi: 10.1016/j.tig.2023.02.004.

Keightley PD, Ness RW, Halligan DL, Haddrill PR. 2014. Estimation of the spontaneous mutation rate per nucleotide site in a *Drosophila melanogaster* full-sib family. Genetics. 196:313–320. doi: 10.1534/genetics.113.158758.

Kelleher J, Etheridge AM, McVean G. 2016. Efficient coalescent simulation and genealogical analysis for large sample sizes. PLoS Comput. Biol. 12:e1004842. doi:

10.1371/journal.pcbi.1004842.

Kelleher J, Thornton KR, Ashander J, Ralph PL. 2018. Efficient pedigree recording for fast population genetics simulation. PLoS Comput. Biol. 14:e1006581. doi: 10.1371/journal.pcbi.1006581.

Kelly JK. 2022. The genomic scale of fluctuating selection in a natural plant population. Evol Lett. 6:506–521. doi: 10.1002/evl3.308.

Kern AD, Hahn MW. 2018. The neutral theory in light of natural selection. Mol. Biol. Evol. 35:1366–1371. doi: 10.1093/molbev/msy092.

Kim Y. 2023. Partial protection from fluctuating selection leads to evolution towards wider population size fluctuation and a novel mechanism of balancing selection. Proc. Biol. Sci. 290:20230822. doi: 10.1098/rspb.2023.0822.

Ludwig A et al. 2015. Twenty-five thousand years of fluctuating selection on leopard complex spotting and congenital night blindness in horses. Philos. Trans. R. Soc. Lond. B Biol. Sci. 370:20130386. doi: 10.1098/rstb.2013.0386.

Lynch M, Wei W, Ye Z, Pfrender ME. 2023. The genome-wide signature of short-term temporal selection. bioRxiv. 2023.04.28.538790. doi: 10.1101/2023.04.28.538790.

Machado HE et al. 2021. Broad geographic sampling reveals the shared basis and environmental correlates of seasonal adaptation in *Drosophila*. eLife. 10:e67577. doi: 10.7554/eLife.67577.

Miles A et al. 2021. *cggh/scikit-allel: v1.3.3*. doi: 10.5281/zenodo.4759368.

Nunez JCB et al. 2023. A cosmopolitan inversion facilitates seasonal adaptation in overwintering *Drosophila*. Genetics. doi: 10.1093/genetics/iyad207.

Park Y, Kim Y. 2019. Partial protection from cyclical selection generates a high level of polymorphism at multiple non-neutral sites. Evolution. 73:1564–1577. doi: 10.1111/evo.13792.

Pfenninger M, Foucault Q. 2022. Population genomic time series data of a natural population suggests adaptive tracking of fluctuating environmental changes. Integr. Comp. Biol. doi: 10.1093/icb/icac098.

Pfenninger M, Foucault Q, Waldvogel A-M, Feldmeyer B. 2022. Selective effects of a short transient environmental fluctuation on a natural population. Mol. Ecol. doi: 10.1101/2022.02.10.479864.

Ralph P, Thornton K, Kelleher J. 2020. Efficiently summarizing relationships in large samples: A general duality between statistics of genealogies and genomes. Genetics. 215:779–797. doi: 10.1534/genetics.120.303253.

Rudman SM et al. 2022. Direct observation of adaptive tracking on ecological time scales in *Drosophila*. Science. 375:eabj7484. doi: 10.1126/science.abj7484.

Schrider DR, Houle D, Lynch M, Hahn MW. 2013. Rates and genomic consequences of

spontaneous mutational events in *Drosophila melanogaster*. Genetics. 194:937–954. doi: 10.1534/genetics.113.151670.

Smith JM, Haigh J. 1974. The hitch-hiking effect of a favourable gene. Genet. Res. 23:23–35. doi: 10.1017/S0016672300014634.

Tajima F. 1983. Evolutionary relationship of DNA sequences in finite populations. Genetics. 105:437–460. doi: 10.1093/genetics/105.2.437.

Tajima F. 1989. Statistical method for testing the neutral mutation hypothesis by DNA polymorphism. Genetics. 123:585–595. doi: 10.1093/genetics/123.3.585.

Takahata N, Ishii K, Matsuda H. 1975. Effect of temporal fluctuation of selection coefficient on gene frequency in a population. Proc. Natl. Acad. Sci. U.S.A. 72:4541–4545. doi: 10.1073/pnas.72.11.4541.

Taylor JE. 2013. The effect of fluctuating selection on the genealogy at a linked site. Theor. Popul. Biol. 87:34–50. doi: 10.1016/j.tpb.2013.03.004.

Virtanen P et al. 2020. SciPy 1.0: fundamental algorithms for scientific computing in Python. Nat. Methods. 17:261–272. doi: 10.1038/s41592-019-0686-2.

Watterson GA. 1975. On the number of segregating sites in genetical models without recombination. Theor. Popul. Biol. 7:256–276. doi: 10.1016/0040-5809(75)90020-9.

Wilks SS. 1932. Certain generalizations in the analysis of variance. Biometrika. 24:471–494. doi: 10.2307/2331979.

Wittmann MJ, Bergland AO, Feldman MW, Schmidt PS, Petrov DA. 2017. Seasonally fluctuating selection can maintain polymorphism at many loci via segregation lift. Proc. Natl. Acad. Sci. U.S.A. 114:E9932–E9941. doi: 10.1073/pnas.1702994114.

Wittmann MJ, Mousset S, Hermisson J. 2023. Modeling the genetic footprint of fluctuating balancing selection: From the local to the genomic scale. Genetics. 223. doi: 10.1093/genetics/iyad022.

Supplementary Information

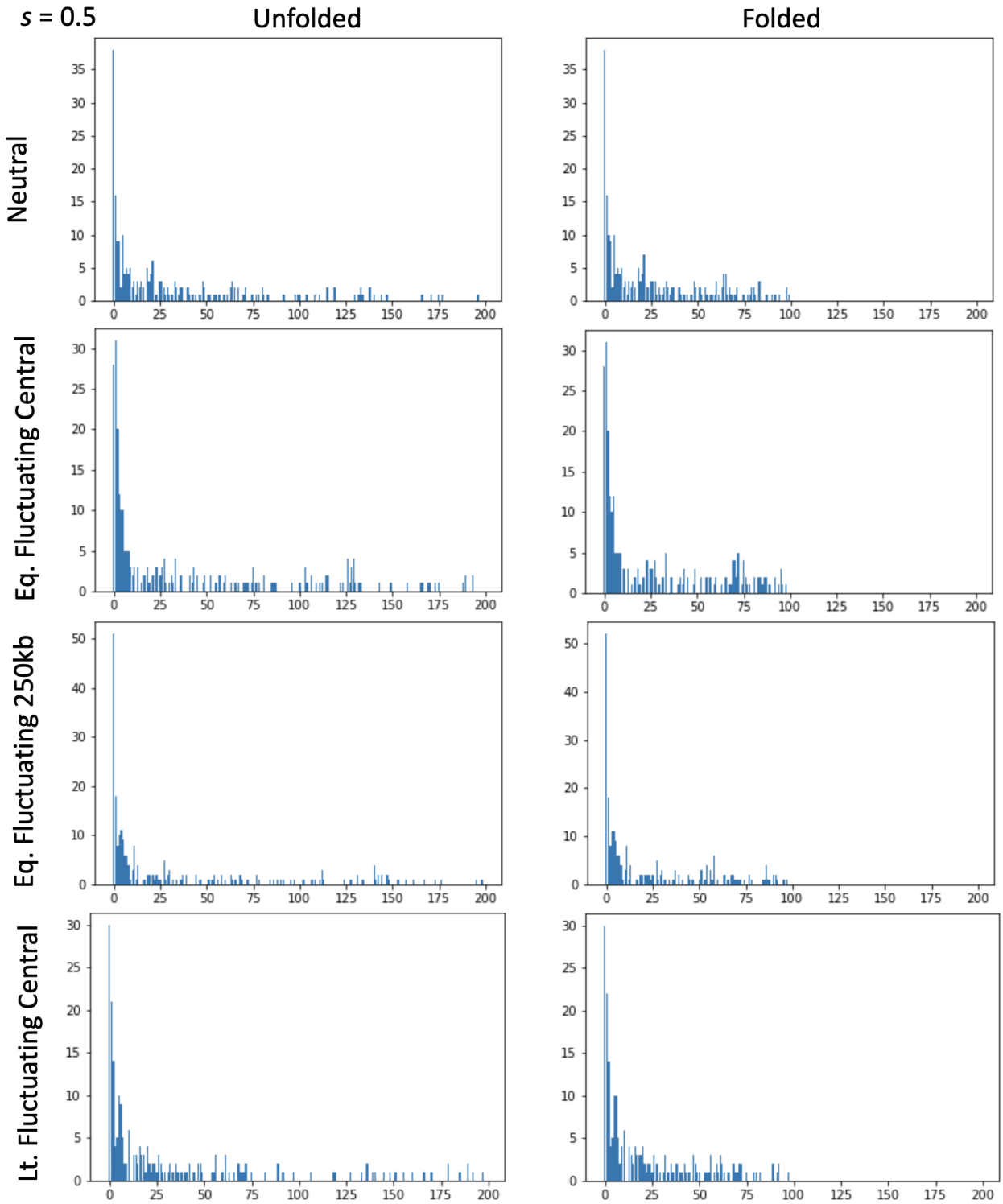

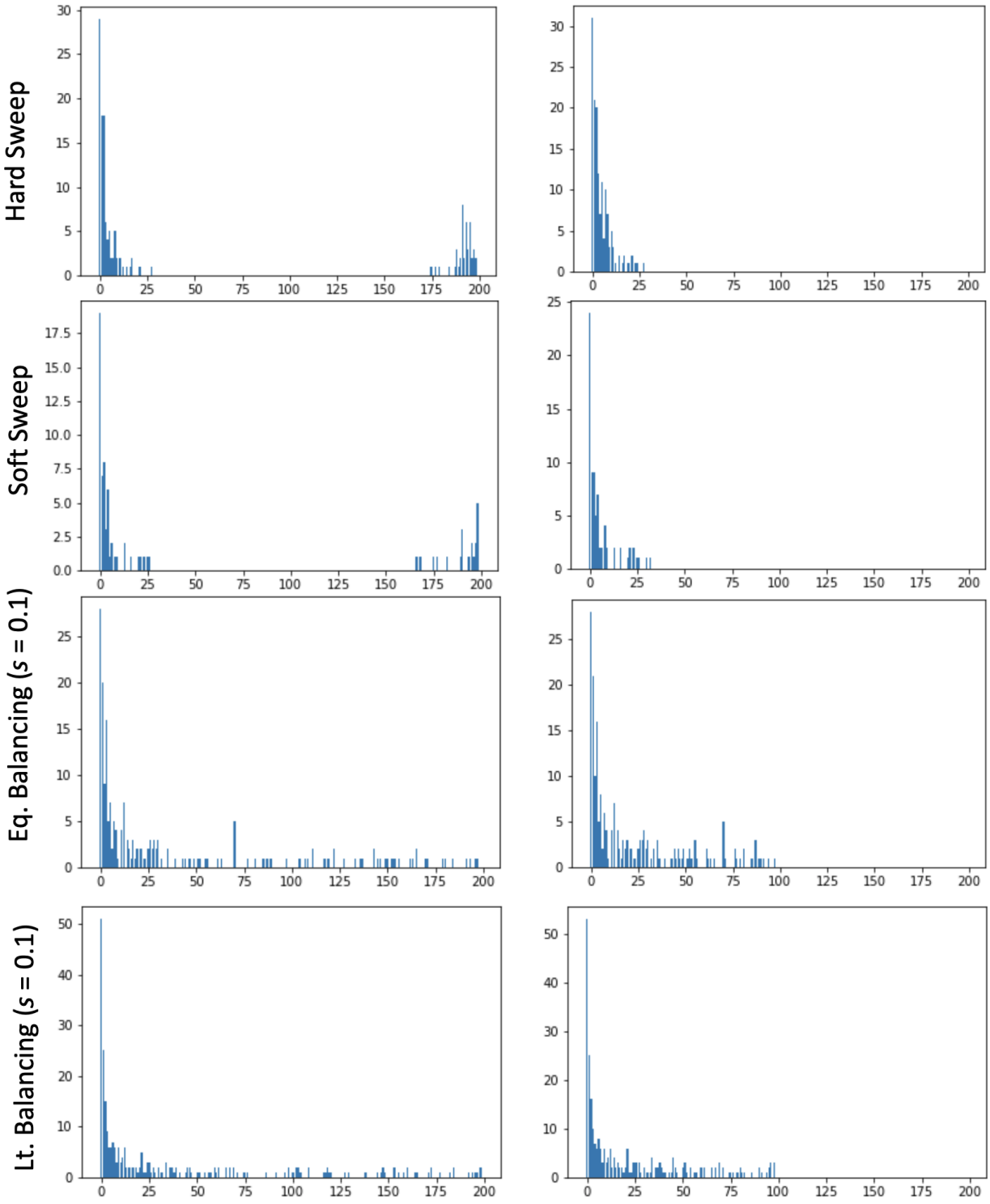

Figure S1. Folded and unfolded site frequency spectrum of a single replicate for each selection type.

Neutral evolution, Early Equilibrium Fluctuating selection (Eq.) at the central window and at a window 250 kb from the selected site, Long-term Fluctuating selection (Lt), hard and soft positive selection after fixation, and Early Equilibrium and Long-term Balancing selection (s = 0.1) all at the central window. Figure extends over two pages.

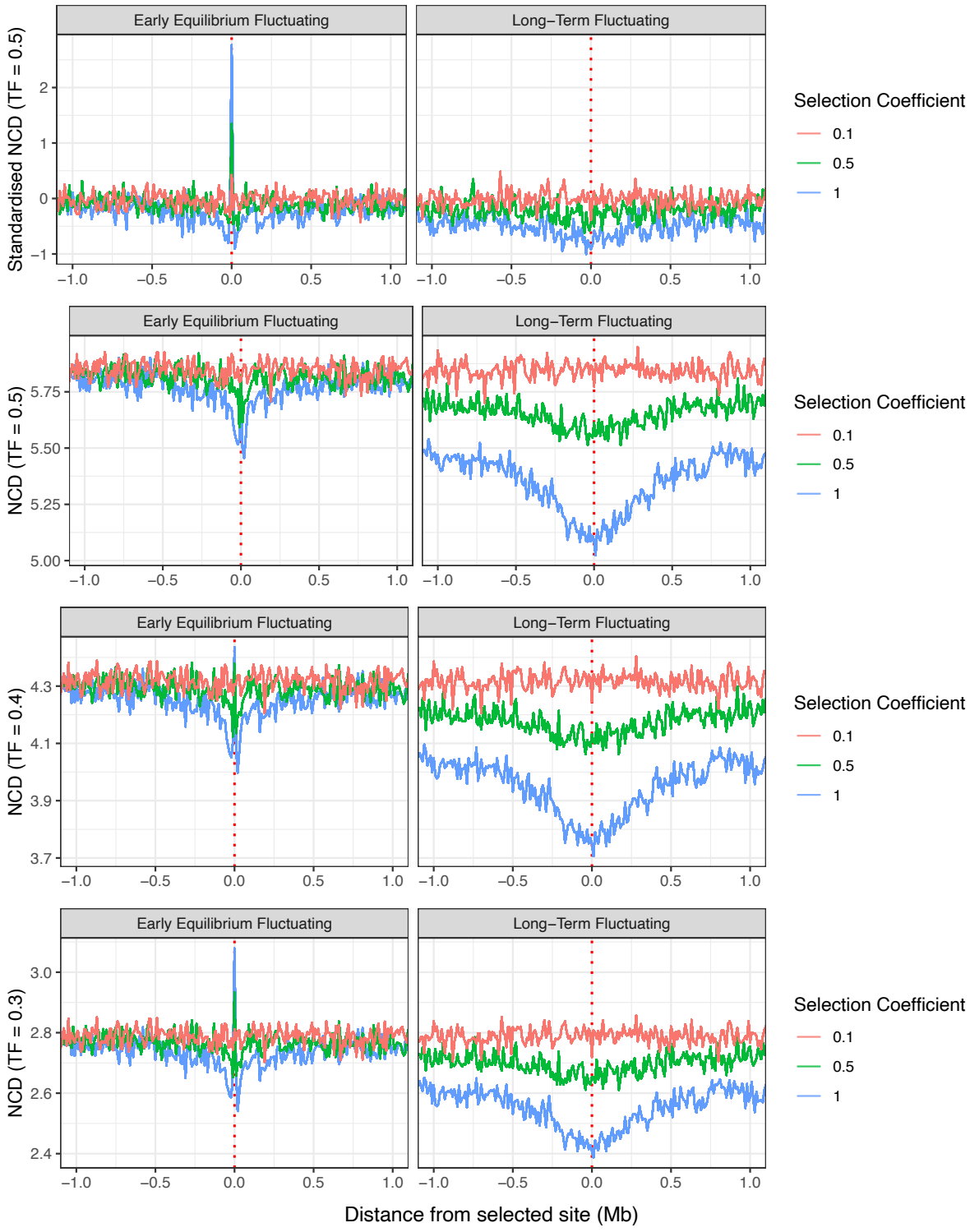

Figure S2. Signatures of fluctuating selection in NCD for all target frequencies.

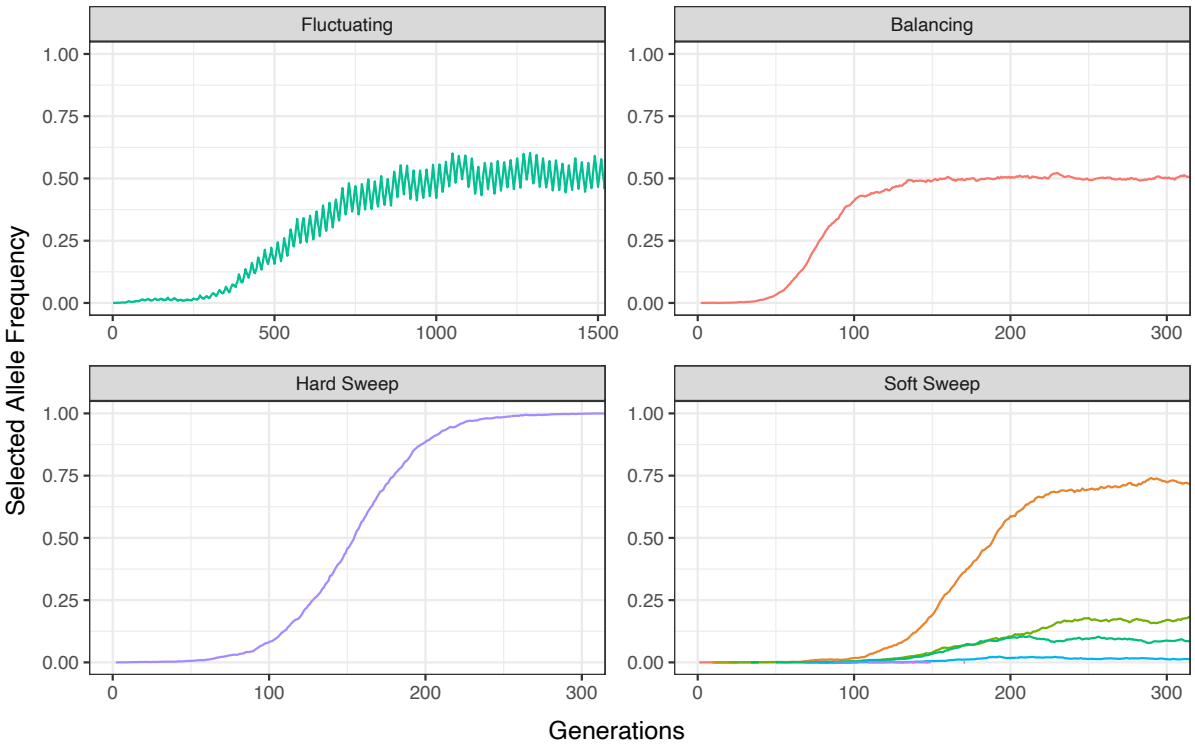

Figure S3. Allele frequency trajectory of single replicate for each form of selection.
Time in simulated generations is shown along the x-axis and the allele frequency of the selected allele is shown on the y-axis. All simulations had a selection coefficient of 0.1 and the data from one replicate is shown on each panel. The establishment of a selected allele/trait is shown for each form of selection. Balancing and fluctuating selection are shown until the allele has reached a stable equilibrium. For fluctuating selection, this follows the summer-favoured allele. For soft sweeps, each beneficial mutation conferring the selected trait is coloured differently, and the combined sum of the frequencies of each mutation gives the frequency of the trait. Hard and soft sweeps are shown until just after fixation.

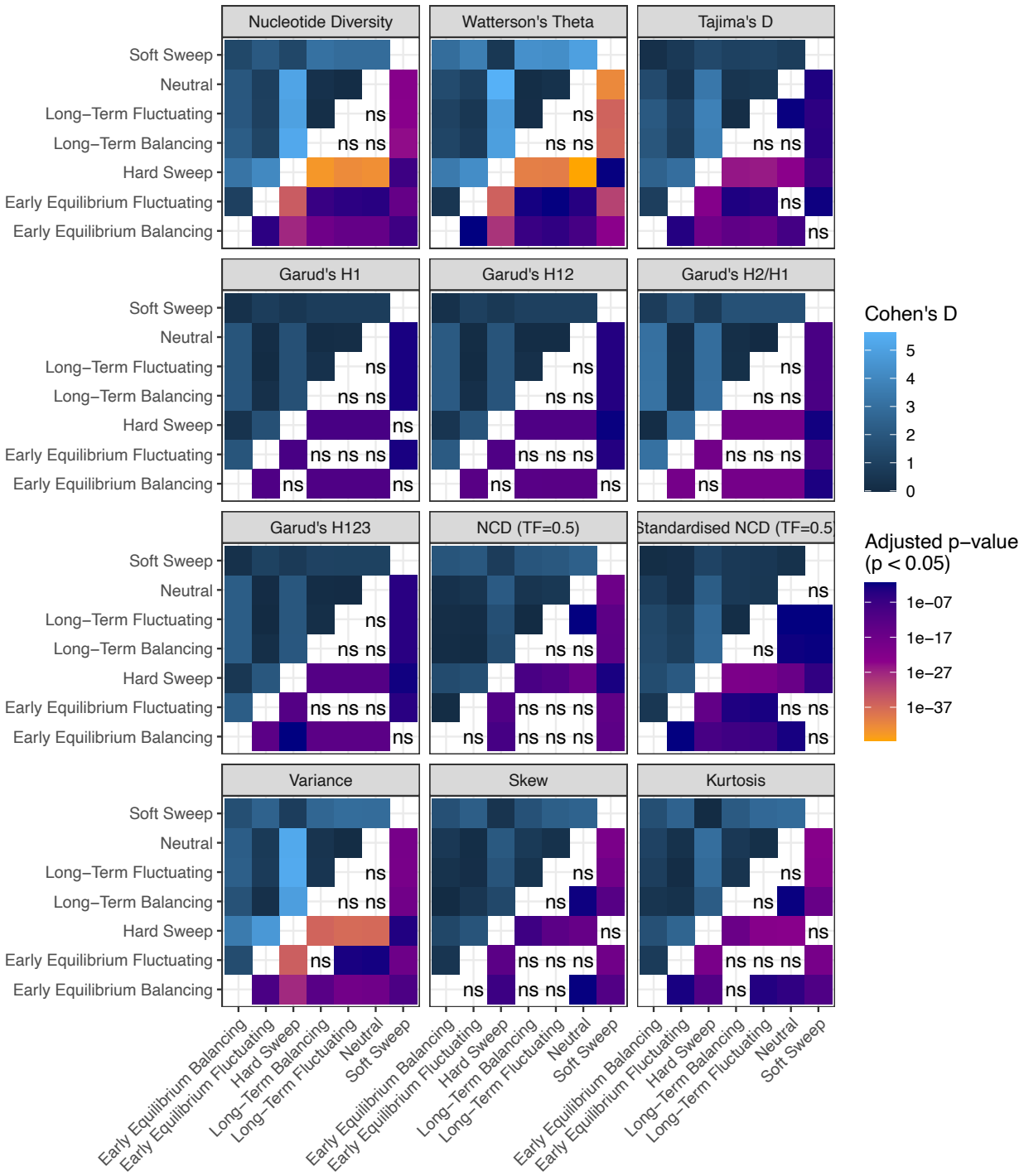

Figure S4. Heatmap of *p*-value and Cohen's D for pairwise comparisons between balancing, fluctuating and positive selection with a selection coefficient of 0.1.

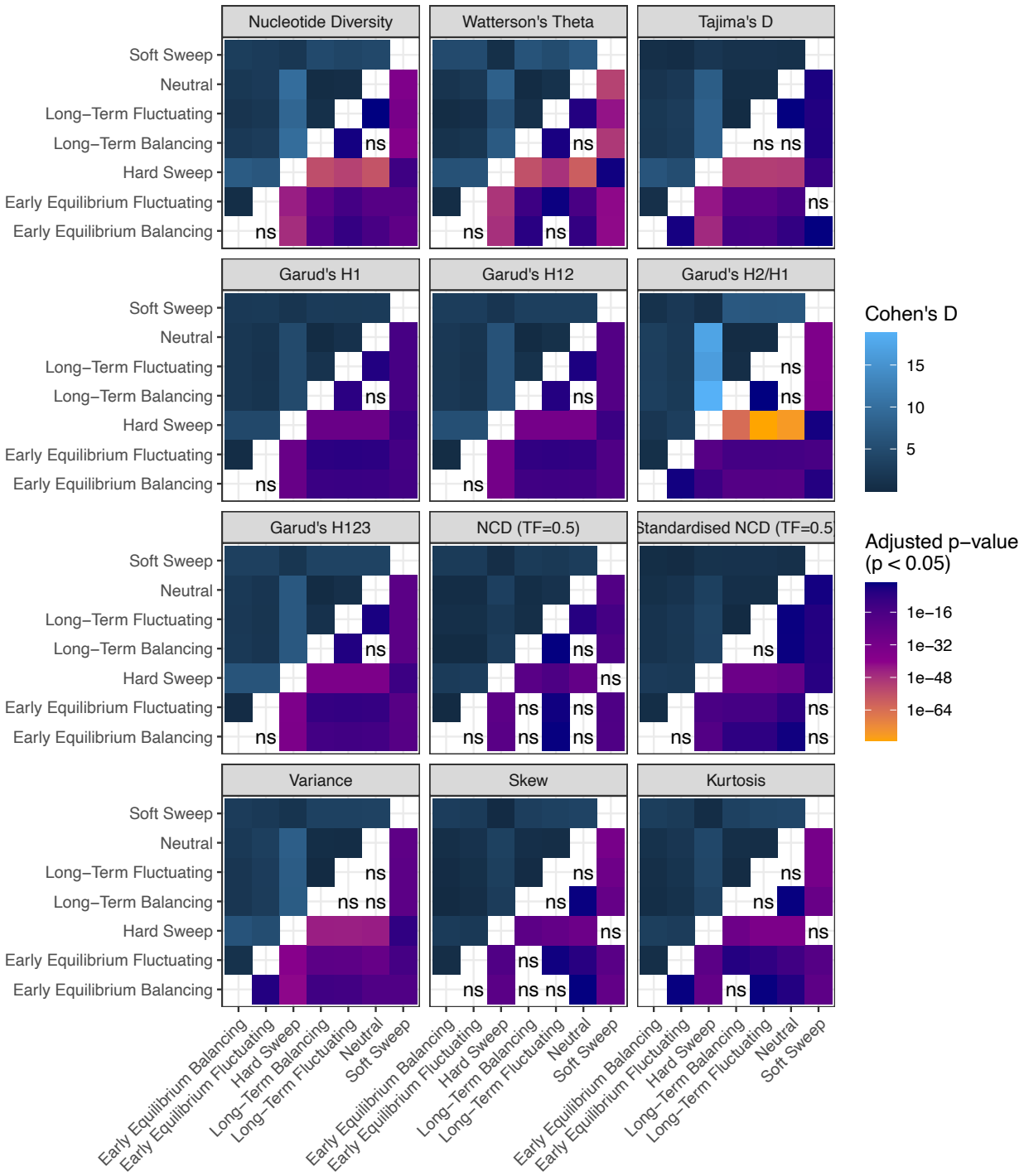

Figure S5. Heatmap of *p*-value and Cohen's D for pairwise comparisons between balancing selection with a selection coefficient of 0.1, with fluctuating selection, and positive selection with a selection coefficient of 0.5.

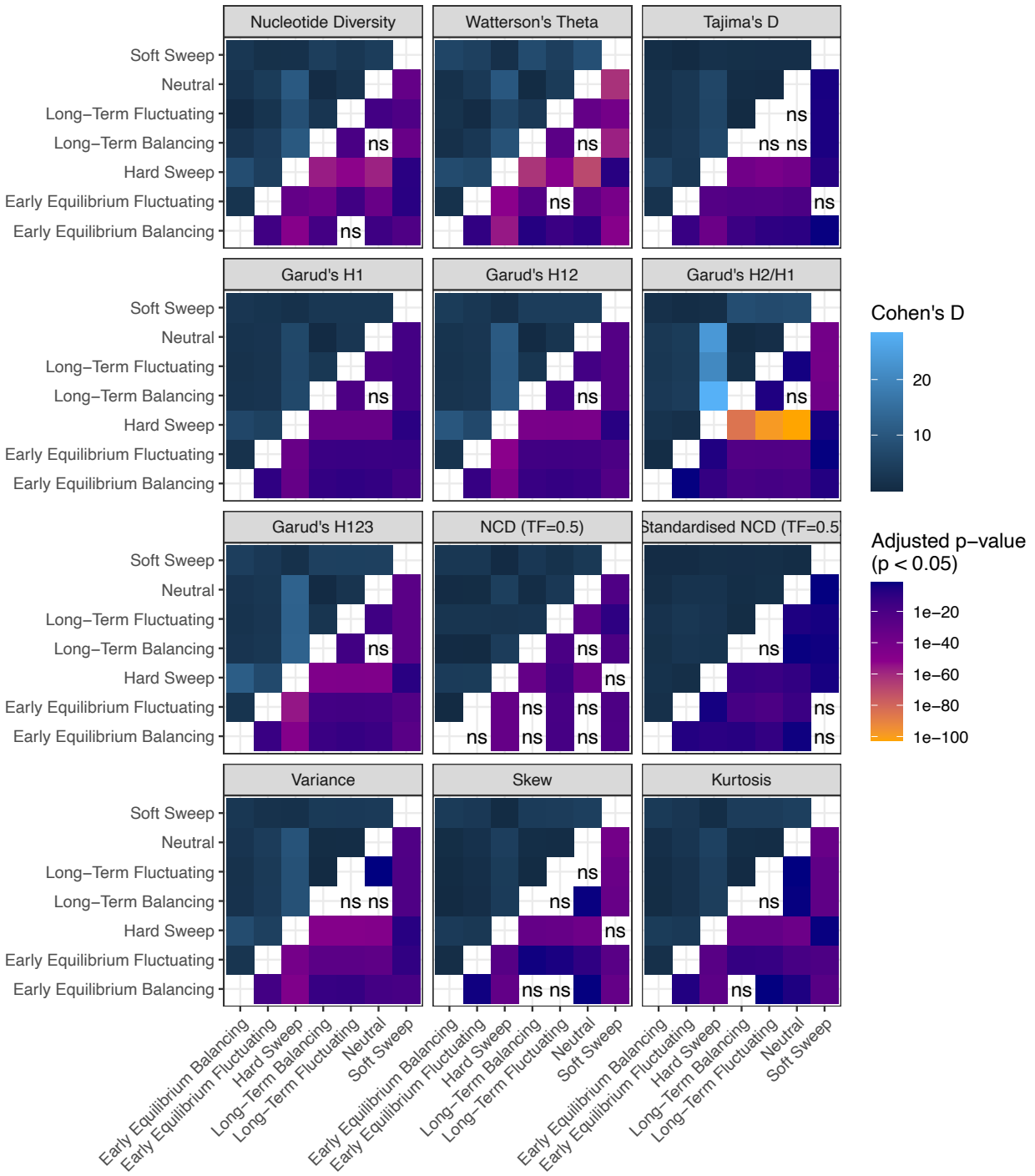

Figure S6. Heatmap of *p*-value and Cohen's D for pairwise comparisons between balancing selection with a selection coefficient of 0.1, with fluctuating selection, and positive selection with a selection coefficient of 1.

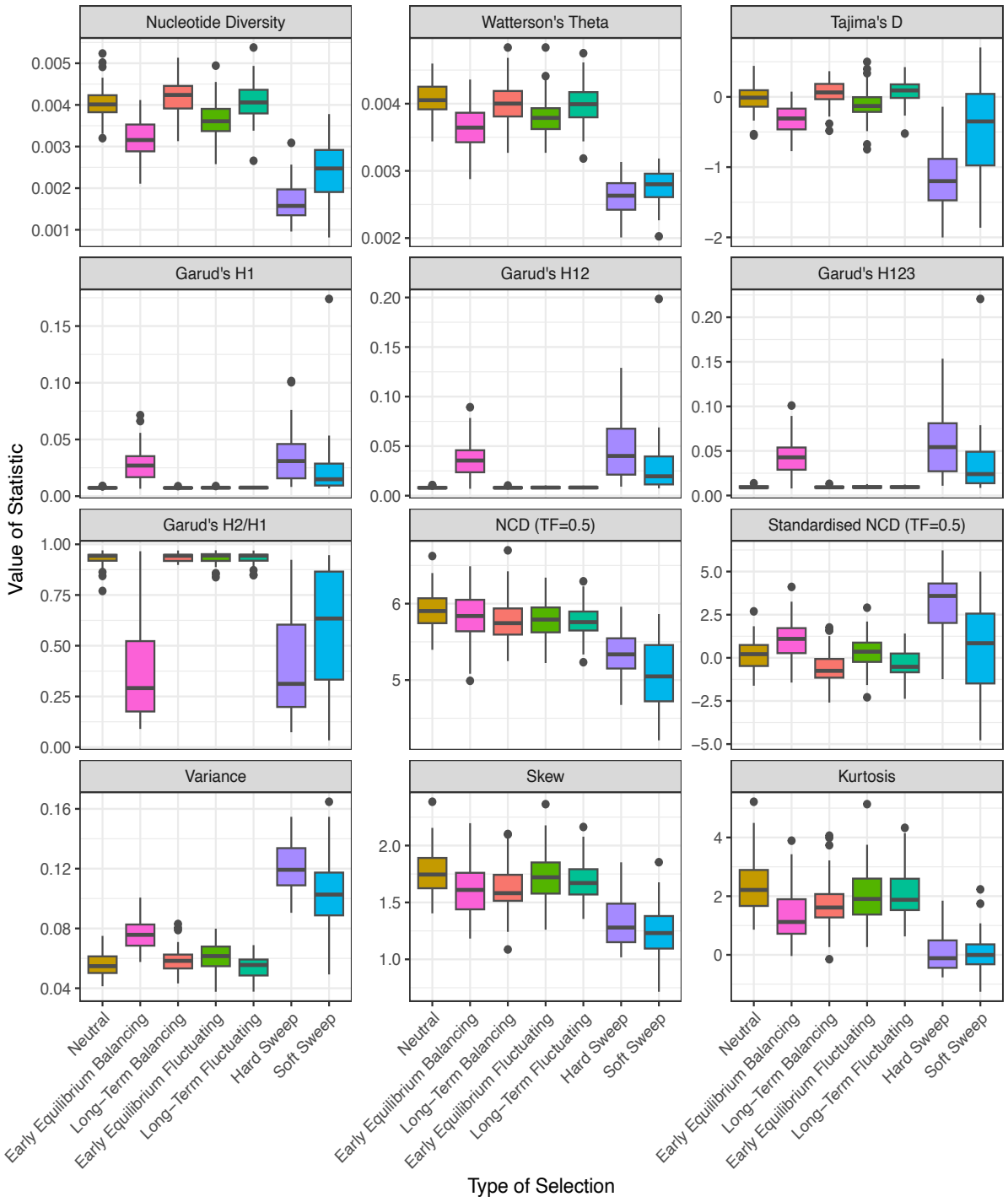

Figure S7. Population genetic statistics at the 10 kb window centred over the selected site for different types of selection (*s* = 0.1).

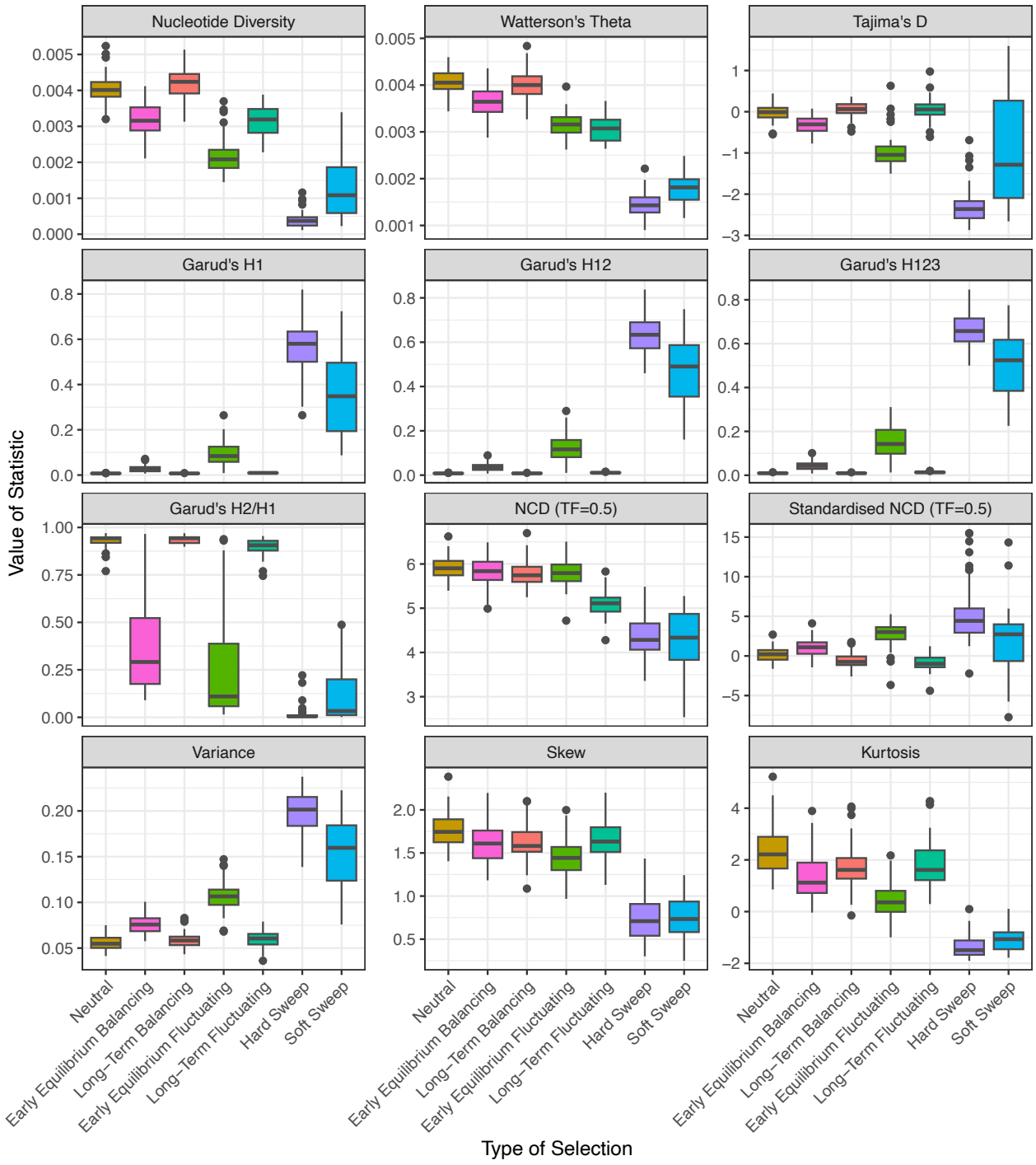

Figure S8. Population genetic statistics at the 10 kb window centred over the selected site for different types of selection (*s* = 1).

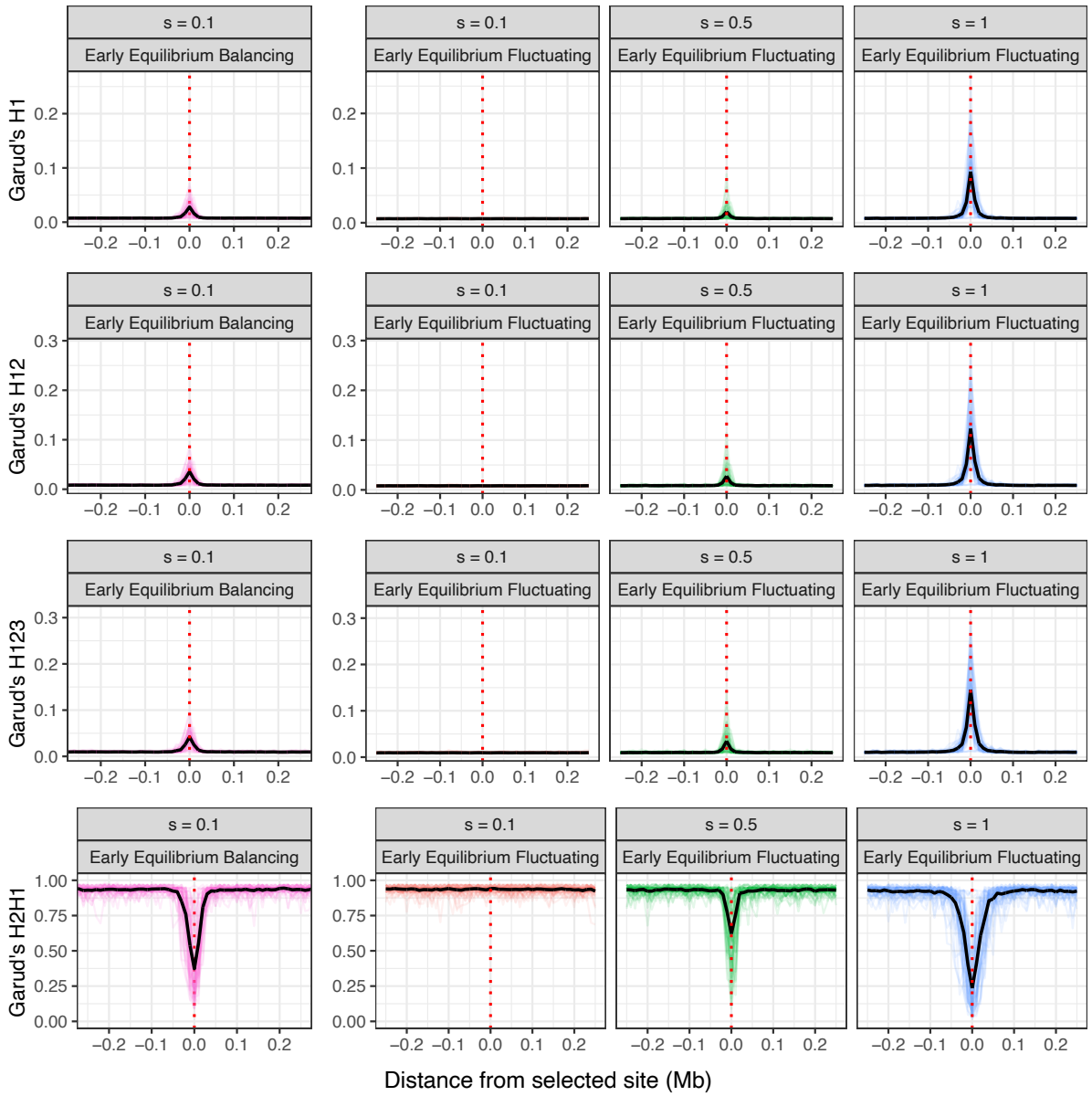

Figure S9. Comparisons of Garud's haplotype statistics between balancing selection (*s* = 0.1) and fluctuating selection of all selection coefficients (*s* = 0.1, 0.5, 1)

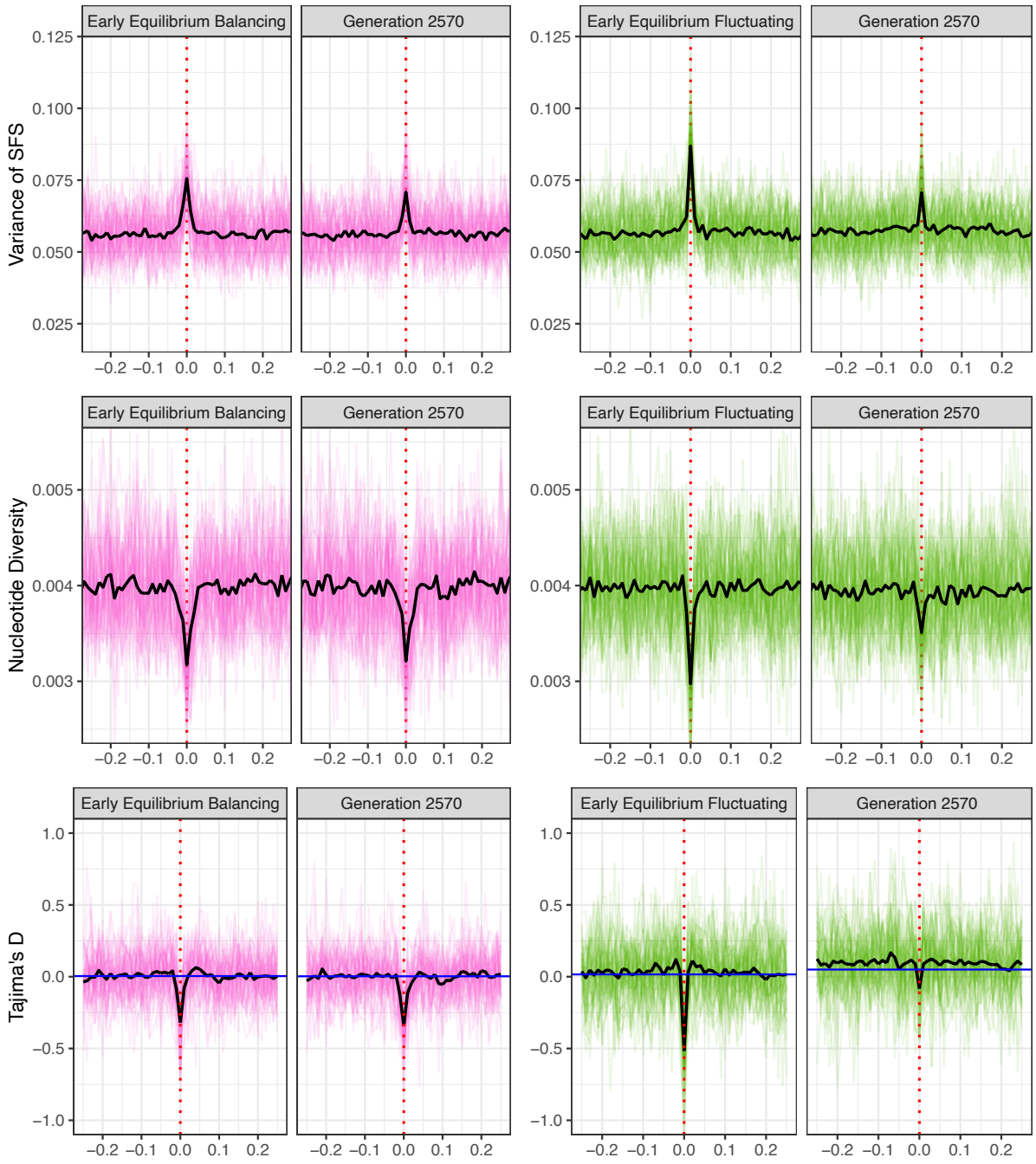

Figure S10. Balancing (*s* = 0.1) and Fluctuating selection (*s* = 0.5) when sampled at the same time point (i.e. 2560 generations) for variance in the SFS, nucleotide diversity, and Tajima's D.

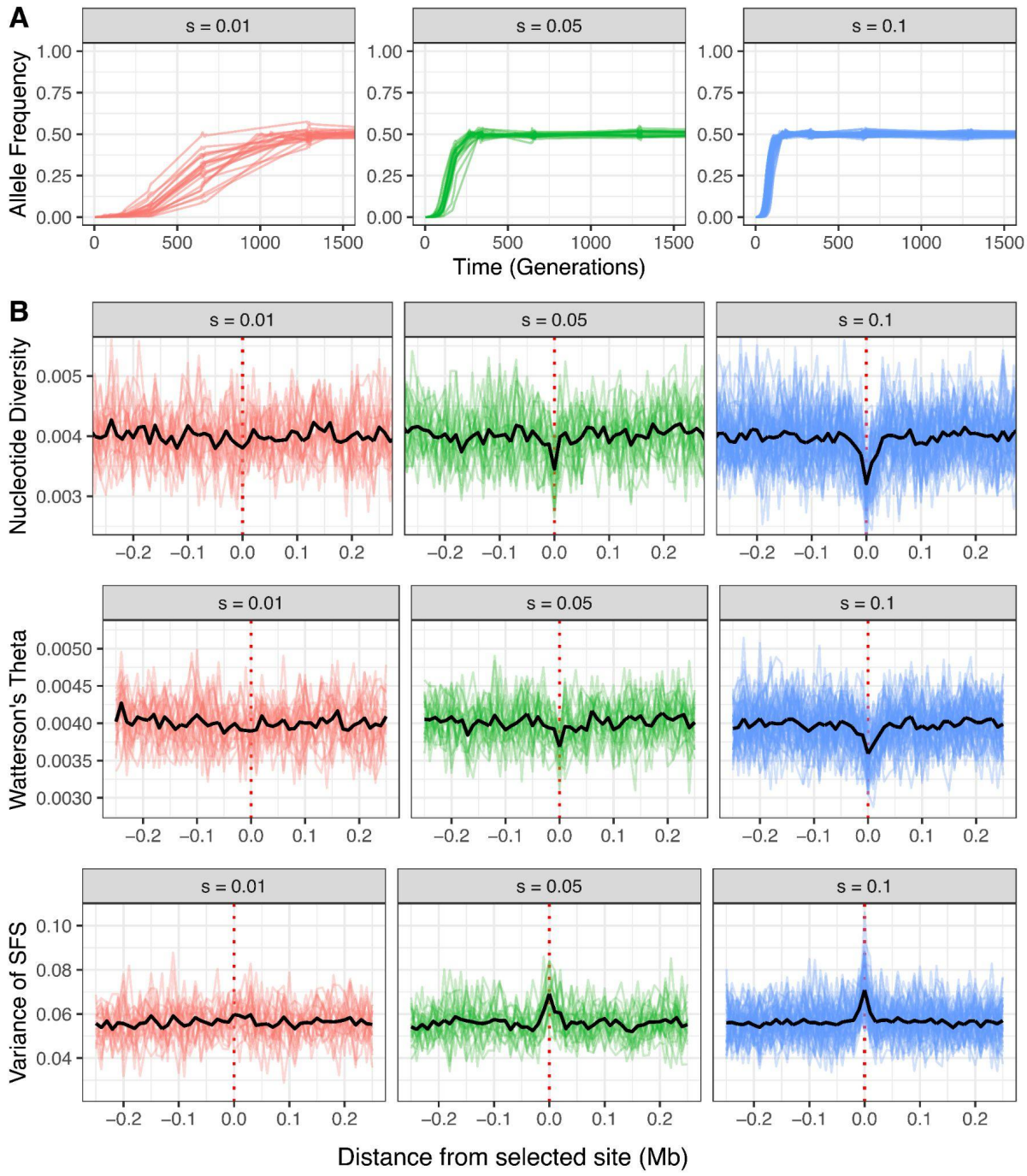

Figure S11. Balancing selection at three selection coefficients (*s* = 0.01, 0.05, 0.1) with the selected allele frequency trajectories from *de novo* to stable equilibrium and associated variance in SFS, Watterson's theta and nucleotide diversity at early equilibrium.

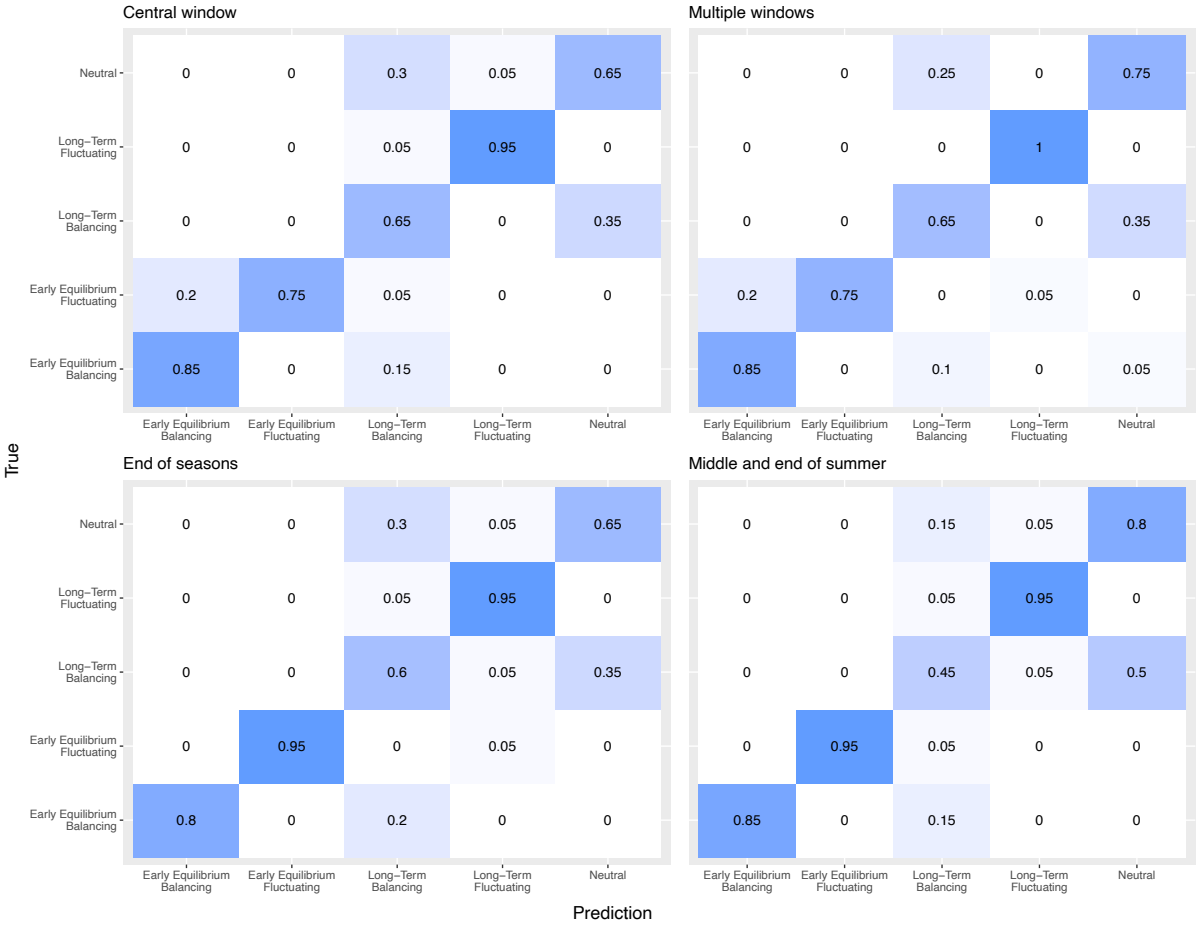

Figure S12. LDA model accuracy for fluctuating selection coefficient of 1.

Figure S13. LDA model accuracy for fluctuating selection coefficient of 0.1.

Appendix 1: Establishment probability

Simulations were restarted if the selected mutation was lost, with fluctuating selection having an increased number of restarts compared to balancing selection and hard selective sweeps (Figure A1-1). Soft sweeps were not investigated due to their differential set-up. The selected allele was most often lost in the first few generations of the simulation for balancing and fluctuating selection and hard selective sweeps. However, though the number of restarts dropped off after this initial peak, for fluctuating selection, the level remained elevated compared to other forms of selection for approximately the next 50 generations, particularly between generations 10 and 20 which was the binary winter season in which the summer-favoured mutation is selected against (Figure A1-2).

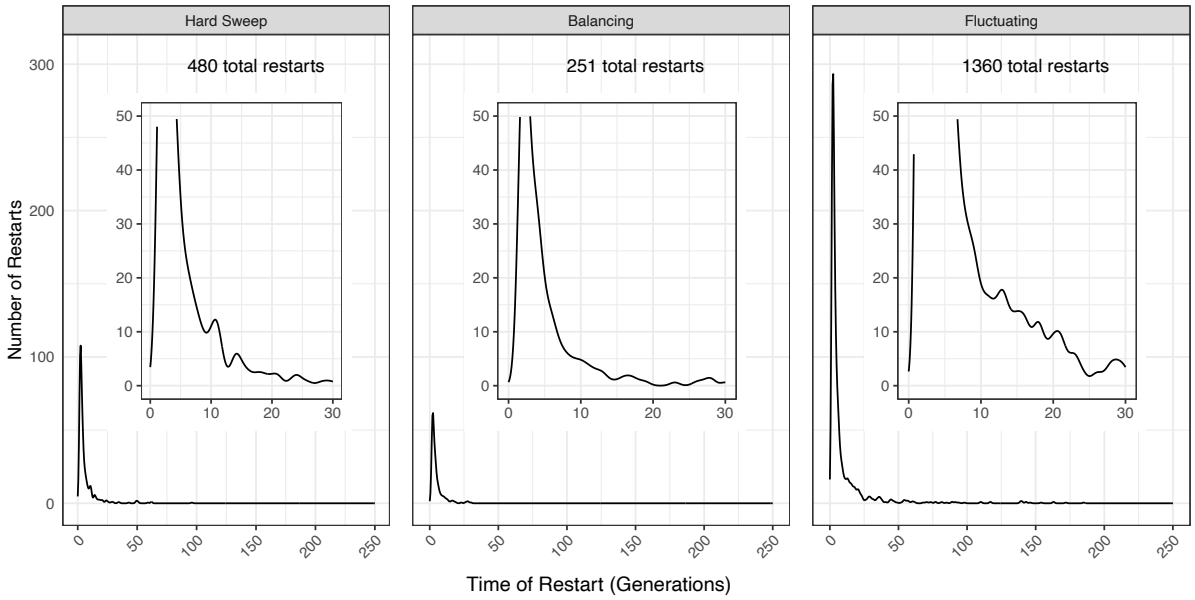

Figure A1-1. Establishment distribution of hard selective sweeps, balancing and fluctuating selection with a selection coefficient of 0.1.

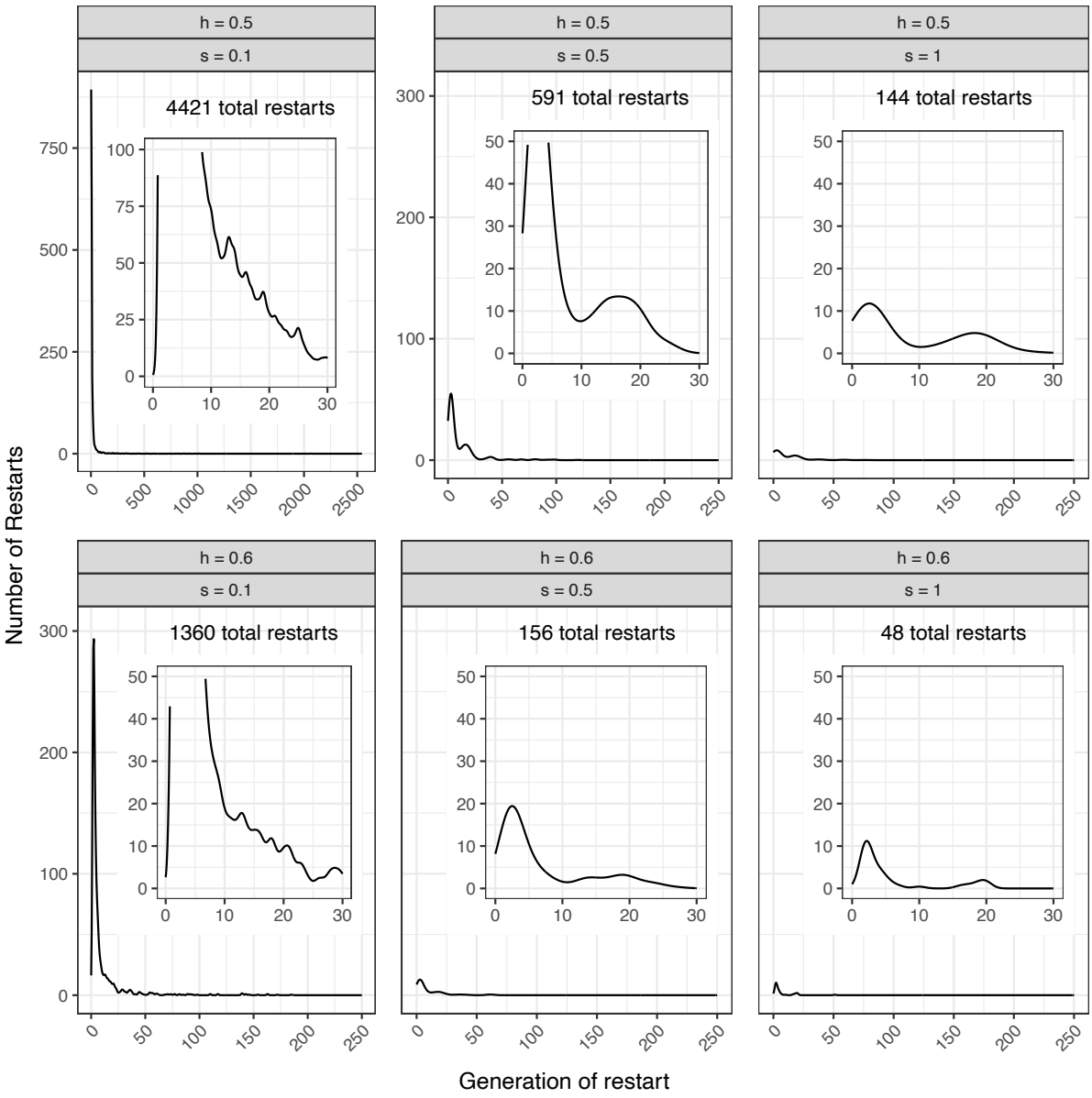

Figure A1-2. Establishment distribution of fluctuating selection for selection coefficients (*s*) 0.1, 0.5, 1 and dominance coefficients (*h*) 0.5, 0.6.

Supplementary tables

s = 0.1, end of summer, central window			
Variables	**Associated Wilks lambda**	***p*-value of difference**	**Model coefficient**
H2/H1	0.181	0.001	-11.633
Variance of SFS	0.138	0.001	51.182
Nucleotide diversity	0.114	0.001	-977.703
H1	0.101	0.005	-339.37
H12	0.093	0.05	215.561
Watterson's theta	0.086	0.05	1082.165

s = 0.1, end of summer, central, adjacent and 250 kb window			
Variables	**Associated Wilks lambda**	***p*-value of difference**	**Model coefficient**
H2/H1 - Central	0.181	0.001	-8.981
Variance of SFS - Central	0.138	0.001	49.18
Nucleotide diversity - Central	0.114	0.001	-1007.584
H1 - Central	0.101	0.005	-373.062
H12 - Central	0.093	0.05	257.284
H2/H1 - Adjacent	0.083	0.02	-3.863
Watterson's theta - Central	0.077	0.05	1142.683

s = 0.1, end of summer and winter, central window			
Variables	**Associated Wilks lambda**	***p*-value of difference**	**Model coefficient**
H2/H1 - Winter	0.138	0.001	-11.983
Variance of SFS - Summer	0.108	0.001	37.191
Tajima's D - Summer	0.090	0.001	-2.94
H1 - Winter	0.082	0.01	-277.256
H123 - Winter	0.072	0.001	166.117
Tajima's D - Winter	0.066	0.05	1.767
Nucleotide diversity - Summer	0.062	0.05	-369.679
Nucleotide diversity - Winter	0.056	0.05	356.483

s = 0.1, middle and end of summer, central window			
Variables	**Associated Wilks lambda**	***p*-value of difference**	**Model coefficient**
H2/H1 - Middle	0.141	0.001	-9.766
Tajima's D- End	0.110	0.001	1.824
Variance of SFS - End	0.092	0.001	-30.421
H1 - Middle	0.083	0.01	302.315
H123 - Middle	0.071	0.001	-221.207

s = 0.5, end of summer, central window			
Variables	**Associated Wilks lambda**	***p*-value of difference**	**Model coefficient**
H2/H1	0.278	0.001	8.229
Variance of SFS	0.161	0.001	-59.51
Tajima's D	0.121	0.001	1.03
H1	0.090	0.001	136.26
Nucleotide diversity	0.076	0.001	1079.059
H123	0.065	0.001	-88.215
H12	0.057	0.001	67.5
Watterson's theta	0.053	0.05	-718.281

s = 0.5, end of summer, central, adjacent and 250 kb window			
Variables	**Associated Wilks lambda**	***p*-value of difference**	**Model coefficient**
H2/H1 - Central	0.278	0.001	7.765
Variance of SFS - Central	0.161	0.001	-57.324
Tajima's D - Central	0.121	0.001	0.788
H1 - Central	0.090	0.001	126.610
Watterson's theta - Adjacent	0.072	0.001	-103.508
H123 - Central	0.061	0.001	80.698
Watterson's theta - Central	0.053	0.001	-939.575
H12 - Central	0.047	0.005	70.000
Watterson's theta – 250 kb	0.042	0.01	-396.169
Nucleotide diversity - Central	0.038	0.005	1299.880
H2/H1 - Adjacent	0.035	0.05	1.655

s = 0.5, end of summer and winter, central window			
Variables	**Associated Wilks lambda**	***p*-value of difference**	**Model coefficient**
H2/H1 - Winter	0.193	0.001	-3.83
H2/H1 - Summer	0.075	0.005	6.386
Variance of SFS - Summer	0.049	0.001	-95.435
Variance of SFS - Winter	0.024	0.001	72.778
H1 - Summer	0.018	0.001	114.468
Tajima's D - Summer	0.014	0.001	1.24
Nucleotide diversity - Summer	0.012	0.001	5796.645
Nucleotide diversity - Winter	0.009	0.001	-5446.187
H123 - Winter	0.007	0.001	-155.476
H12 - Winter	0.006	0.001	87.499

s = 0.5, middle and end of summer, central window			
Variables	**Associated Wilks lambda**	***p*-value of difference**	**Model coefficient**
H2/H1 - Middle	0.258	0.001	-5.016
Variance of SFS - End	0.133	0.001	-99.46
Variance of SFS - Middle	0.058	0.001	60.662
Nucleotide diversity - End	0.047	0.001	4643.404
Nucleotide diversity - Middle	0.036	0.001	-4389.633
Watterson's theta - Middle	0.031	0.001	-103.165
H1 - End	0.026	0.001	121.168
H2/H1 - End	0.022	0.001	7.427
H123 - Middle	0.019	0.001	-537.25
Tajima's D - End	0.017	0.005	2.17
H12 - Middle	0.015	0.005	504.016

s = 1, end of summer, central window			
Variables	**Associated Wilks lambda**	***p*-value of difference**	**Model coefficient**
H2H1	0.212	0.001	5.311
Watterson's theta	0.074	0.001	-379.052
H123	0.032	0.001	-16.487
Variance of SFS	0.022	0.001	-58.557
H1	0.018	0.001	38.695
Nucleotide diversity	0.016	0.05	827.106

s = 1, end of summer, central, adjacent and 250 kb window			
Variables	**Associated Wilks lambda**	***p*-value of difference**	**Model coefficient**
H2/H1 - Central	0.212	0.001	-5.469
Watterson's theta - Central	0.074	0.001	120.781
H123 - Central	0.032	0.001	13.151
Watterson's theta - Adjacent	0.019	0.001	-921.171
Variance of SFS - Central	0.014	0.001	56.767
H1 - Central	0.011	0.001	-366.792
Kurtosis of SFS - Adjacent	0.010	0.05	-0.0275
Nucleotide diversity - Central	0.009	0.05	-794.486

s = 1, end of summer and winter, central window			
Variables	**Associated Wilks lambda**	***p*-value of difference**	**Model coefficient**
H2/H1 - Summer	0.212	0.001	-2.757
H2/H1 - Winter	0.056	0.001	1,909
Watterson's theta - Summer	0.019	0.001	-3513.087
Variance of SFS - Summer	0.012	0.001	6.667
H1 - Summer	0.008	0.001	-16.319
Variance of SFS - Winter	0.007	0.001	9.113
Tajima's D - Winter	0.005	0.001	6.054
Tajima's D - Summer	0.004	0.001	-4.902
Watterson's theta - Winter	0.004	0.001	2750.617

s = 1, middle and end of summer, central window			
Variables	**Associated Wilks lambda**	***p*-value of difference**	**Model coefficient**
H2/H1 - Middle	0.186	0.001	-8.075
Watterson's theta - End	0.064	0.001	-570.102
H123 - End	0.024	0.001	14.754
Variance of SFS - End	0.017	0.001	68.353
Variance of SFS - Middle	0.013	0.001	-12.531
H1 - End	0.011	0.001	-33.935
NCD (TF = 0.3) - Middle	0.009	0.001	1.328
H1 - Middle	0.008	0.005	-33.203

Chapter 4

The effect of fluctuating selection on effective population size

Statement of Authorship

Title of Paper	The effect of fluctuating selection on effective population size
Publication Status	☐ Published ☐ Accepted for Publication ☐ Submitted for Publication ☒ Unpublished and Unsubmitted w ork w ritten in manuscript style
Publication Details	

Principal Author

Name of Principal Author (Candidate)	Olivia L. Johnson		
Contribution to the Paper	Conceptualisation, developed and ran simulations, data analysis, interpretation, wrote the manuscript.		
Overall percentage (%)	85%		
Certification:	This paper reports on original research I conducted during the period of my Higher Degree by Research candidature and is not subject to any obligations or contractual agreements with a third party that would constrain its inclusion in this thesis. I am the primary author of this paper.		
Signature		Date	08/01/2024

Co-Author Contributions

By signing the Statement of Authorship, each author certifies that:

i. the candidate's stated contribution to the publication is accurate (as detailed above);
ii. permission is granted for the candidate in include the publication in the thesis; and
iii. the sum of all co-author contributions is equal to 100% less the candidate's stated contribution.

Name of Co-Author	Christian D. Huber		
Contribution to the Paper	Conceptualisation, development of simulations, data analysis, interpretation, wrote the manuscript.		
Signature		Date	08/01/2024

Name of Co-Author	Raymond Tobler		
Contribution to the Paper	Conceptualisation, development of simulations, data analysis, interpretation, manuscript revision.		
Signature		Date	08/01/24

Name of Co-Author	Joshua M. Schmidt		
Contribution to the Paper	Conceptualisation, development of simulations, data analysis, interpretation, manuscript revision.		
Signature		Date	09/01/24

Introduction

Effective population size (N_e) is a population genetic measure of the ideal population size that explains the levels of genetic drift (i.e. stochastic genetic change) and inbreeding observed in a given population (Wright 1931; Kimura & Crow 1963). In the field of evolutionary biology, effective population size is used as a measure of the amount of genetic drift in a population and is often employed in the estimation of the effects of a number of evolutionary processes (Waples 2022). This includes the rate of loss of genetic diversity and the effectiveness of selection (Kimura 1983; Charlesworth 2009). Effective population size is also a key parameter in plant and animal breeding as well as conservation biology as it can quantify the effects of inbreeding. For example, it is often used to develop targets in conservation efforts as it captures a population's history of inbreeding and genetic drift and aiming to maximise the effective population size should minimise these effects and reduce the loss of genetic diversity (Laikre et al. 2016; Wang et al. 2016).

N_e can be calculated in a myriad of ways using different aspects of population genetic measurements (Wang et al. 2016; Waples 2022). There are three commonly used measures of effective population size. Inbreeding and variance effective population size reflect the number in the parental and offspring generations, respectively. If a population is stable, these values will be equal, however, inbreeding N_e will be large and variance N_e small in declining populations and the opposite will be seen for growing populations (Crow 1954; Crow & Denniston 1988; Waples 2022). Another measure of N_e is the coalescent effective population size, which uses genetic diversity to estimate effective size (Sjödin et al. 2005; Wakeley & Sargsyan 2009; Waples 2022). Consequently, levels of diversity can serve as an indicator of effective population size (Caballero 1994). Such usage of diversity measures has led to the general consensus that effective population sizes are smaller than census population sizes

(N_c). This is used to explain Lewontin's Paradox, the observation that the variance in genetic diversity is substantially smaller (by orders of magnitude) than the variance in census population sizes across species, by asserting that effective population size is more strongly reduced in larger populations than smaller populations decoupling the variance in diversity and census population size (Lewontin 1974; Buffalo 2021; Charlesworth & Jensen 2022).

There have been several potential explanations of Lewontin's paradox put forth since this original finding, all of which would reduce the effective population size relative to the census population size. These proposals have included demographic events such as bottlenecks or extinction and recolonisation events (Ohta & Kimura 1973; Slatkin 1977; Buffalo 2021; Charlesworth & Jensen 2022), as well as a high variance or skew in reproductive success (Waples et al. 2018). Natural selection has also been included in proposals, particularly the influence of selection on diversity at linked neutral sites (Corbett-Detig et al. 2015; Buffalo 2021; Charlesworth & Jensen 2022). Genetic hitchhiking, a hallmark of directional selection, was originally proposed as an explanation for Lewontin's paradox as it describes the decrease in diversity levels caused by selected alleles carrying surrounding neutral variants to extreme frequencies or even fixation when recombination does not have enough time to break up the selected haplotype (Smith & Haigh 1974; Kaplan et al. 1989). Selection models such as recurrent selective sweeps (Buffalo 2021; Charlesworth & Jensen 2022; Achaz & Schertzer 2023) and background selection (Comeron 2014; Charlesworth 2012; Corbett-Detig et al. 2015; Comeron 2017; Buffalo 2021; Charlesworth & Jensen 2022) have also been explored due to the diversity-reducing effects they induce. However, the decrease in diversity that results from these types of selection is not of the magnitude of Lewontin's paradox (Coop 2016; Buffalo 2021) There are several selection forms that remain understudied in their potential contribution to this phenomenon, and fluctuating selection is one such form.

Fluctuating selection, when selection changes in direction or intensity, has recently been shown to have wide-ranging effects on levels of genetic diversity (Taylor 2013; Huang et al. 2014; Wittmann et al. 2023). Genetic evidence of fluctuating selection has been found in a range of species (Kelly 2022; Pfenninger & Foucault 2022; Lynch et al. 2023; reviewed in Johnson et al. 2023) but has been most extensively studied in cosmopolitan *Drosophila melanogaster* populations (Bergland et al. 2014; Behrman et al. 2018; Machado et al. 2021; Rudman et al. 2022; Bitter et al. 2023; Nunez et al. 2023). A recent study of the effects of fluctuating selection on genetic diversity has shown that it leads to genome-wide decreases that can overwhelm any local maintenance of variation at the selected site (Wittmann et al. 2023). This effect can be so widespread that a single site under seasonally fluctuating selection can cause a decrease in diversity in completely unlinked regions, i.e. different chromosomes (Wittmann et al. 2023). This genome-wide decrease was shown to reach levels of up to 30% when multiple additive seasonal loci were simulated across 3 chromosomes. This effect is due to the recurrent bottlenecks caused by alleles under selection switching between favourable and non-favourable environments, leading to an increased variation in offspring number between individuals, i.e. a small fraction of individuals contribute disproportionately to the next generation. Substantial decreases in genome-wide diversity as seen under fluctuating selection suggest this form of selection could have implications for the resolution of Lewontin's paradox, should fluctuating loci reduce effective population size relative to the census size and have a stronger effect in larger populations.

In this study, we simulate numerous seasonally fluctuating loci under the segregation lift model, a multilocus model of seasonal adaptation (Wittmann et al. 2017). We assumed locus-specific parameters of effect size and dominance, and *D. melanogaster* guided parameters of population size, genome size, and recombination rate. By varying the epistasis parameter in the segregation lift model, we were able to vary and fit amplitudes of our simulated allele

frequency fluctuations to empirically observed amplitudes from natural and outdoor experimental populations (Bergland et al. 2014; Machado et al. 2021; Rudman et al. 2022; Bitter et al. 2023). Using the estimated epistasis parameter and number of selected sites, we then simulate a full *Drosophila* genome and measure the effect of these fluctuating loci on the instantaneous variance effective population size. This is a genome-wide measure of effective population size that captures changes in the variance in offspring number which can be influenced by selection. By examining the effect of fluctuating selection on effective population size we aim to determine if it could contribute to an explanation for Lewontin's paradox.

Methods

All simulations are conducted in the forward simulator *SLiM* (v. 4.0.1; Haller & Messer 2023).

Model of multilocus seasonally fluctuating selection

Fluctuating selection is largely evidenced in natural populations of *D. melanogaster* (Bergland et al. 2014; Behrman et al. 2018; Glaser-Schmitt et al. 2021; Machado et al. 2021; Rudman et al. 2022; Bitter et al. 2023; Glaser-Schmitt et al. 2023; Nunez et al. 2023). Consequently, we simulate a randomly mating *D. melanogaster* population of 1 million individuals, in a binary 2-season (summer/winter) environment. We use a multilocus model of seasonally fluctuating selection presented by Wittmann and colleagues, the segregation lift model (Wittmann et al. 2017). This is a dynamic fitness landscape model that consists of multiple parts. Each seasonal locus is allocated a dominance coefficient (d) and effect size (Δ) for each season (summer/winter). The dominance coefficients are drawn from a uniform distribution with a minimum of 0 and a maximum of 1. It was found stable polymorphism is more likely when the average dominance across seasons is greater than 0.5 (Wittmann et al.

2017) and consequently, if the average dominance for a given seasonal locus is less than this value the dominance parameters are redrawn. Positive effect sizes for each locus are drawn from a log-normal distribution (Wittmann et al. 2017), by drawing a pair of parameters from a bivariate normal distribution with a mean of 0, standard deviation of 1, and correlation coefficient of 0.9, and subsequently exponentiating both values. We use correlated values as it was found that smaller differences between the summer and winter effect size resulted in more stable allele frequency fluctuations (Wittmann et al. 2017). These parameters are then used to calculate the contribution of a locus (C_l) to a season-specific seasonal score ($z_{s/w}$).

$$z_{s/w} = \sum_{l=1}^{L} c_l \qquad [1]$$

Thus, the contribution of each locus is dependent on the genotype at the locus and the season it is in, illustrated in Table 1. As an example, in winter if the locus is homozygous for the winter-favoured allele the contribution is the winter effect size (Δ_w), if it is homozygous for the summer allele the contribution is 0, if it is heterozygous the contribution is the product of the winter dominance and effect size of that locus ($d_w\Delta_w$). The sum of the contributions of all seasonal loci form the first part of the selection model, the seasonal score ($z_{s/w}$; equation 1). This seasonal score is then incorporated into the second part of the model, a fitness equation that accounts for different levels of epistasis via the epistasis parameter (y; equation 2).

$$\omega(z) = (1 + z)^y \qquad [2]$$

Multiplicative fitness as well as positive and diminishing-returns epistasis were tested when the model was originally presented but diminishing-returns epistasis was determined to be most plausible having been evidenced in empirical studies (Chou et al. 2011; Khan et al. 2011; Kryazhimskiy et al. 2014; Wittmann et al. 2017). Diminishing-returns was found to be conducive to long-term fluctuating loci that experience reasonable reversals of dominance,

compared to other forms of epistasis that require almost complete reversal of dominance between each season (Wittmann et al. 2017). All values of y in equation 2 confer diminishing-returns epistasis, but greater values signify greater per-locus selection. When simulating in *SLiM* under this model, the fitness of individuals was recalculated each generation using *SLiM*'s 'fitnessEffect' callback (Haller & Messer 2023).

Table 1. Contribution of seasonal loci (C_l) to fitness.

The contribution of a seasonal locus is conditioned on the genotype at that locus and the current season. If the locus is homozygous for the seasonal allele the contribution is the effective size of the seasonal allele. If the locus is homozygous for the allele of the opposing season the contribution is 0. If the locus is heterozygous, the contribution is the product of the effect size and the dominance coefficient for that given season.

Season	$C_{l,ww}$	$C_{l,sw}$	$C_{l,ss}$
Winter	Δ_w	$\Delta_w d_w$	0
Summer	0	$\Delta_s d_s$	Δ_s

Simulating allele frequency trajectories of seasonally fluctuating loci.

We started by simulating the allele frequency trajectories of loci using the outlined multilocus model of selection. We tested different values of the epistasis parameter y, ranging from 0.5 to 20 (0.5, 1, 2, 4, 8, 12, 16, 20) and different counts of seasonal loci (l; 100, 200, 500). In these simulations, l unlinked seasonal loci were drawn in at 50% frequency and their allele trajectories were tracked over time. We downscaled our population parameters by a factor of 2 and simulated a constant population size of 500,000 individuals with 5 generations per season, equivalent to 10 generations per season in a population of 1 million (Wittmann et al. 2017). Due to computational constraints, for a loci number of 500, we only simulated y values of 8, 12 and 20, as preliminary tests with smaller population size suggested this range to be most consistent with empirical data. Simulations were run for 18,000 generations,

sampling allele frequencies for three consecutive seasonal cycles every 9,000 generations. Each combination of parameters was replicated 20 times. We then collated the data and calculated the amplitude of allele frequency change for each seasonal locus across time.

Multiple linear regression of allele frequency amplitude for estimating selection parameters

We used the information obtained in the allele frequency simulations to investigate how the epistasis parameter (y), which determines the strength of per-locus selection, depends on the number of seasonal loci and the amplitude of seasonal allele frequency change. We tested the mean, median and 90% quartile amplitude of seasonal loci as one independent variable, and number of seasonal loci as second independent variable in a multiple regression model, with the epistasis parameter as the dependent variable. The fitted regression model then allowed us to derive the epistasis parameter given amplitude and number of causal loci from empirical studies of fluctuating selection in *Drosophila*. We include both additive effects and two-way interaction of the two independent variables, and tested if certain models significantly improved the fit to the data. We also modelled the number of initial seasonal loci required to result in a specific number of final loci based on the sampled epistasis value, as typically some proportion of seasonal polymorphisms got fixed or lost early on in the simulation. Eventually, these models were used to derive parameters for genome-wide simulations of seasonally fluctuating selection in *D. melanogaster,* depicted in Table 2.

Table 2. Parameters for genome-wide simulations

Number of causal loci	Mean amplitude	References	Derived *y*	Derived initial loci
111	0.05	Number of genes that overlapped with clusters in Rudman et al. 2022.	11	150
90	0.08	Rudman et al. 2022	15	127
264	0.02	Bitter et al. 2023	9.5	340
27	0.04	Rudman et al. 2022	2	37
9	0.35	Causal loci from Rudman et al. 2022. The amplitudes of the top 9 SNPs were averaged for each study of natural populations with available data (Bergland et al. 2014, Machado et al. 2021) and found to be similar.	7.5	19

Genome-wide simulation of seasonally fluctuating selection

The previous simulations assumed that all selected variants are unlinked from each other. To investigate the effect of fluctuating selection on the variance effective population size in a more realistic setting that includes linkage, we conducted genome-wide simulations of 4 *Drosophila* chromosomes: 2L, 2R, 3L, and 3R. We used Comeron et al's recombination maps for these four chromosomes (Comeron et al. 2012). As outlined above, we derived parameters that are consistent with studies of fluctuating selection from natural populations of *D. melanogaster* (Bergland et al. 2014; Machado et al. 2021), as well as from experimental studies using outdoor mesocosms (Rudman et al. 2022; Bitter et al. 2023; Table 2). We drew in an initial number of seasonal alleles at 50% frequency randomly across three chromosomes, leaving the final chromosome with no seasonal loci to allow for measuring the effect on effective population size in unlinked regions. We simulated for 10,000 generations, sampling allele frequencies and calculating the variance effective population size over a

seasonal cycle every 1000 generations. We conducted simulations of a downscaled constant population size of 500,000 individuals as well as a fluctuating population size, to model cosmopolitan *Drosophila's* boom-bust demography, with a summer population size of 500,000 and a winter population size of 50,000. The fluctuating population size simulations used the same parameters as the constant population size simulations to ensure they were comparable. Each simulation of unique parameters was replicated 10 times.

Calculating effective population size

To calculate effective population size, we drew neutral mutations across the four simulated chromosomes, with one variant every 100 kb. These mutations were introduced at 50% frequency and allowed to segregate for one seasonal cycle. After 10 generations, the change in allele frequency of the neutral mutations was recorded and used to calculate the variance effective population size, which is a genome-wide estimation of effective population size (Waples 1989; Jónás et al. 2016). First, the standardised variance, *F,* was calculated for each neutral mutation according to equation 3 (Waples 1989).

$$F = \frac{(allele\ frequency\ change)^2}{0.25} \quad [3]$$

This *F* value was then averaged across either the chromosomes with seasonal mutations (2L, 2R, 3L; linked region) or the chromosome without seasonal mutations (3R; unlinked region). These values were used in equation 4 to calculate the effective population size for both regions (Waples 1989; Jónás et al. 2016).

$$N_e = \frac{-10}{2\ ln(1-F)} \quad [4]$$

Offspring Capping

Our simulation of strong seasonal selection can produce an unrealistically large number of offspring for a small number of highly fit parental individuals. Thus, we also examined if limiting the number of offspring individuals per parent would reduce the effect of fluctuating selection on effective population size. We capped the number of offspring at 10, using *SLiM*'s 'modifyChild' callback. This allowed alternate parents to be allocated to individuals of a new generation if the ones originally picked had already contributed to 10 individuals. This effectively allows less fit individuals to also contribute to the next generation. We also examined the effect of this limitation on the distribution of allele frequency fluctuations.

Results

Simulating allele frequencies of loci under fluctuating selection

We conducted simulations of unlinked seasonal loci to characterise the range of fluctuations for various combinations of initial loci number and epistasis value. We first examined the number of segregating loci across time to investigate to what degree and how quickly fluctuating alleles become fixed or lost in our model (Figure 1). We see two main trends: a slow and steady decrease over time, seen largely for lower epistasis values; or a sharp loss of alleles at the start before the number of segregating loci levels out for the remainder of the simulation. In the latter case, most loci will be lost in the first 9,000 generations with the subsequent loss of segregating loci occurring at a slower rate than this initial phase. Seasonal loci that became fixed or lost were found to have a bimodal distribution of mean effect size across seasons compared to segregating alleles that displayed a more normal distribution (Figure S1). The bimodal distribution would suggest that as the mean effect size moves further away from 1, where the summer and winter effect sizes are equal, alleles are less

likely to remain segregating. This is likely caused by larger differences in effect size leading to less stable fluctuations (Wittmann et al. 2017).

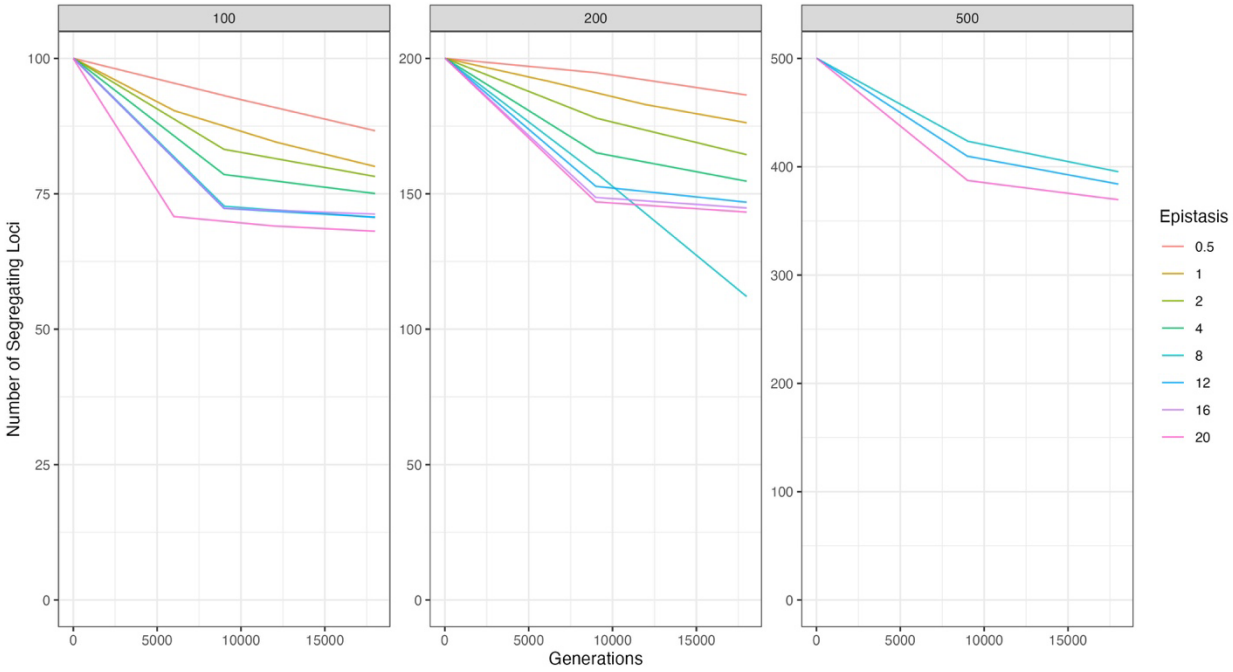

Figure 1. The average number of segregating loci across time.

The time in generations is shown on the x-axis, with the average number of segregating loci shown on the y-axis. Each panel depicts the number of segregating loci for a different number of initial loci. Each line is for a specific epistasis value (*y*), as indicated by the colour of the line.

We also examined the distributions of amplitudes of allele frequency fluctuations to determine if they stabilised over time, similar to the number of segregating loci. We sampled every 9000 generations but found that the distributions of seasonal amplitude were established by this first sampling point at generation 9000 (Figure 2). This suggests that a stable distribution of allele frequency fluctuations is quickly established while there are still segregating loci being lost after the first 9000 generations. This rapid establishment is likely driven by the intermediate initial frequency of mutations (0.5) and instant selection pressure allowing fluctuations to start immediately and from a frequency near that expected at the start of the seasonal cycle.

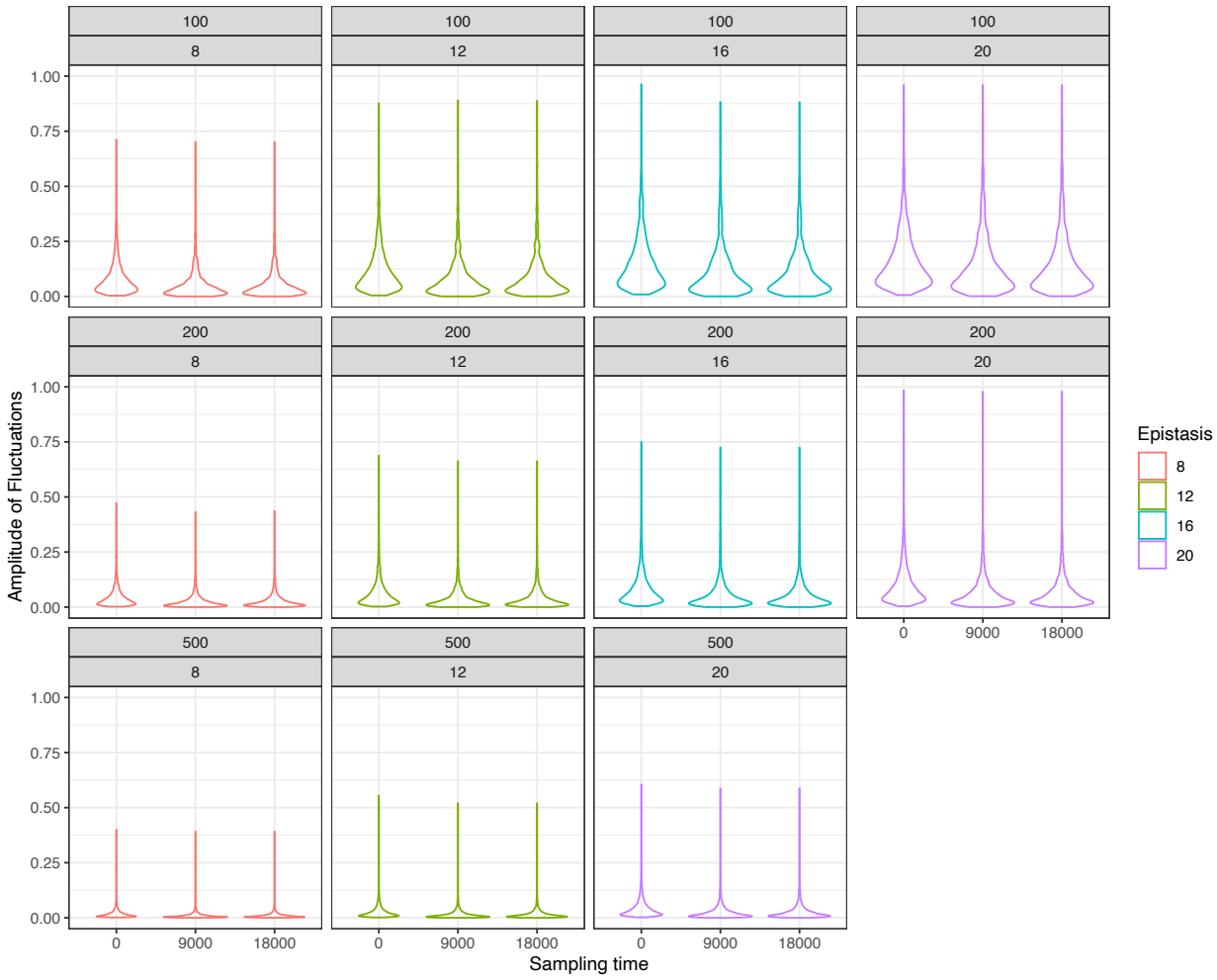

Figure 2. Distribution of the amplitude of allele frequency fluctuations across time.
The distribution of allele frequency fluctuations of segregating seasonal loci at different sampling points (in generations). Each facet displays a different initial loci number (labelled in the top strip) and epistasis (also labelled in the second strip and by the colour of the distributions). The distribution of the amplitude of allele frequency fluctuations is shown on the y-axis. Note that fixed or lost alleles (i.e. non-polymorphic loci) are excluded from the distribution.

Having established that the distributions of seasonal fluctuations become stable within less than 9000 generations, we next investigated how the amplitude distribution changes with loci number and epistasis value *y* for samples after this initial phase. We observed that on a log-log scale, there is a linear relationship between the final number of segregating loci and various aspects of the amplitude of allele frequency fluctuation (i.e. mean, median, 90% quartile; Figure 3) for each epistasis value. The mean amplitude ranged from ~ 0.4% to 16.5% across all epistasis values. The 90% quartile captured the larger allele frequency

fluctuations simulated, ranging to values up to 35%. The largest median amplitude of fluctuation was 11.8%, suggesting that there are many loci with smaller allele frequency fluctuations and a small number of loci with large amplitudes that are inflating the mean. Simulations of 100 loci (largest mean = 16.5%, median = 11.8%, 90% quartile = 35%) show overall larger allele frequency amplitude than simulations of 500 loci (largest mean = 3.2%, median = 2%, 90% quartile = 8.2%). Greater values of the epistasis parameter *y* confer stronger selection, leading to larger allele frequency fluctuations (Figure 3). This suggests that the selection strength per individual locus increases with increasing *y* and decreasing loci number.

We decided to leverage the strong log-linear relationship shown in Figure 3 to derive model parameters that mimic amplitude distributions and loci numbers previously reported in empirical studies of fluctuating selection in *D. melanogaster* (Bergland et al. 2014; Machado et al. 2021; Rudman et al. 2022; Bitter et al. 2023).

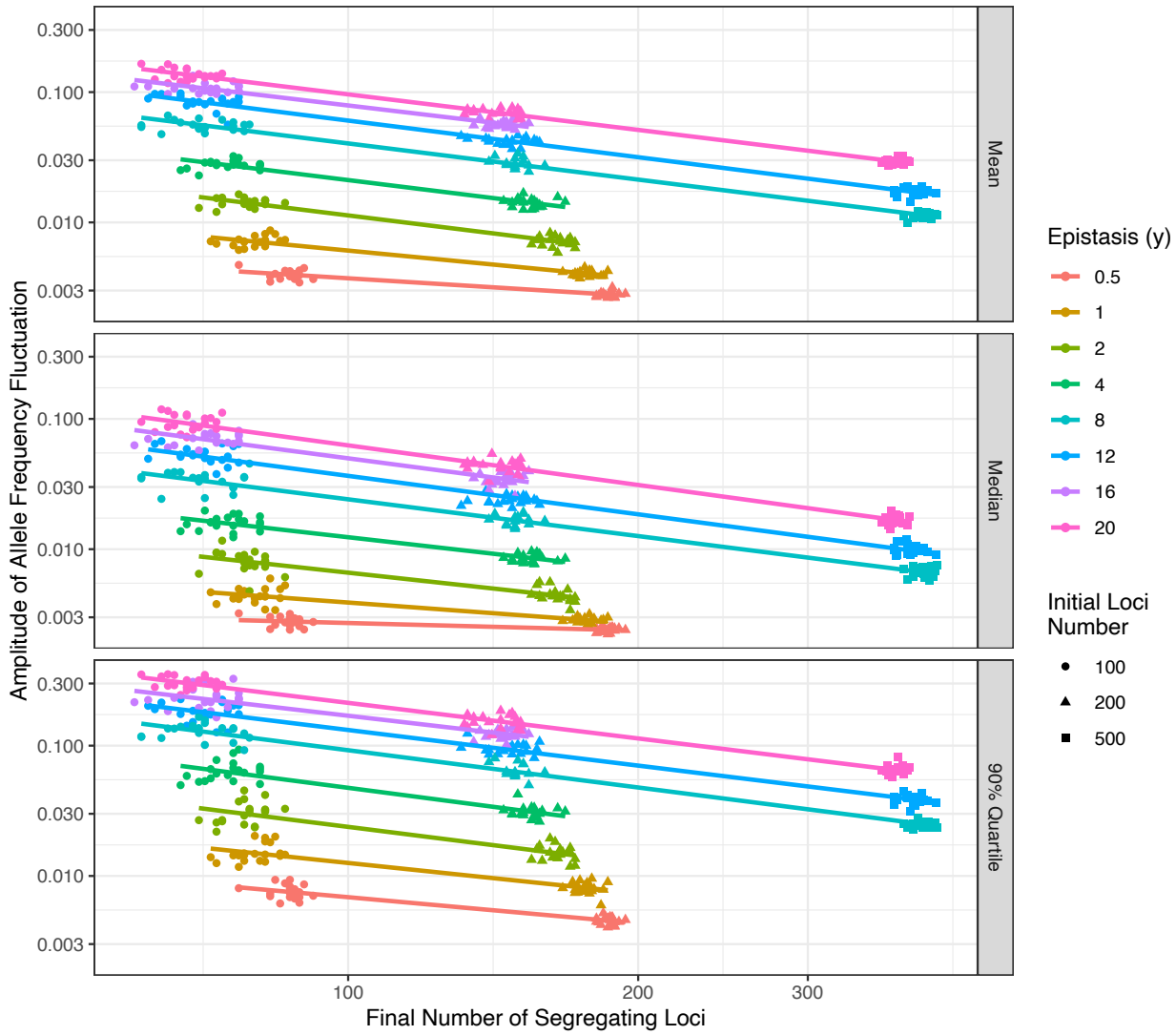

Figure 3. Relationship between number of segregating loci, epistasis, and amplitude of seasonal allele frequency fluctuation.

Each panel depicts the relationship between the initial and final number of segregating loci (sampled at 18,000 generations) and either the mean, median, or 90% quartile of allele frequency fluctuations, for different epistasis values. The amplitude of the seasonal fluctuation is shown on the y-axis. The initial loci number is visualised by the shape of the points, and each point represents a simulated replicate (of which there are 20 for each initial loci number and epistasis value). The epistasis value is illustrated by the colour of the points and lines.

Multiple linear regression model to determine empirically informed parameters of seasonally fluctuating selection

We used a multiple linear regression approach to calculate the epistasis value required to generate allele frequency fluctuations of a given average amplitude and a specified number of segregating loci. To this end, we fit a multiple regression model with epistasis as the dependent variable, and the number of loci and mean amplitude as predictors, after log-transforming all variables. In addition, we also tested the median and 90% quantile of the amplitude as predictors. However, using the mean amplitude gave the best model-fit (r^2 = 0.9922), compared to the median amplitude (r^2 = 0.9787) and the 90% quartile of the amplitude (r^2 = 0.9838). Further, an ANOVA model comparison suggested that adding a two-way interaction term did not significantly improve the model-fit ($p > 0.05$). Hence, the simpler additive model was subsequently used for the prediction of epistasis (y), and mean amplitude was used as one of the predictors. The final regression equation is shown in equation 5,

$$log(y) \sim 0.9949\, log(n) + 1.0926\, log(mean\_x) + 0.4258 \qquad [5]$$

where y is the epistasis value, n is the final number of segregating seasonal loci, and $mean\_x$ is the mean amplitude of seasonal allele frequency fluctuation.

A multiple regression model was also used to determine the number of initially segregating loci required to obtain the final number of segregating loci after the initial loss of alleles. The model predicts the desired final number of segregating loci (L) from the epistasis parameter (y) and initial number of loci (n). In this case, adding an interaction term to the model (equation 6) significantly improved the fit ($p < 0.001$).

$$L \sim 1.1814n + 0.4541y + 0.007179ny + 4.1124 \qquad [6]$$

Using these two fitted regression models, we computed epistasis values based on values of the mean amplitude of allele frequency fluctuation and the final number of segregating loci derived from studies of natural *D. melanogaster* populations (Table 2). We used estimates of the final number of segregating seasonal loci from Rudman et al. and Bitter et al.'s outdoor cage experiments (Rudman et al. 2022; Bitter et al. 2023). In these two studies, the authors used linkage disequilibrium, hitchhiking, and parallel allele frequency change to estimate the number of unlinked 'clusters' that occur in their experimental populations. With the assumption that each cluster is driven by a single seasonal locus, we use the number of clusters as an estimate of the "final" number of segregating loci. We also use the number of genes found to overlap with clusters in Rudman et al. as another alternate estimate for the number of segregating loci (Rudman et al. 2022). For mean amplitude, we used a range of values from published studies of *D. melanogaster* in both natural populations as well as experimental studies (Bergland et al. 2014; Machado et al. 2021; Rudman et al. 2022; Bitter et al. 2023), along with averaging the amplitudes of the top loci from the published seasonal SNP data from the studies by Bergland et al. and Machado et al. corresponding with the number of segregating loci derived from either Rudman et al. or Bitter et al.. For all subsequent simulations, we used our regression model approach to derive an epistasis parameter and the initial number of segregating loci from these empirically derived combinations of mean amplitudes and number of causal loci, as summarized in Table 2.

Genome-wide effect on N_e

We simulated the autosomes of a *Drosophila* genome to evaluate the effect of seasonally fluctuating selection on variance effective population size in a *Drosophila* population (see Methods). We first assessed our regression model approach and found that the final number of segregating loci was slightly higher than the final loci number input into the model, with an average of 5 additional segregating loci and no more than 15 in a single replicate. In

contrast, the mean amplitude was marginally lower than the values used in the model, with a decrease of 0.7%. The maximum discrepancy was 23%, however this occurred when using extreme empirical parameters (i.e. 9 final loci with an average amplitude of 35% to correspond with the mean amplitude of the top 9 SNPs from Bergland et al. and Machado et al's empirical data). Overall, under reasonable conditions, the model results in allele frequency amplitude and final segregating loci numbers close to the empirically derived input values.

We found that fluctuating selection using these empirically based models reduced genome-wide effective population size by as much as 76% and no less than ~7% across a parameter space that conferred mean allele frequency fluctuations between 1.6 and 18.4% (Figure 4). Interestingly, the greatest reduction in effective population size was not observed under parameters that led to the largest mean seasonal fluctuations, but for a combination of 127 initial loci with a *y* value of 15, which had a mean seasonal amplitude of only 6.7%. This allele frequency fluctuation is within the range of estimates from studies of natural populations (Machado et al. 2021; Rudman et al. 2022; Bitter et al. 2023). The least reduction in effective population size resulted from a combination of 37 initial loci and a *y* value of 2, which had a mean amplitude of 3.2%. However, we find a considerable reduction with very similar allele frequency fluctuation for 150 initial loci and a *y* value of 11, suggesting the mean amplitude of allele frequency fluctuation is not the only driver of this reduction in effective population size.

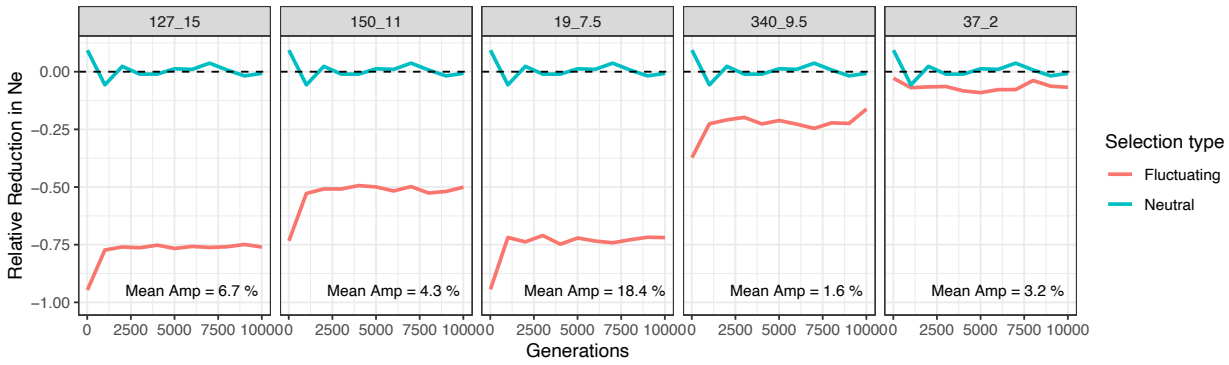

Figure 4. Relative reduction in effective population size due to fluctuating selection

Relative reduction in effective population size across time (simulated generations). Each panel shows effective population size for a different combination of initial loci number and epistasis value (labelled respectively in the top strip). A dashed black line depicts the neutral expectation (i.e. 0% reduction). The blue line demonstrates relative effective population size under neutral evolution, while the red line signifies effective population size under fluctuating selection. The corresponding mean amplitude of each parameter combination is included in the bottom right of each panel.

We then examined whether other aspects of the amplitude of fluctuation are better predictors of the decrease in effective population size (Figure 5). We compare the mean, median, and maximum seasonal fluctuation with the reduction in effective population size and observe that maximum amplitude appears to have a roughly linear relationship with the reduction in effective population size ($r^2 = 0.7621$). The mean and median amplitude do not show such clear patterns, with a steep linear relationship for simulations with initial loci number greater than 19, but the values for the simulations with 19 initial loci and an epistasis value of 7.5 are outliers to this trend. This suggests that the more extreme (i.e. largest) allele frequency fluctuations are the best predictors for a strong reduction in N_e, not the average amplitude or the number of fluctuating sites.

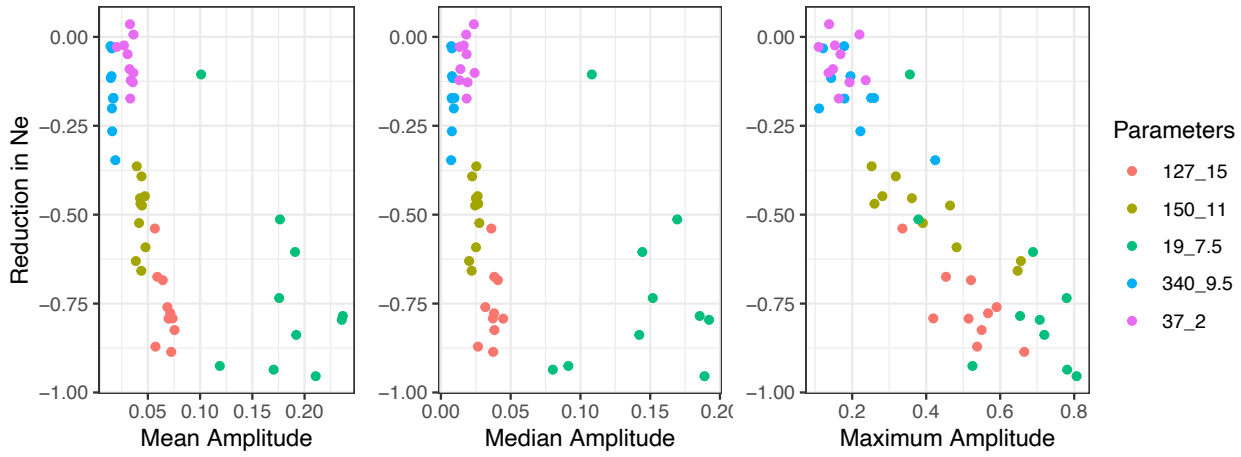

Figure 5. Relationship between reduction in effective population size and aspects of seasonal fluctuation (amplitude).

The relative reduction in effective population size in relation to the mean, median, and maximum amplitude for each simulated replicate of each combination of initial loci number and epistasis value (coloured).

We also explored the relationship between the dominance and effect size of the seasonal loci that remain segregating and the amplitude of allele frequency. We see a general trend across the parameter combinations of increasing seasonal allele frequency fluctuation with greater mean effect size (average of the summer and winter effect size; Figure 6A). The distribution of mean dominance and amplitude demonstrates that smaller dominance sizes can confer a wider range of amplitudes, particularly decreasing the lower range of amplitudes but without decreasing the upper range (Figure 6B). Hence, loci with the largest amplitude, which are likely driving the reduction in effective population size, also have a large mean effect size but are not restricted to any particular range of mean dominance coefficients.

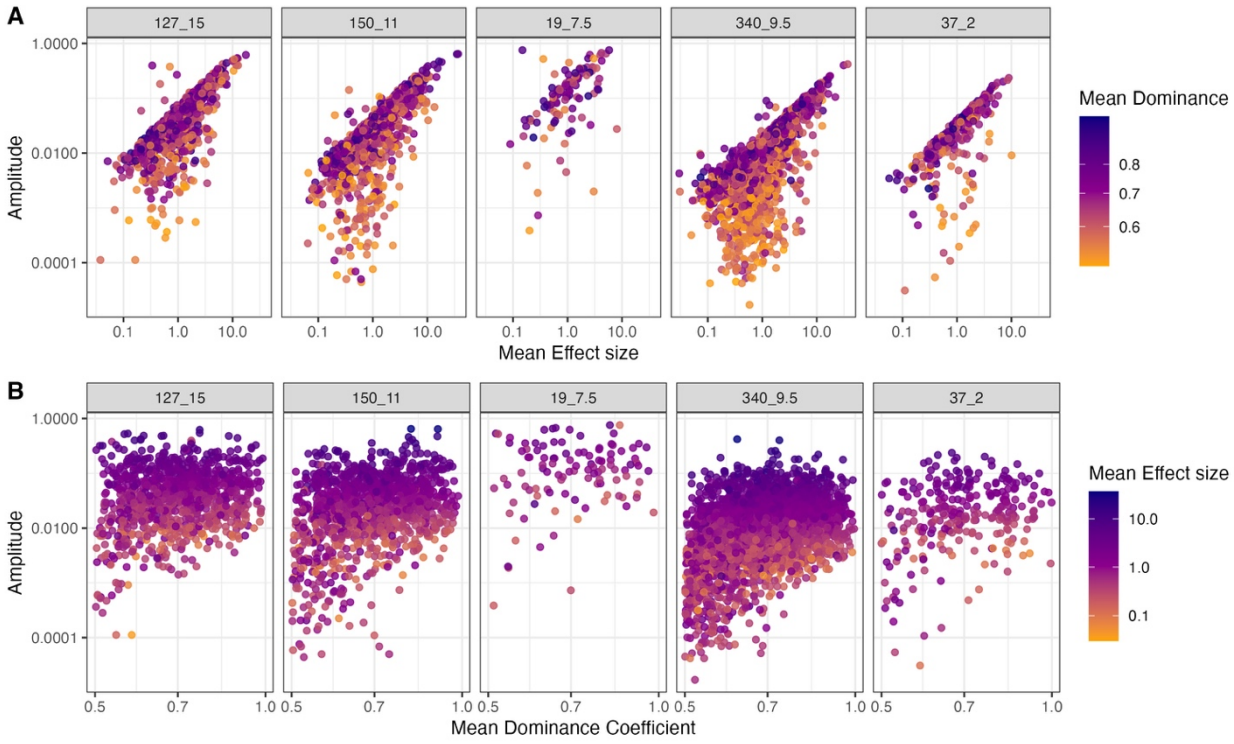

Figure 6. Mean effect size and mean dominance coefficient of seasonal loci segregating at the end of simulations in relation to their amplitude of fluctuation.

A The mean effect size and **B** mean dominance coefficient, calculated as the average of both the summer and winter value for each locus, compared to the amplitude of each locus. The colours of the points illustrate the mean dominance or effect size. Each panel depicts a different parameter combination labelled in the top strip with the initial loci number and epistasis value, respectively.

Offspring capping

It was noted previously that under the segregation lift model, unrealistically large offspring numbers per parent might occur, but restricting the offspring number per parent did not qualitatively change the allele frequency fluctuations (Wittmann et al. 2017). Thus, we aimed to determine if the reduction in effective population size would be less substantial if offspring output, the number of offspring any individual can have, was capped. We also observed little difference between the distributions of allele frequency fluctuations with and without offspring capping, with amplitudes from capped simulations only being slightly less than those without offspring limitation. Using 150 initial loci and an epistasis value of 11 as an example, we see that the mean amplitude is 0.041 with capping and 0.043 without. Further,

the maximum amplitude only differed by 1% between simulations with capping and without for this parameter combination (0.646 and 0.656, respectively). When examining levels of effective population size, we observe that if the original reduction in effective population size was approximately 50% or less, capping offspring does not reduce the effect of fluctuating selection on effective population size. However, capping offspring did limit the reduction in effective population size compared to when the original reduction in effective population size was more severe (Figure 7). With capping, the most extreme reduction in effective population size was less than ~75% in the initial 'burn-in' phase of the simulation and approximately 60% at equilibrium.

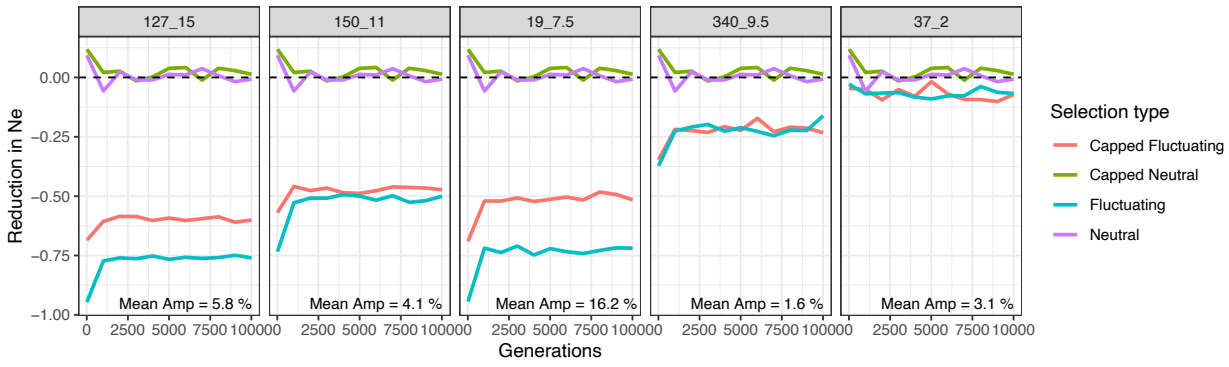

Figure 7. Reduction in effective population size with and without offspring capping. Effective population size under neutral evolution, with and without offspring capping, are depicted in purple and green respectively. The neutral expectation is shown by the dashed black line. Effective population size under fluctuating selection with standard offspring generation is shown in blue, and fluctuating selection with offspring capping is shown in red. The mean amplitude of fluctuating loci with offspring capping is written in the bottom of each respective panel.

Fluctuating population size

We also tested the effects of fluctuating selection on a population of fluctuating size. It is known that *D. melanogaster* in temperate environments undergo a boom-bust demography where population sizes grow (boom) in the summer, when conditions are optimal and resources are abundant, and crash (bust) in winter when resources are sparse. We simulate a

step wise population decrease of 1 order of magnitude (500,000 to 50,000 individuals) at the start of the winter season that increases again at the beginning of summer. Interestingly, we find similar proportions of reduction in effective population relative to the harmonic mean population size as was seen in the constant-sized model (i.e., ~10-75% reduction; Figure 8). In some cases, this equates to a reduction of an order of magnitude compared to the peak summer census population. For example, when simulating 150 initial loci, with a *y* value of 11 with an amplitude of 4.6%, the harmonic mean effective population size is reduced by approximately 55%. The resulting effective population size is approximately 41,000 individuals, down from a summer census population size of 500,000. Hence, fluctuating selection combined with recurring bottlenecks may be able to explain a substantial discrepancy between census and effective population size.

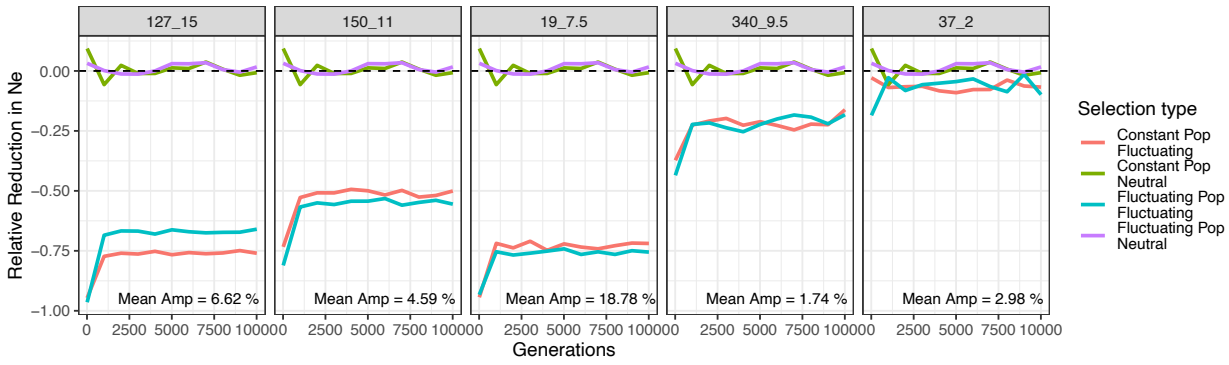

Figure 8. Reduction in effective population size due to fluctuating selection in a population with boom-bust demography.

The dashed line depicts the neutral expectation, and the purple line represents the estimated effective population size of a fluctuating population size (relative to the harmonic mean population size) under neutral evolution, while the green line is neutral evolution in a constant population size. The red line shows the effective population size under fluctuating selection for a constant size population size, and for a fluctuating population size in blue. The mean amplitude of allele frequency fluctuation in a fluctuating population is included in the bottom right of the respective panel.

Discussion

Fluctuating selection was shown to have genome-wide effects on levels of diversity, even in regions that are completely unlinked to any selected sites (Wittmann et al. 2023). This is an indication that fluctuating selection impacts effective population size by increasing the variance in offspring number. In this study, we quantify this effect on effective population size (i.e., the variance effective population size) in a simulated *Drosophila* population and investigate the relationship between the reduction in effective population size and factors such as mean, median, and maximum amplitude, as well as the effect size and dominance coefficient of the seasonally selected loci. We test both a constant and a fluctuating population size, and additionally determined if capping the number of offspring limits the reduction in N_e.

We use a model of fluctuating selection that simulates seasonal alleles with different dominance and effect sizes, this implies that the seasonal allele frequency fluctuations (amplitudes) are different for each locus. We find a strong positive relationship between the maximum seasonal amplitude and the reduction in N_e. The maximum amplitude of seasonal SNPs identified in Bergland and colleagues' 2014 study as well as Machado et al's 2021 study is approximately 0.37 and 0.45, respectively (Bergland et al. 2014; Machado et al. 2021). When comparing this to our simulations, this suggests there is potentially a reduction in effective population size of between 40-60% in the natural populations in these studies due to fluctuating selection (Figure 5). Further investigation into this relationship between maximum amplitude and effective population size under additional ecological realism and estimation of effective population size from natural populations in which fluctuating selection had been identified may inform whether this effect is maintained when there are additional

forces at play. Notably, we observed that the reduction in effective population size is robust to fluctuations in population size and capping of the offspring number per parent.

Lewontin's paradox pertains to the much smaller variance in genetic diversity between species compared to the variance in census population size, which spans several orders of magnitude. One possible solution to this paradox is that natural selection reduces effective population size to a larger degree in larger populations, thus leading to less variation in genetic diversity between species than predicted from their census population sizes. This explanation is only feasible if there is actually a strong effect of natural selection on levels of neutral diversity, i.e. a strong reduction in N_e. We observed reductions in effective population size of up to 75%. In our simulated constant population of 500,000, this confers an effective population size of 125,000 individuals. While this is not several orders of magnitude, this is still a substantial decrease and suggests fluctuating selection may play a key role in explaining Lewontin's paradox, in combination with other types of selection and demographic effects such as recurrent bottlenecks (Buffalo 2021; Charlesworth & Jensen 2022). For instance, when we combined fluctuating selection with a fluctuating population size model, we were able to capture differences between census and effective population size that correspond to an order of magnitude, with realistic values of mean amplitude of fluctuating alleles. This suggests fluctuating selection combined with population demography may be able to explain a large portion of the discrepancy between census and effective population sizes. Fluctuating selection is also a more plausible cause of this disparity than recurrent positive selection as it can be sustained for as long as the oscillating pressure is active, as selected alleles are being maintained for extended periods of time. Previous proposals of positive selection as the cause of Lewontin's paradox rely on a constant supply of positively selected mutations (Buffalo 2021; Charlesworth & Jensen 2022; Achaz & Schertzer 2023) as diversity in the regions surrounding the selected allele is slowly regained

after the selected allele becomes fixed and diversity recovers. In contrast, the recurrent selective bottlenecks caused by a large proportion of individuals being strongly maladapted after each seasonal transition lead to a consistently reduced effective population size throughout time.

Conclusion

Under an empirically informed model, fluctuating selection was found to reduce effective population size by as much as 75%, and even when individuals were limited to only 10 offspring per parent, a maximum reduction of 60% was observed. We found that the maximum amplitude of the seasonal allele frequency fluctuation, i.e. the largest amplitude over all selected loci, was a crude indicator of the reduction in effective population size that is independent of the number of loci. When fluctuating selection was simulated in addition to a fluctuating population size, we were able to capture reductions in variance effective population size one order of magnitude lower than the peak census population size. Together, the significant reduction in effective population size, combined with the ability of fluctuating selection to maintain segregating alleles for long periods of time, make it a plausible contributor to resolving Lewontin's paradox. Further investigations with additional ecological realism, and fitting the segregation lift model to species other than *Drosophila*, will improve our understanding of the broader implications of this reduction in effective population size across the tree of life.

Acknowledgements

Thanks go to Ben Haller for assistance with *SLiM* code and bug fixes. Thank you to Dr. Fabien Vosin, Dr. Gludhug Purnomo, Dr. Xavier Roca-Rada and Shyamsundar Ravishankar for their assistance with computational issues.

References

Achaz G, Schertzer E. 2023. Weak genetic draft and the Lewontin's paradox. bioRxiv. 2023.07.19.549703. doi: 10.1101/2023.07.19.549703.

Behrman EL et al. 2018. Rapid seasonal evolution in innate immunity of wild *Drosophila melanogaster*. Proc. Biol. Sci. 285. doi: 10.1098/rspb.2017.2599.

Bergland AO, Behrman EL, O'Brien KR, Schmidt PS, Petrov DA. 2014. Genomic evidence of rapid and stable adaptive oscillations over seasonal time scales in *Drosophila*. PLoS Genet. 10:e1004775. doi: 10.1371/journal.pgen.1004775.

Bitter MC et al. 2023. Continuously fluctuating selection reveals extreme granularity and parallelism of adaptive tracking. bioRxiv. 2023.10.16.562586. doi: 10.1101/2023.10.16.562586.

Buffalo V. 2021. Quantifying the relationship between genetic diversity and population size suggests natural selection cannot explain Lewontin's paradox. eLife. 10:e67509. doi: 10.7554/eLife.67509.

Caballero A. 1994. Developments in the prediction of effective population size. Heredity. 73:657–679. doi: 10.1038/hdy.1994.174.

Charlesworth B. 2009. Fundamental concepts in genetics: effective population size and patterns of molecular evolution and variation. Nat. Rev. Genet. 10:195–205. doi: 10.1038/nrg2526.

Charlesworth B. 2012. The role of background selection in shaping patterns of molecular evolution and variation: evidence from variability on the *Drosophila* X chromosome. Genetics. 191:233–246. doi: 10.1534/genetics.111.138073.

Charlesworth B, Jensen JD. 2022. How can we resolve Lewontin's paradox? Genome Biol. Evol. doi: 10.1093/gbe/evac096.

Chou H-H, Chiu H-C, Delaney NF, Segrè D, Marx CJ. 2011. Diminishing returns epistasis among beneficial mutations decelerates adaptation. Science. 332:1190–1192. doi: 10.1126/science.1203799.

Comeron JM. 2014. Background selection as baseline for nucleotide variation across the *Drosophila* genome. PLoS Genet. 10:e1004434. doi: 10.1371/journal.pgen.1004434.

Comeron JM. 2017. Background selection as null hypothesis in population genomics: insights and challenges from *Drosophila* studies. Philos. Trans. R. Soc. Lond. B Biol. Sci. 372:20160471. doi: 10.1098/rstb.2016.0471.

Comeron JM, Ratnappan R, Bailin S. 2012. The many landscapes of recombination in *Drosophila melanogaster*. PLoS Genet. 8:e1002905. doi: 10.1371/journal.pgen.1002905.

Coop G. 2016. Does linked selection explain the narrow range of genetic diversity across species? bioRxiv. 042598. doi: 10.1101/042598.

Corbett-Detig RB, Hartl DL, Sackton TB. 2015. Natural selection constrains neutral diversity across a wide range of species. PLoS Biol. 13:e1002112. doi: 10.1371/journal.pbio.1002112.

Crow JF. 1954. Breeding structure of populations. II. Effective population number. Statistics and mathematics in biology.

Crow JF, Denniston C. 1988. Inbreeding and variance effective population numbers. Evolution. 42:482–495. doi: 10.2307/2409033.

Glaser-Schmitt A, Ramnarine TJS, Parsch J. 2023. Rapid evolutionary change, constraints and the maintenance of polymorphism in natural populations of *Drosophila melanogaster*. Mol. Ecol. doi: 10.1111/mec.17024.

Glaser-Schmitt A, Wittmann MJ, Ramnarine TJS, Parsch J. 2021. Sexual antagonism, temporally fluctuating selection, and variable dominance affect a regulatory polymorphism in *Drosophila melanogaster*. Mol. Biol. Evol. 38:4891–4907. doi: 10.1093/molbev/msab215.

Haller BC, Messer PW. 2023. SLiM 4: Multispecies eco-evolutionary modeling. Am. Nat. 201:E127–E139. doi: 10.1086/723601.

Huang Y, Wright SI, Agrawal AF. 2014. Genome-wide patterns of genetic variation within and among alternative selective regimes. PLoS Genet. 10:e1004527. doi: 10.1371/journal.pgen.1004527.

Johnson OL, Tobler R, Schmidt JM, Huber CD. 2023. Fluctuating selection and the determinants of genetic variation. Trends Genet. 39:491–504. doi: 10.1016/j.tig.2023.02.004.

Jónás Á, Taus T, Kosiol C, Schlötterer C, Futschik A. 2016. Estimating the effective population size from temporal allele frequency changes in experimental evolution. Genetics. 204:723–735. doi: 10.1534/genetics.116.191197.

Kaplan NL, Hudson RR, Langley CH. 1989. The “hitchhiking effect” revisited. Genetics. 123:887–899. doi: 10.1093/genetics/123.4.887.

Kelly JK. 2022. The genomic scale of fluctuating selection in a natural plant population. Evol Lett. 6:506–521. doi: 10.1002/evl3.308.

Khan AI, Dinh DM, Schneider D, Lenski RE, Cooper TF. 2011. Negative epistasis between beneficial mutations in an evolving bacterial population. Science. 332:1193–1196. doi: 10.1126/science.1203801.

Kimura M. 1983. *The neutral theory of molecular evolution*. Cambridge University Press.

Kimura M, Crow JF. 1963. The measurement of effective population number. Evolution. 17:279–288. doi: 10.2307/2406157.

Kryazhimskiy S, Rice DP, Jerison ER, Desai MM. 2014. Microbial evolution. Global epistasis makes adaptation predictable despite sequence-level stochasticity. Science. 344:1519–1522. doi: 10.1126/science.1250939.

Laikre L, Olsson F, Jansson E, Hössjer O, Ryman N. 2016. Metapopulation effective size and conservation genetic goals for the Fennoscandian wolf (*Canis lupus*) population. Heredity.

117:279–289. doi: 10.1038/hdy.2016.44.

Lewontin RC. 1974. *The genetic basis of evolutionary change*. Columbia University Press https://play.google.com/store/books/details?id=rLMTAQAAIAAJ.

Lynch M, Wei W, Ye Z, Pfrender ME. 2023. The genome-wide signature of short-term temporal selection. bioRxiv. 2023.04.28.538790. doi: 10.1101/2023.04.28.538790.

Machado HE et al. 2021. Broad geographic sampling reveals the shared basis and environmental correlates of seasonal adaptation in *Drosophila*. eLife. 10:e67577. doi: 10.7554/eLife.67577.

Nunez JCB et al. 2023. A cosmopolitan inversion facilitates seasonal adaptation in overwintering *Drosophila*. Genetics. doi: 10.1093/genetics/iyad207.

Ohta T, Kimura M. 1973. A model of mutation appropriate to estimate the number of electrophoretically detectable alleles in a finite population. Genet. Res. 22:201–204. doi: 10.1017/s0016672300012994.

Pfenninger M, Foucault Q. 2022. Population genomic time series data of a natural population suggests adaptive tracking of fluctuating environmental changes. Integr. Comp. Biol. doi: 10.1093/icb/icac098.

Rudman SM et al. 2022. Direct observation of adaptive tracking on ecological time scales in *Drosophila*. Science. 375:eabj7484. doi: 10.1126/science.abj7484.

Sjödin P, Kaj I, Krone S, Lascoux M, Nordborg M. 2005. On the meaning and existence of an effective population size. Genetics. 169:1061–1070. doi: 10.1534/genetics.104.026799.

Slatkin M. 1977. Gene flow and genetic drift in a species subject to frequent local extinctions. Theor. Popul. Biol. 12:253–262. doi: 10.1016/0040-5809(77)90045-4.

Smith JM, Haigh J. 1974. The hitch-hiking effect of a favourable gene. Genet. Res. 23:23–35. doi: 10.1017/S0016672300014634.

Taylor JE. 2013. The effect of fluctuating selection on the genealogy at a linked site. Theor. Popul. Biol. 87:34–50. doi: 10.1016/j.tpb.2013.03.004.

Wakeley J, Sargsyan O. 2009. Extensions of the coalescent effective population size. Genetics. 181:341–345. doi: 10.1534/genetics.108.092460.

Wang J, Santiago E, Caballero A. 2016. Prediction and estimation of effective population size. Heredity. 117:193–206. doi: 10.1038/hdy.2016.43.

Waples RS. 1989. A generalized approach for estimating effective population size from temporal changes in allele frequency. Genetics. 121:379–391. doi: 10.1093/genetics/121.2.379.

Waples RS. 2022. What is Ne, anyway? J. Hered. 113:371–379. doi: 10.1093/jhered/esac023.

Waples RS, Grewe PM, Bravington MW, Hillary R, Feutry P. 2018. Robust estimates of a high Ne/N ratio in a top marine predator, southern bluefin tuna. Sci Adv. 4:eaar7759. doi:

10.1126/sciadv.aar7759.

Wittmann MJ, Bergland AO, Feldman MW, Schmidt PS, Petrov DA. 2017. Seasonally fluctuating selection can maintain polymorphism at many loci via segregation lift. Proc. Natl. Acad. Sci. U.S.A. 114:E9932–E9941. doi: 10.1073/pnas.1702994114.

Wittmann MJ, Mousset S, Hermisson J. 2023. Modeling the genetic footprint of fluctuating balancing selection: From the local to the genomic scale. Genetics. 223. doi: 10.1093/genetics/iyad022.

Wright S. 1931. Evolution in Mendelian Populations. Genetics. 16:97–159. doi: 10.1093/genetics/16.2.97.

Supplementary Information

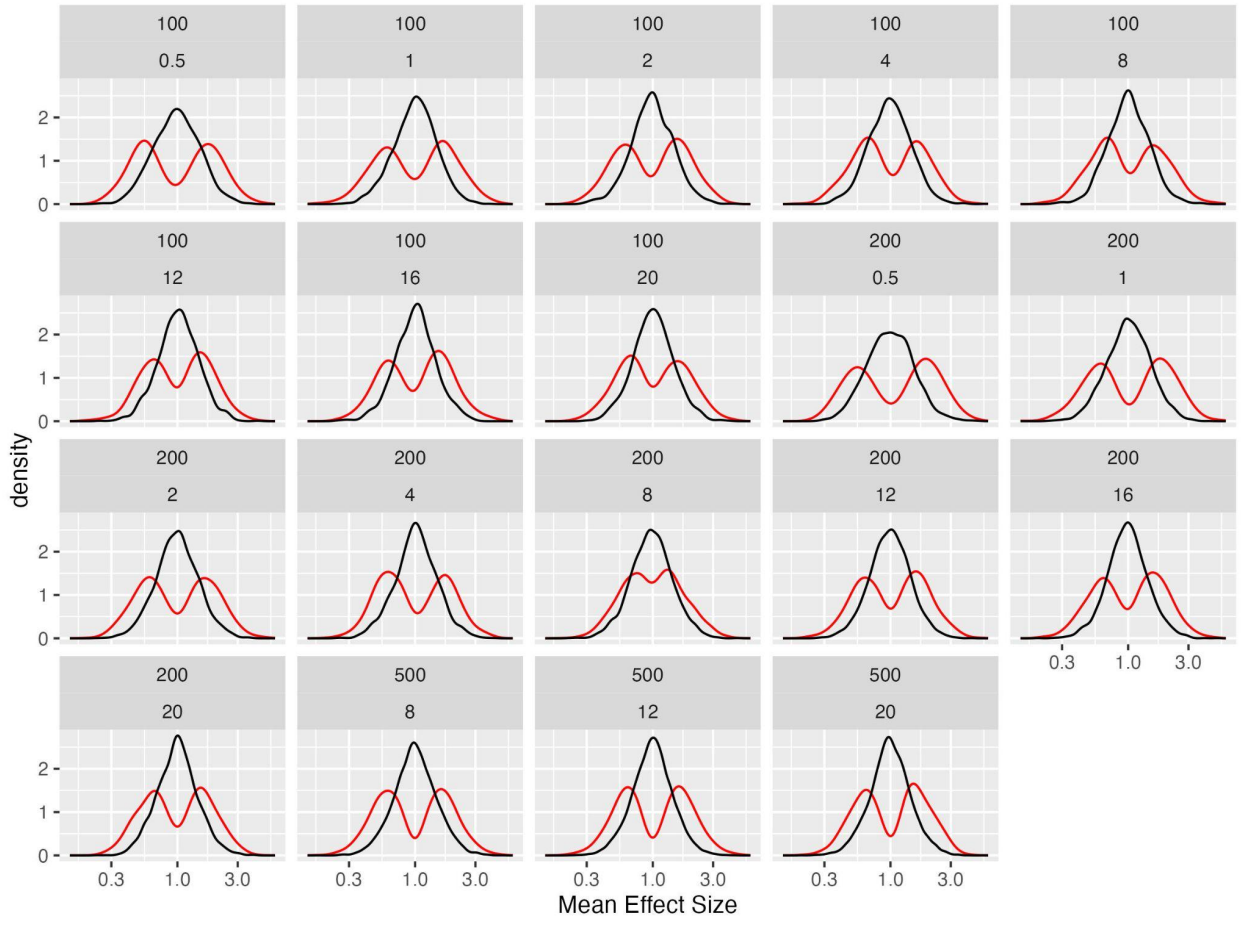

Figure S1. Distribution of mean effect size for segregating (black) and fixed/lost (red) alleles. The number of initial loci and *y* parameters are labelled at the top of each panel. A mean effect size of 1 signifies that the summer and winter effect sizes are equal.

Thesis Discussion

Overview

Natural selection is a key principle in biology. The study of this evolutionary phenomenon has evolved from observing phenotypes (Darwin 1859; Fisher & Ford 1947) to directly discerning it at the molecular level through allele frequencies and patterns of neutral genetic variation (Smith & Haigh 1974; Berry et al. 1991; Bergland et al. 2014). This has allowed the investigation of natural selection in species throughout all life and on a broad range of timescales, from evolve-and-resequence studies of species with short generation times (Petersen et al. 2007; Abdul-Rahman et al. 2021; Rudman et al. 2022) to the use of ancient DNA in larger mammals (Ludwig et al. 2015; Souilmi et al. 2022). With an extensive body of research regarding common types of selection such as positive and classical balancing selection (Charlesworth 2006; Stephan 2019), attention has now turned to more complex forms of selection which benefit from advances in sequencing and computational technology and increasing accessibility to these resources due to declining costs.

Fluctuating selection is a type of selection that has long been theorised but has yet to be consistently studied in the same manner as other selection forms. This has left us with a number of gaps in our current knowledge. In addition to this, recent improvements in sequencing and associated costs have allowed for the direct identification of fluctuating allele frequency trajectories across time (Bergland et al. 2014; Machado et al. 2021; Pfenninger et al. 2022; Pfenninger & Foucault 2022; Rudman et al. 2022; Bitter et al. 2023). This has brought fluctuating selection to the forefront of the field of natural selection resulting in an abundance of new studies over the last decade; however, much of the focus has been on identifying fluctuating alleles in natural populations and modeling the dynamics of such loci. This thesis takes an alternate approach. Instead, I aimed to characterise the effects of fluctuating loci on linked neutral genetic variation to determine if it can be discriminated

from other common forms of selection. In addition, I explored the influence of fluctuating selection on population genetic statistics and measures, such as effective population size.

An updated review of fluctuating selection

In Chapter 1, I lead a review of the field of fluctuating selection, synthesising the abundance of evidence that has been published since the previous review conducted in 2010 (Bell 2010). Bell's review challenges the idea that selection is gradual and slow which was first perpetuated by Darwin (Darwin 1859) and led to the development of the infinitesimal model in population genetics (Fisher 1930). Bell highlights that environments are constantly changing which is more likely to result in rapid adaptation to varying selection pressures. As a consequence, Bell proposed that fluctuating selection is expected to be common and summarises the evidence of this in a number of species (Bell 2010). Notably, evidence in *Drosophila* is not included in this prior review but has since been a key species in the study of fluctuating selection, both experimentally and in natural populations (Bergland et al. 2014; Huang et al. 2014; Glaser-Schmitt et al. 2021; Machado et al. 2021; Behrman & Schmidt 2022; Rudman et al. 2022; Bitter et al. 2023; Glaser-Schmitt et al. 2023; Nunez et al. 2023). Moreover, additional evidence has also been found in a variety of other species spanning all forms of life and a range of time scales; from plants and insects to mammals ranging from seasonal scales to thousands of years (Ludwig et al. 2015; Busoms et al. 2018; Garcia-Elfring et al. 2021; Pfenninger et al. 2022; Pfenninger & Foucault 2022). In addition to recapitulating studies of empirical data, I also summarise the abundance of theoretical studies of fluctuating selection. This includes a discussion of models of fluctuating loci, including the segregation lift model used in Chapters 2 and 4, as well as the influence of fluctuating selection on genome-wide diversity, explored further in Chapter 4.

Ecological mechanisms for fluctuating selection

My review also covers theoretical models that involve ecological mechanisms of fluctuating selection. In this thesis, I largely simulate a constant population size and an equal number of generations per season. It is understood that, in reality, *Drosophila* experience a boom-bust demography, whereby the population increases over summer and decreases over winter due to abiotic factors such as temperature and humidity and biotic factors such as food availability (Varpe 2017; Bertram & Masel 2019). In addition, *D. melanogaster* has been suggested to undergo 'overwintering', such that there are fewer generations in the winter compared to summer (Bergland et al. 2014; Nunez et al. 2023). In Chapter 4, I simulate a fluctuating population size to emulate the boom-bust demography observed in natural *Drosophila* populations. I also simulate fluctuating selection with offspring capping, limiting the number of offspring per parent, to ensure I am encapsulating effects likely to be seen in nature to compare against idealised population genetic effects (i.e. where individuals can contribute to a larger portion of offspring than biologically viable). I find that the effects of fluctuating selection on variance effective population size are robust to both of these ecological mechanisms. In addition, the combination of fluctuating selection and boom-bust demography produces a reduction in effective population size on the order of a magnitude, suggesting that ecological mechanisms in conjunction with fluctuating selection may be able to explain the large disparity between effective and census population size seen in many insect species.

Limitations in ecological realism

Some of the limitations of the work in this thesis relate to the ecological parameters under which simulations are conducted (i.e. generations per season, population size across seasons). I use constant population sizes and equal generations per season to untangle the effects of

selection from the influence of demographic events, this provides an effective foundation for our understanding of the impacts of fluctuating selection. However, ecological parameters in natural populations might be very different from those simulated, and future studies could include additional ecological realism to capture any additional features that may result from these ecological influences. In addition, protection from selection, where a portion of the population is replaced as juveniles and selection is not acting on the remaining adult population (Bertram & Masel 2019; Park & Kim 2019; Kim 2023; Yamamichi et al. 2023), is another ecological mechanism that was not included in the work in this thesis but may add further ecological realism to simulations as another contributor to fluctuating allele frequencies. An additional limitation is that I do not simulate recurrent mutation, instead investigating only the fluctuating loci that are introduced at the initiation of simulations. The mutation rates of *Drosophila* are large enough that some seasonal loci could mutate over the timescales simulated in these studies (Keightley et al. 2014). This is again an additional feature that could be included in future work to add realism. It is important to note that there are likely a myriad of factors, some of which we still may not fully appreciate, acting on natural populations. Thus, while the addition of ecological factors may generate the impacts of fluctuating selection more similar to what is seen in natural populations, simulations can never perfectly replicate what happens in nature. That being said, simulation does provide us with a suitable understanding that can then be tested against empirical data.

Simulations of fluctuating selection

In Chapter 2, I evaluate simulation frameworks for complex selection models, like fluctuating selection. Most studies that benchmark population genetic simulation programs only simulate simplified forms of selection with constant pressure, such as selective sweeps or purifying selection (Shlyakhter et al. 2014; Thornton 2014; Haller & Messer 2017; Kelleher et al. 2018; Haller et al. 2019; Baumdicker et al. 2022). This makes evaluating the appropriate simulation

program difficult when aiming to model non-standard forms of selection, with resource usage for static models of selection not always providing an accurate approximation for models of fluctuating selection. This chapter allows for the consideration of realistic resource usage when complex models of selection are implemented. I tested four workflows, two of which have not been benchmarked previously. Two simulation programs are utilised, *msprime* (Baumdicker et al. 2022), a coalescent simulator, and *SLiM* (Haller & Messer 2023), a forward-in-time simulator. I found that using a coalescent burn-in simulated in *msprime* considerably reduces computational resource usage. This approach not only ensured the coalescence of lineages across the whole of the simulated segment but also established levels of diversity equivalent to the neutral expectation. In comparison, I found that when using forwards-in-time approaches for the burn-in, the simulation must be run for an average of $28N_e$ generations to ensure coalescence across a simulated segment of 1 Mb. This is considerably longer than the $10N_e$ generations that are typically recommended to reach an equilibrium state when conducting simulations. In addition to having uncoalesced lineages when using this $10N_e$ approximation, levels of diversity are significantly lower than the neutral expectation, which can be an issue when examining the effects of a selection form on diversity over time as I did in Chapter 3.

For the selection phase of our benchmarking workflows, I used the forward population genetic simulator, *SLiM.* The use of *SLiM* allowed for additional complexity to be incorporated into simulations beyond simplified models of constant selection, from the implementation of seasonal selection pressures to capping offspring numbers. I compared the resource usage of classical mutation recording to a recently developed computational technique using a novel data structure, tree sequence recording (Haller et al. 2019; Haller & Messer 2023). I found that mutation recording was substantially slower but used less computational memory, compared to tree sequence recording which was faster but required

more RAM. The tree sequence recording approach also retains genealogical information which can be utilised in the analysis of the simulation output, with tree sequence-based statistics being considerably faster to compute.

The workflow consisting of a coalescent burn-in in *msprime* followed by a selection phase simulated in *SLiM* with tree sequence recording was used in Chapter 3, where I investigated the effects of fluctuating selection on established levels of neutral diversity at different time points. Chapter 4 did not require an established level of initial neutral diversity, since here we measure the instantaneous effective population size that does not rely on information from established neutral variants. Thus, I only simulated the forward selection phase using the classical mutation recording approach over a reasonable number of generations. This drastically improved the performance of the simulation and allowed me to simulate the full extent of the two major *Drosophila* autosomes under realistically large population sizes.

Answering outstanding questions

I identified several outstanding questions in my review in Chapter 1. Some of these were addressed in the subsequent chapters of this thesis. In the review I ask, is there power to discriminate the population genetic signatures of fluctuating selection from those of simple forms of balancing selection or soft selective sweeps? In Chapter 3, I determine that fluctuating selection can be readily distinguished from positive selection, in the form of hard and soft selective sweeps, using single statistics. Differentiation between balancing and fluctuating selection is more challenging, particularly when alleles have recently reached equilibrium and are established in similar time frames. This generates partial sweep patterns of comparable magnitude that are difficult to discriminate. In addition, when comparing single statistics, balancing and fluctuating selection failed to be discriminated from one another, this highlights that there are potentially cases of fluctuating selection that have been

mistaken for balancing selection if statistics that struggled to distinguish these forms were used. Using linear discriminant analysis, I found that balancing selection can be well distinguished from fluctuating selection by using multiple statistics in combination. For example, utilising multiple time points, observed across the season, allowed for the correct classification of short-term fluctuating and balancing selection in 90% of cases. In contrast, in the case of long-term selection multiple windows around the selected site (i.e. the window over the selected size, the window adjacent to the selected side, and a window 250 kb away from the selected site) allowed for 85% correct classification of the two forms of selection, suggesting that the spatial genomic pattern allows further power for discrimination. In sum, our results suggest that utilising multiple statistics that leverage different types of information (i.e., spatial across the genome, and temporal across the season) may significantly help to reliably classify fluctuating selection.

My review also highlights that fluctuating selection may have important implications for the resolution of Lewontin's Paradox. In Chapter 4, I investigate the effect of fluctuating selection on effective population size in this context. Fluctuating selection was seen to reduce effective population size by up to 75%, whilst maintaining alleles with a mean allele frequency fluctuation within the range observed in natural populations (Bergland et al. 2014; Machado et al. 2021; Rudman et al. 2022; Bitter et al. 2023). This suggests that fluctuating selection may be a conceivable explanation for some degree of this discrepancy between measures of effective and census population size.

Future work

Many of our remaining questions concern fluctuating alleles in natural populations, i.e. how long are alleles under fluctuating selection typically maintained in natural populations? How do fluctuating alleles become established? Is it through *de novo* mutation or through

introgression from populations in extreme environments? In Chapter 3, I determined that it is possible for a single *de novo* mutation to become established and observed a unique fluctuating allele frequency trajectory (i.e. frequency fluctuates around an increasing average frequency) before alleles reached a stable oscillation. This pattern could be utilised for the estimation of the age and origin of fluctuating alleles in empirical data. I also characterise the patterns of neutral variation expected around loci under short and long-term fluctuating selection. Future work scrutinising the patterns of diversity around fluctuating SNPs identified in empirical data may confirm if the signatures identified in this thesis hold true under all the additional forces experienced by individuals in natural populations. *Drosophila* parameters are used in this thesis to conduct empirically informed investigations; however, this work could be extended to the multitude of species in which fluctuation has been identified or could potentially be occurring. In particular, examination of the effect of fluctuating selection on effective population size in other species may bring us closer to explaining Lewontin's Paradox.

Conclusions

While our understanding of fluctuating selection has advanced considerably over the last decade, each development incites a myriad of additional questions, highlighted throughout this discussion. Overall, this thesis provides an updated review of the field; a unique benchmarking of workflows for population genetic simulation of non-standard models of selection; the characterisation of the signatures of fluctuating selection and their discrimination from other selection types; and an investigation into the effects of fluctuating selection on effective population size. Fluctuating selection has the potential to be prolific throughout species and time; this thesis contributes significantly to this exciting new area of research with major implications for the conservation of species and our understanding genetic diversity across the tree of life.

References

Abdul-Rahman F, Tranchina D, Gresham D. 2021. Fluctuating environments maintain genetic diversity through neutral fitness effects and balancing selection. Mol. Biol. Evol. 38:4362–4375. doi: 10.1093/molbev/msab173.

Baumdicker F et al. 2022. Efficient ancestry and mutation simulation with msprime 1.0. Genetics. 220. doi: 10.1093/genetics/iyab229.

Behrman EL, Schmidt P. 2022. How predictable is rapid evolution? bioRxiv. 2022.10.27.514123. doi: 10.1101/2022.10.27.514123.

Bell G. 2010. Fluctuating selection: The perpetual renewal of adaptation in variable environments. Philos. Trans. R. Soc. Lond. B Biol. Sci. 365:87–97. doi: 10.1098/rstb.2009.0150.

Bergland AO, Behrman EL, O'Brien KR, Schmidt PS, Petrov DA. 2014. Genomic evidence of rapid and stable adaptive oscillations over seasonal time scales in Drosophila. PLoS Genet. 10:e1004775. doi: 10.1371/journal.pgen.1004775.

Berry AJ, Ajioka JW, Kreitman M. 1991. Lack of polymorphism on the *Drosophila* fourth chromosome resulting from selection. Genetics. 129:1111–1117. doi: 10.1093/genetics/129.4.1111.

Bertram J, Masel J. 2019. Different mechanisms drive the maintenance of polymorphism at loci subject to strong versus weak fluctuating selection. Evolution. 73:883–896. doi: 10.1111/evo.13719.

Bitter MC et al. 2023. Continuously fluctuating selection reveals extreme granularity and parallelism of adaptive tracking. bioRxiv. 2023.10.16.562586. doi: 10.1101/2023.10.16.562586.

Busoms S et al. 2018. Fluctuating selection on migrant adaptive sodium transporter alleles in coastal *Arabidopsis thaliana*. Proc. Natl. Acad. Sci. U.S.A. 115:E12443–E12452. doi: 10.1073/pnas.1816964115.

Charlesworth D. 2006. Balancing selection and its effects on sequences in nearby genome regions. PLoS Genet. 2:e64. doi: 10.1371/journal.pgen.0020064.

Darwin C. 1859. *On the origin of species by means of natural selection or the preservation of favoured races in the struggle for life*. H. Milford; Oxford University Press.

Fisher RA. 1930. *The genetical theory of natural selection*. The Clarendon Press: Oxford.

Fisher RA, Ford EB. 1947. The spread of a gene in natural conditions in a colony of the moth *Panaxia dominula L.* Heredity. 1:143–174. doi: 10.1038/hdy.1947.11.

Garcia-Elfring A et al. 2021. Using seasonal genomic changes to understand historical adaptation to new environments: Parallel selection on stickleback in highly-variable estuaries. Mol. Ecol. 30:2054–2064. doi: 10.1111/mec.15879.

Glaser-Schmitt A, Ramnarine TJS, Parsch J. 2023. Rapid evolutionary change, constraints and the maintenance of polymorphism in natural populations of *Drosophila melanogaster*. Mol. Ecol. doi: 10.1111/mec.17024.

Glaser-Schmitt A, Wittmann MJ, Ramnarine TJS, Parsch J. 2021. Sexual antagonism, temporally fluctuating selection, and variable dominance affect a regulatory polymorphism in *Drosophila melanogaster*. Mol. Biol. Evol. 38:4891–4907. doi: 10.1093/molbev/msab215.

Haller BC, Galloway J, Kelleher J, Messer PW, Ralph PL. 2019. Tree-sequence recording in SLiM opens new horizons for forward-time simulation of whole genomes. Mol. Ecol. Resour. 19:552–566. doi: 10.1111/1755-0998.12968.

Haller BC, Messer PW. 2017. SLiM 2: Flexible, interactive forward genetic simulations. Mol. Biol. Evol. 34:230–240. doi: 10.1093/molbev/msw211.

Haller BC, Messer PW. 2023. SLiM 4: Multispecies eco-evolutionary modeling. Am. Nat. 201:E127–E139. doi: 10.1086/723601.

Huang Y, Wright SI, Agrawal AF. 2014. Genome-wide patterns of genetic variation within and among alternative selective regimes. PLoS Genet. 10:e1004527. doi: 10.1371/journal.pgen.1004527.

Keightley PD, Ness RW, Halligan DL, Haddrill PR. 2014. Estimation of the spontaneous mutation rate per nucleotide site in a *Drosophila melanogaster* full-sib family. Genetics. 196:313–320. doi: 10.1534/genetics.113.158758.

Kelleher J, Thornton KR, Ashander J, Ralph PL. 2018. Efficient pedigree recording for fast population genetics simulation. PLoS Comput. Biol. 14:e1006581. doi: 10.1371/journal.pcbi.1006581.

Kim Y. 2023. Partial protection from fluctuating selection leads to evolution towards wider population size fluctuation and a novel mechanism of balancing selection. Proc. Biol. Sci. 290:20230822. doi: 10.1098/rspb.2023.0822.

Ludwig A et al. 2015. Twenty-five thousand years of fluctuating selection on leopard complex spotting and congenital night blindness in horses. Philos. Trans. R. Soc. Lond. B Biol. Sci. 370:20130386. doi: 10.1098/rstb.2013.0386.

Machado HE et al. 2021. Broad geographic sampling reveals the shared basis and environmental correlates of seasonal adaptation in *Drosophila*. eLife. 10:e67577. doi: 10.7554/eLife.67577.

Nunez JCB et al. 2023. A cosmopolitan inversion facilitates seasonal adaptation in overwintering *Drosophila*. Genetics. doi: 10.1093/genetics/iyad207.

Park Y, Kim Y. 2019. Partial protection from cyclical selection generates a high level of polymorphism at multiple non-neutral sites. Evolution. 73:1564–1577. doi: 10.1111/evo.13792.

Petersen L, Bollback JP, Dimmic M, Hubisz M, Nielsen R. 2007. Genes under positive selection in *Escherichia coli.* Genome Res. 17:1336–1343. doi: 10.1101/gr.6254707.

Pfenninger M, Foucault Q. 2022. Population genomic time series data of a natural population suggests adaptive tracking of fluctuating environmental changes. Integr. Comp. Biol. doi: 10.1093/icb/icac098.

Pfenninger M, Foucault Q, Waldvogel A-M, Feldmeyer B. 2022. Selective effects of a short transient environmental fluctuation on a natural population. Mol. Ecol. doi: 10.1101/2022.02.10.479864.

Rudman SM et al. 2022. Direct observation of adaptive tracking on ecological time scales in *Drosophila*. Science. 375:eabj7484. doi: 10.1126/science.abj7484.

Shlyakhter I, Sabeti PC, Schaffner SF. 2014. Cosi2: An efficient simulator of exact and approximate coalescent with selection. Bioinformatics. 30:3427–3429. doi: 10.1093/bioinformatics/btu562.

Smith JM, Haigh J. 1974. The hitch-hiking effect of a favourable gene. Genet. Res. 23:23–35. doi: 10.1017/S0016672300014634.

Souilmi Y et al. 2022. Admixture has obscured signals of historical hard sweeps in humans. Nat. Ecol. Evol. 1–13. doi: 10.1038/s41559-022-01914-9.

Stephan W. 2019. Selective sweeps. Genetics. 211:5–13. doi: 10.1534/genetics.118.301319.

Thornton KR. 2014. A C++ template library for efficient forward-time population genetic simulation of large populations. Genetics. 198:157–166. doi: 10.1534/genetics.114.165019.

Varpe Ø. 2017. Life history adaptations to seasonality. Integr. Comp. Biol. 57:943–960. doi: 10.1093/icb/icx123.

Yamamichi M, Letten AD, Schreiber SJ. 2023. Eco-evolutionary maintenance of diversity in fluctuating environments. Ecol. Lett. 26 Suppl 1:S152–S167. doi: 10.1111/ele.14286.